

Copyright is owned by the Author of the thesis. Permission is given for a copy to be downloaded by an individual for the purpose of research and private study only. The thesis may not be reproduced elsewhere without the permission of the Author.

Characterisation of the maize leaf patterning mutants
Wavy auricle in blade1-R and *milkweed pod1-R*

A thesis presented in partial fulfillment of the requirements for the
degree of
Doctor of Philosophy
in
Plant Biology

at Massey University, Palmerston North, New Zealand.

Robyn Maree Johnston

2007

Abstract

The maize leaf has three main axes of growth, with an asymmetric distribution of tissue types along each axis. This study focuses on three mutants, *Wavy auricle in blade1-R* (*Wab1-R*), *liguleless1-R* (*Lg1-R*) and *milkweed pod1-R* (*mwp1-R*) that disrupt axial patterning of maize leaves. Dominant *Wab1* mutations disrupt both medial-lateral and proximal-distal patterning. *Wab1* leaf blades are narrow and ectopic auricle and sheath-like tissues extend into the leaf blade. Previous analyses have shown that *Lg1* acts cell-autonomously to specify ligule and auricle tissues. The current study reveals additional roles in defining leaf shape. The recessive *Lg1-R* mutation exacerbates the *Wab1-R* phenotype; in the double mutants, most of the proximal blade is deleted and sheath tissue extends along the residual blade.

A mosaic analysis of *Wab1-R* was conducted in *Lg1* and *Lg1-R* backgrounds to determine if *Wab1-R* affects leaf development in a cell-autonomous manner. Normal tissue identity was restored in all *wab1/-* sectors in a *Lg1-R* mutant background, and in three quarters of sectors in a *Lg1* background. These results suggest that *Lg1* can influence the autonomy of *Wab1-R*. In both genotypes, leaf-halves with *wab1/-* sectors were significantly wider than non-sectored leaf-halves, suggesting that *Wab1-R* acts cell-autonomously to affect lateral growth.

mwp1-R is a recessive mutation that specifically affects patterning of sheath tissue. Characterisation of the *mwp1-R* phenotype revealed that *mwp1-R* husk leaves and the sheaths of vegetative leaves develop pairs of outgrowths on the abaxial surface associated with regions of adaxialised tissue. *In situ* hybridisation confirmed that disruptions to adaxial-abaxial patterning are correlated with misexpression of leaf polarity genes. Leaf margins and fused organs such as the prophyll are most severely affected by *mwp1-R*. The first two husk leaves normally fuse along adjacent margins to form the bi-keeled prophyll. In the most severe cases the *mwp1-R* prophyll is reduced to an unfused, two-pronged structure and keel outgrowth is significantly reduced. We speculate that the adaxial-abaxial patterning system has been co-opted during evolution to promote outgrowth of the keels in normal prophyll development.

The results of this study place *Mwp1*, *wab1* and *Lg1* in a network of genes that regulate leaf polarity and axial patterning.

Acknowledgements

I would like to thank my parents, Mum and Owl, for their unconditional love and support. Owl – you have taught me so much more than you imagine. Mum – I am so sorry that you are not here to see me finish. I thank you for your understanding and belief in me and for your sheer common sense.

I thank Paula Jameson for encouraging me to come to Massey (although I didn't realise then how long I would stay!) and for supporting me at every step since. Thanks to Barbara Ambrose for always providing useful and enthusiastic feedback.

A big thank you to Doug Hopcroft and Crunch (Raymond) Bennett for assistance with SEM and photography. Thanks to Keith Croft and Ben Parkinson at the Palmerston North Hospital for irradiating seeds, and to Alla Seleznyova for help with data analysis. Thank you to Chris Kirk for all the patient advice and assistance in the lab.

I would like to thank Sarah Hake for sharing this project, for your warmth and generosity, and for opening your home to me while I was in the US. I thank Hector Candela for generously sharing knowledge and maize seed and for answering a multitude of annoying questions. Thanks to Bruce Veit for the advice, encouragement and random *in situ* reagents.

Ben – thank you for your support while I was finding my way and for always being there for me. Thank you for challenging me and for teaching me the value (and pleasure) of a good argument. >:D<

Thanks to Sacha for providing so much encouragement, for the trips to the airport and for convincing me that I could run 21.1km in the midst of it all. Thanks to Denise for the Word long document tuition and for being a good friend.

Richard – thank you for your unflinching support even at my soggiest. Thanks for the pool tutelage, for walking me and for help with the giraffes.

Sarah Dorling – you turned up just when I needed you and have given me so much love. Thank you for feeding me when I was carb-deprived, sending me to bed when I was exhausted and most of all, thank you for being the sloth to my mould.

Toshi, I cannot thank you enough for making my PhD such an amazing and festive experience. Thank you for being a friend first and for being the best supervisor I could ever have hoped for. Thank you for sharing your love of plant development, for showing me my first meristem and for speaking the same language. Who else will understand the hand gestures and twitching of the shoulder blades that denote particular parts of the maize plant? Thank you for the weekend retreats, wine, meals, nights dancing, cake and lunches at the Gallery.

I wish to acknowledge and thank the Tertiary Education Commission who provided my Top Achiever Doctoral Scholarship and the Marsden Foundation who provided funding for this project.

This thesis is dedicated to my parents, Gaile and Vern Johnston.

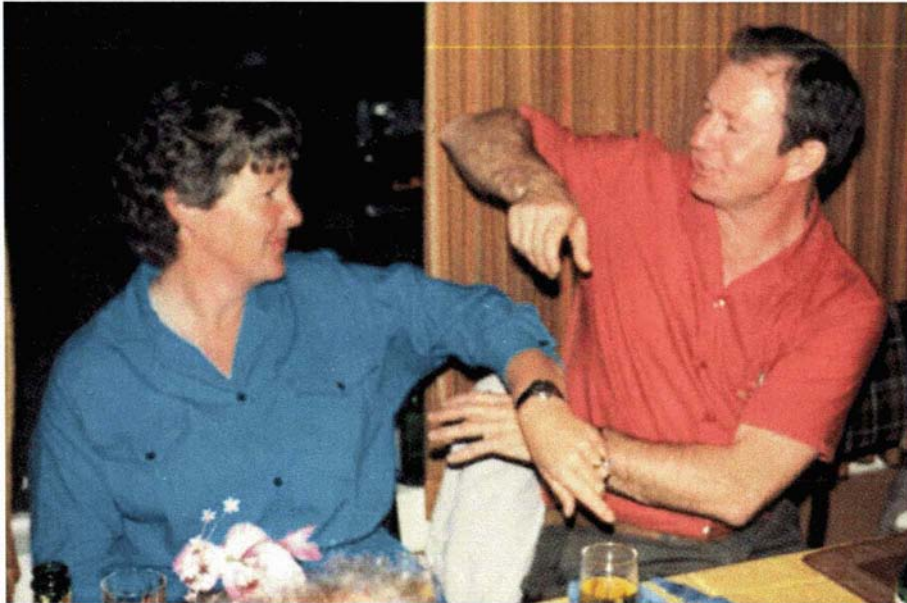


Table of Contents

Abstract	II
Acknowledgements	IV
Dedication	VI
Table of Contents	VII
List of Figures	X
List of Tables	XII
List of Abbreviations	XIII
1. Introduction	1
1.1 Background	1
1.2 Growth of the maize plant	2
1.3 Leaves have three main axes of growth	3
1.4 Leaf initiation and early development	4
1.4.1 Founder cells	4
1.4.2 Development of dicot leaves.....	5
1.4.3 Development of maize leaves.....	6
1.5 Developmental compartments and axial patterning	7
1.5.1 Developmental compartments	7
1.5.2 Analysis of leaf patterning mutants.....	8
1.5.3 Proximal-distal patterning	8
1.5.4 Adaxial-abaxial patterning	11
1.5.5 Medial-lateral patterning	20
1.5.6 Summary of axial patterning	21
1.6 Establishment and maintenance of developmental domains	22
1.6.1 MicroRNAs and gene regulation.....	22
1.6.2 Protein trafficking.....	23
1.7 Homologies between lateral organs	25
1.7.1 Plants are comprised of repeated structural units.....	25
1.7.2 Mutant phenotypes provide a tool for detecting organ homologies within a species	27
1.7.3 Mutations to orthologous genes in diverse species	27
1.8 Genome duplication and subfunctionalisation	29
1.9 Maize inbred lines	30
1.10 Aims and objectives	31

2. General Materials and Methods	33
2.1 Maize nomenclature	33
2.2 Inbred lines	33
2.3 Growth conditions	34
2.4 Stereomicroscope and light microscopy	34
2.5 Scanning electron microscopy	34
2.5.1 Preparation of specimens	34
2.5.2 Preparation of replicas.....	35
2.5.3 Viewing and photography	35
2.6 Histology	36
2.6.1 Paraffin sections	36
2.6.2 Staining.....	37
2.6.3 Resin sections	38
2.6.4 Distinguishing xylem and phloem in sectioned material	38
3. Wavy auricle in blade1-R	39
3.1 Introduction	39
3.2 Specific materials and methods	40
3.2.1 Phenotypic analysis of <i>Wab1-R</i> and <i>Ig1-R;Wab1-R</i> plants.....	40
3.2.2 Mosaic and clonal analyses.....	40
3.2.3 <i>Ig1-R</i> leaf measurements.....	45
3.2.4 Lateral vein count in <i>Wab1-R</i> leaf primordia.....	45
3.3 Results	46
3.3.1 <i>Ig1-R</i> enhances the <i>Wab1-R</i> mutant phenotype.....	46
3.3.2 <i>Ig1-R</i> alters leaf shape.....	48
3.3.3 Mosaic analysis of <i>Wab1-R</i>	50
3.3.4 Mosaic analysis of <i>Ig1-R</i>	57
3.3.5 Clonal analysis of <i>Wab1-R</i> leaves	61
3.3.6 <i>Wab1-R</i> leaves have fewer lateral veins by plastochron 4	63
3.4 Discussion	66
3.4.1 <i>Lg1</i> influences cell-autonomy of the <i>Wab1-R</i> phenotype	66
3.4.2 Loss of <i>Wab1-R</i> is associated with an increase in leaf width.....	68
3.4.3 The role of <i>Lg1</i> in leaf morphogenesis	69
3.4.4 Ectopic auricle tissue in <i>Wab1-R</i> leaves is conditioned by <i>Lg1</i> ...	70
3.4.5 Effects of <i>Ig1-R/-</i> sectors on <i>Wab1-R</i> ectopic sheath tissue.....	73
3.4.6 <i>Lg1</i> promotes lateral growth in a non-cell autonomous manner ..	73
3.4.7 <i>Lg1</i> has both cell-autonomous and non-autonomous functions...74	
3.4.8 <i>Wab1-R</i> leaf primordia are narrower and initiate fewer lateral veins than wild-type leaf primordia	74

4. milkweed pod1-R	77
4.1 Introduction	77
4.2 Specific Materials and Methods	78
4.2.1 Material for SEM and histology	78
4.2.2 Measurements of <i>mwp1-R</i> and wild-type lateral organs	79
4.2.3 SEM of developing prophylls	80
4.2.4 Measurements of developing prophylls	80
4.2.5 <i>In situ</i> hybridisation	80
4.2.6 Husk leaf and prophyll material for <i>in situ</i> hybridisation	85
4.3 Results	85
4.3.1 Husk leaf phenotype	85
4.3.2 Prophyll phenotypes	91
4.3.3 <i>mwp1-R</i> sheath margin phenotype	105
4.3.4 <i>mwp1-R</i> floral organ phenotypes	108
4.3.5 Measurements of mature wild-type and <i>mwp1-R</i> lateral organs	110
4.3.6 The <i>mwp1-R</i> ; <i>Wab1-R</i> leaf blade phenotype	118
4.4 Discussion	120
4.4.1 <i>mwp1-R</i> disrupts adaxial-abaxial polarity	120
4.4.2 <i>mwp1-R</i> affects lateral and proximal-distal growth	129
4.4.3 <i>Mwp1</i> interacts with networks that establish leaf polarity	133
4.4.4 Expression of the <i>mwp1-R</i> phenotype varies in different inbred backgrounds	136
4.4.5 <i>mwp1-R</i> specifically affects sheath tissue	138
4.4.6 <i>mwp1-R</i> interacts with proximal-distal patterning mutants	138
4.4.7 Comparison of grass and dicot modes of growth	139
4.4.8 Prophyll morphogenesis	140
5. Conclusions and future work	145
5.1 Conclusions	145
5.2 Future work	148
References	150

List of Figures

Figure 1.1 Leaf axes	3
Figure 1.2 Founder cells.....	4
Figure 1.3 Generation of albino sectors for clonal analysis	5
Figure 1.4 Maize leaf patterning mutants	13
Figure 1.5 Interactions between factors involved in the specification of adaxial-abaxial polarity in <i>Arabidopsis</i> and maize leaves.....	20
Figure 1.6 Lateral organ homologies in maize	26
Figure 1.7 Upper and lower leaf zones.....	28
Figure 3.1 Scheme for mosaic analysis of <i>Wab1-R</i>	41
Figure 3.2 Scheme for mosaic analysis of <i>lg1-R</i>	42
Figure 3.3 Leaf and whole plant phenotypes.....	47
Figure 3.4 Epidermal and histological features of wild-type, <i>Wab1-R</i> and <i>lg1-R;Wab1-R</i> leaves.....	48
Figure 3.5 Phenotypes of <i>wab1/-</i> sectors in <i>Wab1-R</i> leaves.....	53
Figure 3.6 Phenotypes of <i>wab1/-</i> sectors in <i>lg1-R;Wab1-R</i> leaves	55
Figure 3.7 Phenotypes of <i>lg1-R/-</i> sectors in <i>Lg1;Wab1-R</i> leaves.....	60
Figure 3.8 Calculation of radial position of clonal sectors in culm	63
Figure 3.9 Lateral vein number in wild-type and <i>Wab1-R</i> leaf primordia.....	65
Figure 3.10 <i>Lg1</i> affects cell-autonomy of the <i>Wab1-R</i> phenotype.....	68
Figure 3.11 Model for <i>Lg1</i> function in leaf morphogenesis.....	70
Figure 4.1 Wild-type and <i>mwp1-R</i> ears	86
Figure 4.2 Ectopic outgrowths on <i>mwp1-R</i> husk leaves are associated with adaxialised tissue.....	87
Figure 4.3 <i>rd1</i> is misexpressed in <i>mwp1-R</i> husk leaf primordia	89
Figure 4.4 <i>zyb9</i> is misexpressed in <i>mwp1-R</i> husk leaf primordia.....	90
Figure 4.5 The prophyll	91
Figure 4.6 <i>mwp1-R</i> disrupts prophyll development	93

Figure 4.7 Vascular polarity in wild-type prophyll keel.....	94
Figure 4.8 The <i>mwp1-R</i> prophyll defect is apparent by plastochron four	96
Figure 4.9 The <i>mwp1-R</i> unfused prophyll phenotype is associated with <i>rld1</i> misexpression early in development	98
Figure 4.10 <i>rld1</i> expression in wild-type prophyll primordium.....	99
Figure 4.11 Morphometric analysis of <i>mwp1-R</i> and wild-type prophyll development	100
Figure 4.12 The <i>mwp1-R</i> prophyll “tab”phenotype	101
Figure 4.13 <i>rld1</i> expression in <i>mwp1-R</i> prophyll exhibiting the “tab” phenotype	103
Figure 4.14 <i>mwp1-R</i> subdivided keel phenotype	104
Figure 4.15 Outgrowths at <i>mwp1-R</i> sheath margins are associated with ectopic <i>rld1</i> expression.....	106
Figure 4.16 Adaxial epidermal characteristics continue onto the abaxial side of <i>mwp1-R</i> sheath margins with ectopic outgrowths	107
Figure 4.17 <i>mwp1-R</i> silks are twisted and have ectopic outgrowths	109
Figure 4.18 Adaxial-abaxial polarity is disrupted in regions adjacent to ectopic sheath-like tissue in <i>mwp1-R;Wab1-R</i> leaf blades.....	119
Figure 4.19 Model for establishment of polarity in wild-type and <i>mwp1-R</i> prophyll primordia and resulting prophyll phenotypes	127
Figure 4.20 The adaxial-abaxial boundary promotes both lateral and proximal-distal growth.....	131
Figure 4.21 Model for outgrowth of the prophyll keels.....	143

List of Tables

Table 3.1 Comparison of <i>Ig1-R</i> and wild-type (<i>Lg1/Ig1-R</i>) leaf shape	49
Table 3.2 Median width of clonal sectors in <i>Lg1/Ig1-R</i> and <i>Ig1-R/Ig1-R</i> plants	50
Table 3.3 Summary of <i>wab1/-</i> sector phenotypes	52
Table 3.4 Median differences in the width of <i>wab1/-</i> sectored and non-sectored leaf-halves at the blade-sheath boundary and sheath midpoint	56
Table 3.5 Median differences in <i>wab1/-</i> sectored and non-sectored leaf-half widths, and effect of sector position.	57
Table 3.6 Summary of <i>Ig1-R/-</i> sector phenotypes	58
Table 3.7 Median differences in the width of <i>Ig1-R/-</i> sectored and non-sectored leaf-halves.....	61
Table 3.8 Mean widths of clonal sectors in <i>Wab1-R</i> and wild-type leaves.....	62
Table 4.1 Measurements of mature <i>mwp1-R</i> and wild-type prophylls... ..	111
Table 4.2 Measurements of mature wild-type and <i>mwp1-R</i> husk leaves.....	112
Table 4.3 Measurements of mature wild-type and <i>mwp1-R</i> vegetative leaves... ..	113
Table 4.4 Measurements of mature wild-type and <i>mwp1-R</i> glumes.....	115
Table 4.5 Measurements of mature wild-type and <i>mwp1-R</i> paleae.	116
Table 4.6 Measurements of wild-type and <i>mwp1-R</i> silks.....	117

List of abbreviations

BSA	bovine serum albumin
°C	degrees Celsius
d	day
DEPC	diethylpyrocarbonate
dicot	dicotyledon
DIG	digoxigenin
DNA	deoxyribonucleic acid
DPX	dibutylphthalate polystyrene xylene
DTT	dithiothreitol
EDTA	ethylenediaminetetraacetic acid
FAA	formaldehyde, acetic acid, ethanol
GFP	green fluorescent protein
h	hour
kV	kilovolt
L1, L2, L3	cell layers in the shoot apical meristem and lateral organs
LM	lateral meristem
M	molar
mg	milligram
min	minute
miRNA	microRNA
ml	millilitre
mm	millimetre
mM	millimolar
monocot	monocotyledon
mRNA	messenger ribonucleic acid
NBT/BCIP	5-bromo-4-chloro-3'-indolyphosphate p-toluidine salt/nitro-blue tetrazolium chloride
nm	nanometre
NTP	nucleotide triphosphates
P0, P1, P2	plastochron number
PBS	phosphate buffered saline
RNA	ribonucleic acid
s	second
SAM	shoot apical meristem

SEM	scanning electron microscopy
SSC	sodium chloride, sodium citrate
SSPE	sodium chloride, sodium phosphate, EDTA
TBS	tris buffered saline
TE	tris, EDTA
tRNA	transfer ribonucleic acid
μg	microgram
μl	microlitre
μm	micron
w/v	weight by volume ratio
v/v	volume to volume ratio

1. Introduction

1.1 Background

A central issue in developmental biology is how pattern is superimposed on initially uniform groups of cells (Russo, 1999; Gilbert, 2000). A primary mechanism in animal development is the subdivision of fields of cells into smaller compartments defined by differential gene expression (Lawrence and Struhl, 1996). New axes of growth can form where two compartments are juxtaposed (Diaz-Benjumea and Cohen, 1993).

There is evidence that similar mechanisms operate in leaf development. Distinct cell types develop on the adaxial (upper) and abaxial (lower) surfaces of most leaves (Steeves and Sussex, 1984). The complete loss of either domain results in radial leaves whereas partial loss generates new boundaries, resulting in ectopic outgrowths (Sussex, 1954; Waites and Hudson, 1995; McConnell and Barton, 1998; Eshed *et al.*, 2001). Many genes involved in the establishment of leaf polarity have been identified in dicots (McConnell and Barton, 1998; Alvarez and Smyth, 1999; Siegfried *et al.*, 1999; Eshed *et al.*, 2001; Kerstetter *et al.*, 2001; McConnell *et al.*, 2001). However, mechanisms controlling leaf polarity in monocots are less well known.

One approach that has been successful in elucidating the mechanisms that control development is the study of mutants that exhibit developmental defects. The current study focuses on two maize mutants that disrupt leaf polarity. *Wavy auricle in blade1-R* (*Wab1-R*) is a dominant mutation that disrupts medial-lateral and proximal-distal patterning of leaves, resulting in narrow leaves and inappropriate cell differentiation (Hay and Hake, 2004). I have used mosaic analysis to investigate the mode of action of *Wab1-R* and to elucidate genetic interactions between *Wab1-R* and *Liguleless1* (*Lg1*).

The recessive *milkweed pod1-R* (*mwp1-R*) mutation was first identified by ectopic outgrowths on the abaxial surface of the husk leaves. This phenotype suggested that *Mwp1* may be required for the establishment or maintenance of

leaf polarity. The *mwp1-R* mutation specifically affects sheath tissue, the basal part of the lower leaf zone. This part of the leaf is extremely reduced in dicots (Troll, 1955; Kaplan, 1973). The *mwp1-R* phenotype is particularly severe in the prophyll and silks – organs that are thought to form via phytomer fusion (Bossinger *et al.*, 1992). Thus, this mutant affords the opportunity to investigate the establishment of polarity in lateral organs with diverse morphologies.

1.2 Growth of the maize plant

In maize, the primary axis is generated by a single shoot apical meristem (SAM). The SAM initiates a series of vegetative leaves in an alternate pattern before terminating in the tassel (male inflorescence) (Poethig, 1994).

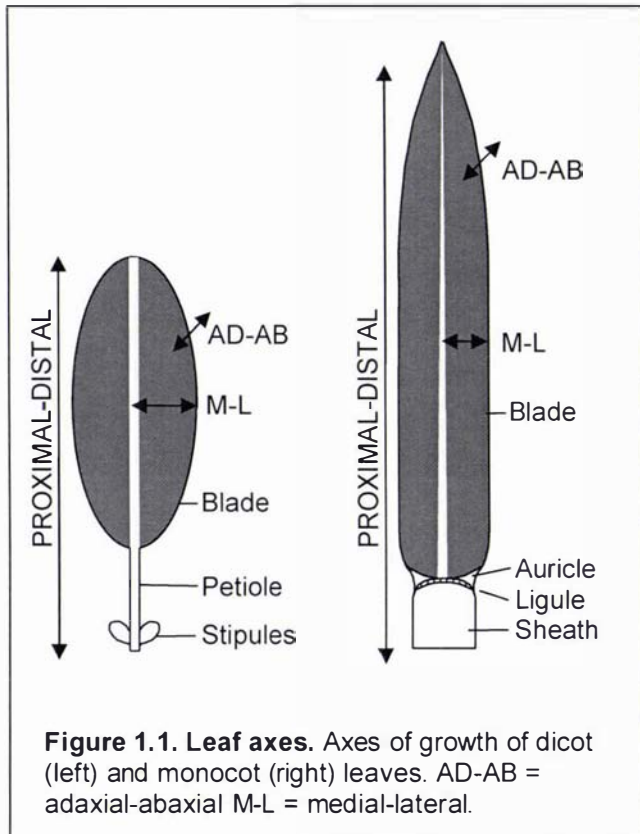
The male and female inflorescences are borne separately. The female inflorescences (ears) arise from meristems in the axils of vegetative leaves at the upper nodes. The SAM terminates in the tassel after the production of vegetative leaves has ceased. Flowers are initially bisexual and become unisexual by the abortion of gynoecia in male flowers, and of stamens in female flowers.

The early stages of spikelet and flower development are similar for male and female flowers (Cheng *et al.*, 1983). Inflorescence meristems produce spikelet pair primordia. Each spikelet pair primordium produces two spikelet primordia which in turn initiate two florets each. There are two flowers per male spikelet. In female spikelets, the lower floret is repressed so that only one functional floret develops per spikelet. The spikelet primordia each initiate a series of bract-like organs - two glumes and two lemmas - before the lower floret is initiated in the axil of the outer lemma. Each floret meristem initiates a bi-keeled palea then lodicules, stamens and the gynoecium. The gynoecium is formed by the outgrowth of a ridge which overgrows the apical meristem, giving rise to the stylar canal and silk. In maize, the styles are fused and very short. The stigmas are very long and can reach up to 75cm. They arise close to the ovary and are fused for most of their length, bifurcating at the very tip (Clifford, 1988). There is evidence that the silks are formed via the preprimordial fusion of the two

posterior carpels along two sets of margins (see Figure 1.6 D) (Cronquist, 1988; Scanlon and Freeling, 1998).

1.3 Leaves have three main axes of growth

Leaves have three main axes of growth defined with reference to the SAM. These are the proximal-distal axis, the adaxial-abaxial axis and the medial-lateral axis (Figure 1.1). The proximal end is attached and closest to the SAM,



while the distal end is unattached. The adaxial surface of a leaf is the one adjacent to the SAM, generally the top surface of the mature leaf, while the abaxial surface is the one furthest from the SAM. The medial-lateral axis is defined as midrib to margin. In most species there are characteristic anatomical and morphological asymmetries along each axis that specialise different regions of the leaf for particular functions (Sylvester *et al.*, 1990; Kerstetter *et al.*, 2001).

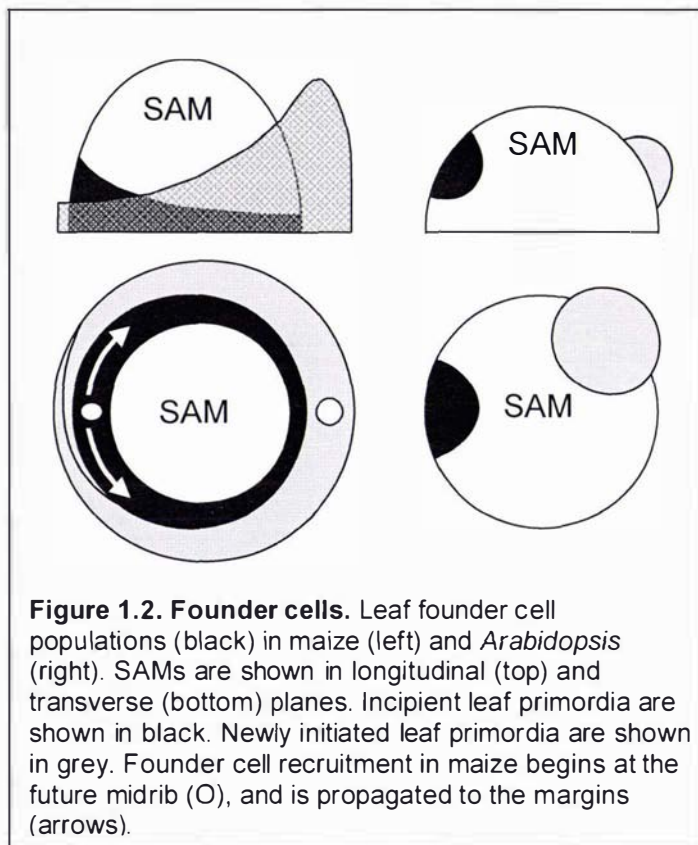
The maize leaf is divided into sheath and blade along the proximal-distal axis (Figure 1.1). The sheath wraps tightly around the culm (stem) of the plant and is separated from the blade by a fringe of ligule tissue and two wedges of auricle tissue. Each of the tissue types has characteristic epidermal and anatomical features (Sylvester *et al.*, 1990). The adaxial blade surface is characterised by rows of bulliform cells and three types of hair. Cell wall junctions are crenulated and interlocking. Sheath cells are non-crenulated and elongated, the abaxial surface has long hairs whereas the adaxial surface has shorter prickly-type hairs. The leaves of dicots such as *Arabidopsis* have a proximal petiole and a

distal lamina. Dicot petioles are often radial in transverse section, whereas the blade has distinct adaxial and abaxial surfaces (Kerstetter *et al.*, 2001).

1.4 Leaf initiation and early development

1.4.1 Founder cells

Morphological differences in the development of dicot and grass leaves are apparent from the time the leaf primordia emerge. Dicot leaf primordia emerge as peg-like outgrowths on the flanks of the SAM, whereas the maize leaf

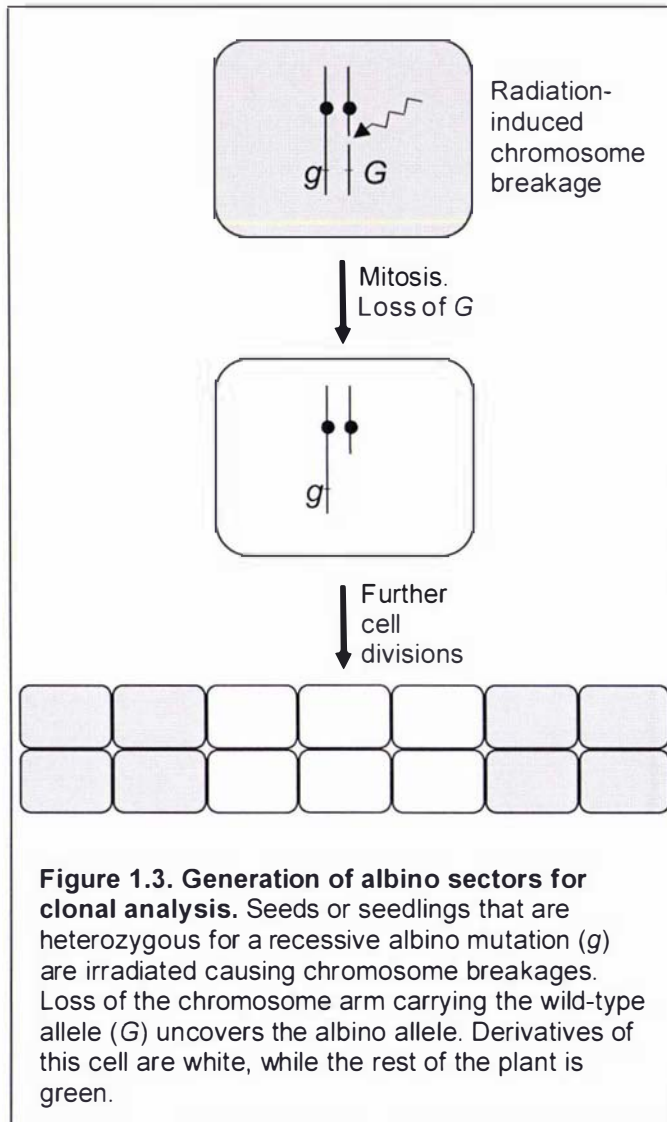


primordium emerges as a ridge of cells that encircles the SAM. Differences in the morphology of dicot and grass leaf primordia reflect differences in the distribution of leaf founder cells (Figure 1.2). The term "founder cell population" refers to those cells within the meristem that are specified to become incorporated into a lateral organ (Poethig, 1984).

In *Arabidopsis*, a small group of about 30 leaf

founder cells is recruited, while in tobacco, the founder cell population is about 50-100 cells (Poethig and Sussex, 1985a; Irish and Sussex, 1992). In maize, the founder cell number is estimated to be about 200 cells (Poethig and Szymkowiak, 1995). Leaf founder cells in dicots occupy only a fraction of the circumference of the SAM, whereas in maize, founder cells are recruited from the entire circumference of the SAM (Figure 1.2). Initialisation of leaf founder cells in maize begins at the future midrib, and is propagated outward toward the margins (Sharman, 1942). The domains that give rise to the sheath margins overlap, so that clonal sectors arising in this part of the SAM include both

margins of the sheath (Poethig, 1984). A number of maize mutants have narrow leaves due to defects in founder cell recruitment (Timmermans *et al.*, 1998; Scanlon, 2000).



Clonal analysis has been used to trace cell lineage and patterns of cell division, both within the meristem and in developing organs, and to estimate leaf founder cell numbers (Steffensen, 1968; Poethig and Sussex, 1985b; Irish and Sussex, 1992; Poethig and Szymkowiak, 1995). Clonal analysis requires that a cell be marked with a heritable, visible, cell-autonomous marker. This allows derivatives of the marked cell to be identified (Figure 1.3). Hyperploidy has been used as a marker of cell lineage within the SAM (Steeves and Sussex, 1984). Albino mutations are

commonly used to investigate cell lineage and cell division patterns in leaves (Steffensen, 1968; Poethig and Sussex, 1985b; Langdale *et al.*, 1989; Irish and Sussex, 1992; Poethig and Szymkowiak, 1995).

1.4.2 Development of dicot leaves

Dicot leaves are initiated by periclinal divisions in a subset of cells in the peripheral zone of the SAM. The first periclinal divisions are generally in the subsurface layers, and are followed by anticlinal divisions in the surface layer (Esau, 1960). These divisions result in a bulge on the flank of the SAM, referred

to as the leaf buttress. The leaf primordium emerges from the leaf buttress as a peg-like outgrowth. Esau (1960) refers to this phase as formation of the leaf axis. At this stage there is no distinction between the blade and petiole (Poethig and Sussex, 1985a). During this phase, the procambium is differentiated in continuity with the procambium of the internode below. The lamina is initiated from cells at the boundary between the adaxial and abaxial faces of the primordium (Poethig and Sussex, 1985a). Subsequent lateral growth of the lamina gives the leaf obvious medial-lateral, and adaxial-abaxial axes (Esau, 1960). Lateral veins are initiated at an oblique angle to the midrib (Poethig and Sussex, 1985a).

A series of classic surgical experiments provided evidence that communication between the SAM and developing leaf primordia is required for the establishment of adaxial cell identity, and for subsequent lamina outgrowth (Sussex, 1955; Snow, 1959). Sussex (1955) found that leaf anlagen (incipient leaf primordia) isolated from the shoot apex by tangential incisions developed as radially symmetrical, abaxialised organs. Leaf primordia isolated after emergence developed flattened laminae. Sussex proposed that communication between the shoot apex and developing leaf primordia is required for the development of adaxial features and lateral growth. These experiments imply that adaxial and abaxial domains are established during the transition from anlagen to leaf primordium. Furthermore, they suggest that abaxial identity is the default state when the leaf primordium is deprived of positional cues.

1.4.3 Development of maize leaves

The maize leaf is derived from cells of the two outer layers of the SAM, the L1 and L2 (Sharman, 1942; Poethig, 1984). Periclinal cell divisions are initiated in a position that corresponds to the future midrib, and are propagated laterally in both directions until they encircle the SAM. The leaf primordium appears first as a crescent shaped protrusion and then as a ridge of cells that encircles the apex (Sharman, 1942; Esau, 1965). Vascularisation begins with the acropetal (base to tip) development of the midvein into the P0 or P1 primordium. This occurs in continuity with the procambium of the shoot apex (Sharman, 1942).

Sylvester *et al.* (1990) have defined three phases of leaf development following emergence of the leaf primordium. Initially, cell division is even throughout the leaf primordium and the sheath and blade regions are morphologically indistinguishable. Lateral veins differentiate acropetally during this primordial stage, beginning near the midrib (Sharman, 1942).

During the second stage, a localised increase in cell division rate, accompanied by a decrease in cell extension, generates a band of small cells (the preligule band) near the base of the leaf primordium. Formation of the preligule band separates the future blade and sheath. Periclinal divisions by epidermal cells at the base of the preligule band form the ligule, and the remaining cells of the preligule band form the auricle. During this phase, cell divisions in the leaf blade become exclusively transverse and differentiation begins at the tip of the blade. Intermediate veins differentiate basipetally, subdividing the regions between the laterals. Transverse veins develop and connect the system of longitudinal veins (Sharman, 1942). During the third stage, the sheath grows rapidly. Differentiation proceeds basipetally, with the sheath being the last part of the leaf to differentiate (Sharman, 1942).

1.5 Developmental compartments and axial patterning

1.5.1 Developmental compartments

A primary mechanism in animal development is the subdivision of fields of cells into progressively smaller compartments (Lawrence and Struhl, 1996). Compartments are defined by differential gene expression. New axes may form when two compartments are juxtaposed. In *Drosophila* limb development, the boundaries between anterior and posterior, and dorsal and ventral, compartments act as organising centres. Experiments show that generation of ventral cell-types in the dorsal compartment creates an ectopic boundary, resulting in the formation of a secondary axis (Diaz-Benjumea and Cohen, 1993). There is evidence for similar mechanisms in leaf development, although compartment boundaries are less rigid. Analysis of genetic mosaics in *Drosophila* demonstrates that cells do not divide across compartment boundaries (Garcia-Bellido *et al.*, 1973). In plants, developmental compartments are more plastic. Cells may divide into adjacent compartments, and

subsequently differentiate according to position rather than lineage (Steeves and Sussex, 1984).

1.5.2 Analysis of leaf patterning mutants

Analysis of mutants that show defects at different stages of leaf development provide clues about the genetic pathways that regulate normal development. Maize is a useful model for such investigations as it is amenable to genetic analysis. Many mutants have been described and the leaves are large, with distinct boundaries and cell types distinguishing different compartments (Freeling and Hake, 1985; Freeling, 1992). Information about the normal role of a gene may be obtained by comparisons of normal and mutant morphogenesis, and of mature organ phenotypes (Sylvester *et al.*, 1990). Interactions between mutants can help determine their order in genetic pathways, whilst analysis of dominant mutations allows identification of genes that may be obscured by genetic redundancy in single loss-of-function mutants (Freeling and Fowler, 1994). Mapping and cloning of genes opens the way for further functional analyses such as studies of gene expression in wild-type and in other mutant backgrounds.

1.5.3 Proximal-distal patterning

The maize leaf is comprised of a proximal sheath and distal blade, separated by a fringe of ligule tissue and two wedges of auricle tissue. Mutants that affect proximal-distal patterning of the maize leaf include dominant *Knox* mutants and *Wab1* mutants (Sinha and Hake, 1990; Hay and Hake, 2004). The *liguleless (lg)* mutants, *lg1* and *lg2*, remove ligule and auricle tissue, but maintain a boundary between blade and sheath (Emerson, 1912; Brink, 1933). Although dominant *Knox* mutations disrupt proximal-distal patterning, their normal function is not specification of the blade-sheath boundary.

Dominant *Knox* mutations

In maize, a number of dominant *Knox* mutations disrupt proximal-distal patterning of the leaf (Sinha and Hake, 1990; Becraft and Freeling, 1994; Foster *et al.*, 1999). The mutants are characterised by the development of proximal tissue types, such as sheath and auricle, in the leaf blade. *Knotted1 (Kn1)*

mutants were the first of these to be identified. Cloning of dominant *Kn1* alleles revealed that mutations in non-coding regions are responsible for ectopic expression of *kn1* (Hake *et al.*, 1989; Veit *et al.*, 1990). *In situ* hybridisation and immunolocalisation have shown that the wild-type gene (*kn1*) is expressed in the SAM, and is downregulated in incipient leaf primordia (Smith *et al.*, 1992). The region of *knox* downregulation correlates with estimates of founder cell populations obtained from clonal analysis. In *Kn1* mutants, the gene is ectopically expressed in the vascular bundles of developing leaves. Based on these results, it is hypothesised that the normal function of *kn1* is to maintain cells in a meristematic state, and that ectopic expression delays differentiation, thus altering cell fates (Smith *et al.*, 1992).

Knox genes appear to have similar functions in dicots and grasses.

SHOOTMERISTEMLESS (*STM*), the *kn1* homologue in *Arabidopsis*, has an expression pattern that is comparable to *kn1*. Loss-of function *stm* mutations result in embryos that lack SAMs, whereas overexpression of *Knox* genes is associated with less determinate patterns of growth, such as lobed leaves and ectopic meristem formation (Barton and Poethig, 1993; Sinha *et al.*, 1993; Chuck *et al.*, 1996).

Rough sheath2 (*Rs2*) negatively regulates *knox* expression in maize. *rs2* loss-of-function mutants ectopically express *knox* genes and have phenotypes similar to *Knox* misexpression (Schneeberger *et al.*, 1998). Ectopic *knox* expression in *rs2* mutants is patchy and appears clonal in nature (Timmermans *et al.*, 1999). There is evidence that *Rs2* and the *Arabidopsis* orthologue, *ASYMMETRIC LEAVES1*, act as epigenetic regulators of *knox* genes, possibly by modifying chromatin structure (Phelps-Durr *et al.*, 2005).

Freeling (1992) has proposed a "maturation schedule" hypothesis to account for dominant *Knox* phenotypes. These mutations cause proximal tissues to extend into the blade, and immature cell types are often associated with regions of displaced tissue (Freeling and Hake, 1985). Freeling (1992) speculates that the ectopic tissues are the result of a retarded maturation schedule. According to this model, ectopic expression of *Knox* genes delays the maturation of cells. Affected cells are not competent to respond to signals to differentiate at the time

when the rest of the blade is differentiating. Instead, they differentiate as the more juvenile sheath tissue.

Although proximal-distal patterning is disrupted by dominant *Knox* mutations, the normal role of these genes is not to specify blade or sheath compartments, nor to demark a boundary between these regions. In wild-type maize, *knox* genes are not expressed in the leaf primordium. Rather, their normal role seems to be to define a "meristematic domain".

***Wab1-R* causes proximal-to-distal tissue displacement**

In maize, dominant *Wab1* mutations cause displacement of proximal tissues such as sheath and auricle into the leaf blade (Hay and Hake, 2004). In addition, the leaf blade is narrower than normal. This defect is apparent by P3-P5 (i.e. in leaf primordia that are third to fifth from the SAM). Although the phenotype is similar to dominant *Knox* mutations, *Wab1* mutants show no alteration in *knox* expression (Hay and Hake, 2004).

***liguleless1* and *liguleless2* delete ligule and auricle tissue**

Lg1 and *Lg2* act in a pathway that specifies ligule and auricle tissues. Loss of either gene function results in deletion of these tissues. However, leaves retain distinct regions of blade and sheath (Becraft *et al.*, 1990; Harper and Freeling, 1996). *Lg1* encodes a novel protein that localises to the nucleus (Moreno *et al.*, 1997). *Lg2* encodes a basic leucine zipper protein (Walsh *et al.*, 1997). Mosaic analysis indicates that *Lg1* has a role in signal propagation, and acts cell-autonomously to specify ligule and auricle tissues (Becraft *et al.*, 1990; Becraft and Freeling, 1991). *Lg2* acts non-cell autonomously (Walsh *et al.*, 1997). Sylvester *et al.* (1990) have analysed cell division in *lg1* mutants. They found that the localised cell divisions that normally give rise to the preligule band are absent in *lg1* leaves.

Mosaic analyses have been used to investigate the roles of *Lg1* and *Lg2* in maize leaf development. Mosaic analysis combines clonal analysis and analysis of mutant phenotypes. The technique involves the generation of organisms that are genetic mosaics for a gene of interest and a linked marker gene. Mosaic analysis has shown that *Lg1* acts cell-autonomously to specify ligule and auricle

tissues (Becraft *et al.*, 1990). When *lg1-R/-* sectors are induced in *Lg1/lg1-R* plants, the ligule and auricle are deleted within the sector and reinitiate at the marginal sector boundary. The reinitiated ligule and auricle are often displaced towards the base of the leaf (Becraft and Freeling, 1991). One interpretation is that *Lg1* is involved in the reception and/or transmission of a "make ligule and auricle" signal that emanates from the midrib towards the margins. As differentiation proceeds basipetally, the time taken for the signal to cross the *lg1-R/-* sector means that the tissue directly opposite the initiation point is no longer competent to respond to the signal. Cells in more proximal positions respond, resulting in displacement of the ligule and auricle at the outer sector border (Becraft and Freeling, 1991).

1.5.4 Adaxial-abaxial patterning

Perhaps the most compelling example of compartments in leaf development is adaxial-abaxial patterning. In dicots, the leaf primordium emerges as a radial or peg-like outgrowth and polarity genes are expressed uniformly. As the primordium emerges, adaxial and abaxial patterning genes become confined to their respective domains (Sawa *et al.*, 1999; Siegfried *et al.*, 1999; Kerstetter *et al.*, 2001; McConnell *et al.*, 2001). One theme that has emerged from mutant studies is that the juxtaposition of adaxial and abaxial compartments is required for subsequent lamina outgrowth (Waites and Hudson, 1995). It is hypothesised that signalling at the boundary between the two domains creates a lateral axis, and in some way induces growth along this axis. Complete loss of either adaxial or abaxial identity results in the formation of radialised lateral organs. Conversely, when ectopic patches of either adaxial or abaxial tissue occur next to tissue with the opposite identity, ectopic outgrowths occur. It is proposed that the adaxialising signal originates in the centre of the SAM (McConnell *et al.*, 2001). These studies are consistent with, and extend, classic surgical investigations of leaf development (Sussex, 1955; Snow, 1959).

***phantastica* and the juxtaposition model**

The juxtaposition hypothesis for lamina development was inspired by the *phantastica* (*phan*) loss-of-function phenotype in *Antirrhinum* (Waites and Hudson, 1995). *phan* mutants exhibit a range of phenotypes including radial

leaves with abaxial cell types, and leaves with outgrowths at the boundaries between adaxial and ectopic abaxial tissues. It was hypothesised that signalling between adjacent adaxial and abaxial domains induces lamina outgrowth.

The *phan* phenotype was initially characterised as a loss of adaxial identity. An alternative explanation has been offered by Tsiantis and co-workers (1999) who propose that *phan* is primarily a proximal-distal patterning defect, with the radialised leaves resulting from extension of the proximal petiole. This hypothesis will be discussed further with reference to the maize homologue *Rough sheath2 (Rs2)*. Nonetheless, the juxtaposition model has provided a key to interpreting the phenotypes of other mutants that affect adaxial-abaxial polarity.

HD-ZIPIII genes specify adaxial cell fate

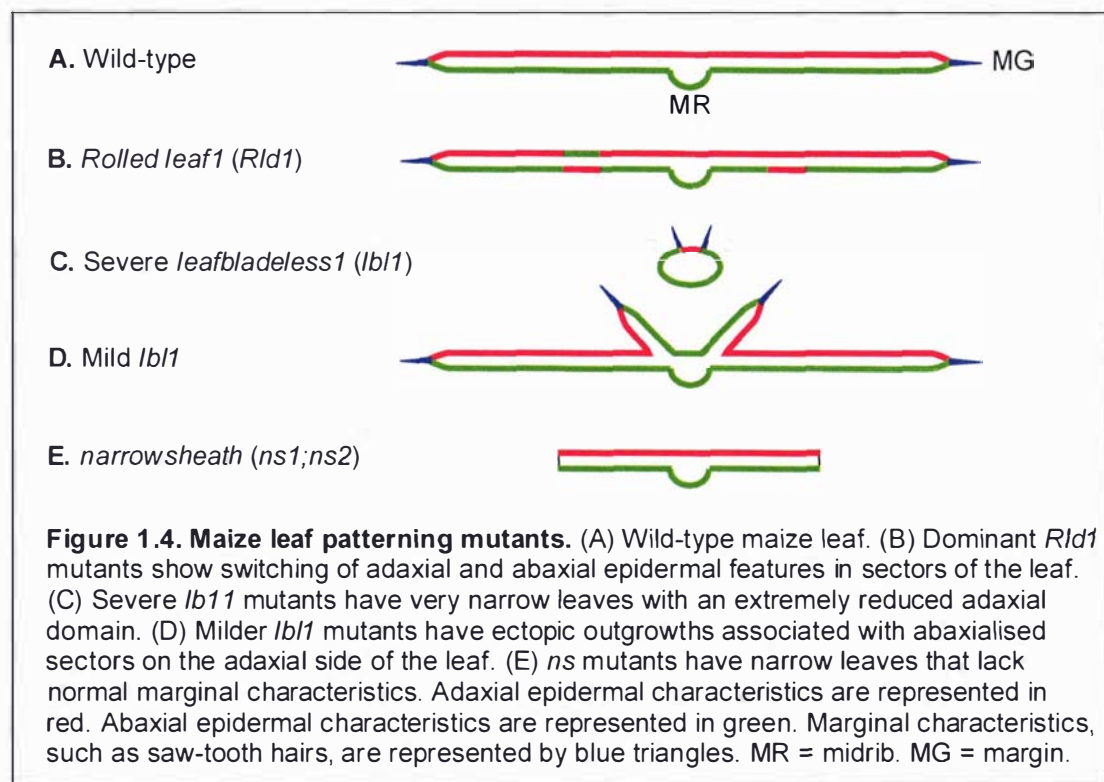
Genetic analyses indicate that the *Class III homeodomain-leucine zipper (HD-ZIPIII)* genes specify adaxial identity in lateral organs in dicot species and in maize. HD-ZIPIII proteins have a homeodomain-leucine zipper domain and a START domain similar to mammalian sterol/lipid-binding proteins (Sessa *et al.*, 1998; Pontig and Aravind, 1999; McConnell *et al.*, 2001; Juarez *et al.*, 2004a).

Dominant mutations in the *Arabidopsis HD-ZIPIII* genes, *PHABULOSA (PHB)*, *PHAVOLUTA (PHV)* and *REVOLUTA (REV)*, result in their ectopic expression and adaxialisation of lateral organs (McConnell and Barton, 1998; McConnell *et al.*, 2001). *REV* mutants have an additional phenotype – the development of radial, adaxialised vascular bundles in the stem (Emery *et al.*, 2003). Triple loss-of-function mutants have abaxialised cotyledons, and the SAM fails to form. Vascular bundles in the cotyledons are radialised, with phloem surrounding xylem (Emery *et al.*, 2003).

Expression studies show that *PHB*, *PHV* and *REV* are initially expressed throughout leaf anlagen, and become localised to the adaxial domain by the P2 stage of leaf development. They are also expressed in the central part of the embryo from the globular stage, and in xylem of developing vascular bundles (McConnell *et al.*, 2001; Emery *et al.*, 2003). In dominant mutants, *HD-ZIPIII*

genes are expressed in both the adaxial and abaxial domains and are expressed at higher levels than in wild-type (McConnell and Barton, 1998; McConnell *et al.*, 2001). The expression patterns, along with the mutant phenotypes suggest multiple roles in patterning the embryo, lateral organs and vasculature (McConnell *et al.*, 2001; Emery *et al.*, 2003).

Dominant mutations in a maize *HD-ZIPIII* gene, *rolled leaf1* (*rld1*), also affect adaxial-abaxial polarity. *rld1* is the maize homologue of *REV* (Juarez *et al.*, 2004b). Dominant *Rld1* mutants show partial to complete switching of adaxial and abaxial epidermal features in sectors of the leaf (Figure 1.4 B) (Nelson *et al.*, 2002). These switches involve adaxialisation of abaxial regions, such as ligule flaps on the abaxial surface, or a complete switching of epidermal features.



Like the *Arabidopsis HD-ZIPIII* genes, *rld1* and a maize *PHB* homologue are normally expressed at the tip of the SAM and on the adaxial side of incipient and young leaf primordia (Juarez *et al.*, 2004b). Expression persists in the vasculature and at the margins. The dominant *Rld1-O* allele is misexpressed on the abaxial side of leaf primordia, although expression in the meristem is not altered.

Regulation of *HD-ZIPIII* genes by microRNAs

McConnell and co-workers (2001) proposed that *PHAB* acts as a receptor for an adaxialising signal that originates in the centre of the SAM. Dominant alleles have mutations in the START domain and initially it was thought these mutations caused the protein to be constitutively active in the absence of ligand binding (McConnell *et al.*, 2001). However, subsequent investigations indicate that this domain overlaps with a miRNA-complementary region and that ectopic expression is due to loss of regulation by the miRNAs miR165 and miR166 (Rhoades *et al.*, 2002; Emery *et al.*, 2003). Similarly, dominant *Rld1* alleles in maize have nucleotide changes in the miRNA-complementary region, indicating that regulation by miRNA165/166 is a conserved mechanism (Juarez *et al.*, 2004b). In maize, miRNA166 is expressed immediately below the incipient leaf primordium. Subsequently, the expression domain expands to include the abaxial side of the primordium (Juarez *et al.*, 2004b).

These findings do not preclude a role for a ligand that activates HD-ZIPIII proteins in adaxial regions of lateral organs. Regulation by miRNAs and a ligand produced in the SAM could act together to specify and refine the domain of active HD-ZIPIII protein (Emery *et al.*, 2003; Juarez *et al.*, 2004b). Juarez *et al.* (2004b) suggest that *rld1* may act to integrate positional information from the SAM and from below the leaf primordium.

***KANADI* genes specify abaxial cell fate**

Members of the *Arabidopsis KANADI* (*KAN*) gene family are expressed abaxially in lateral organs, and analysis of loss-of-function and overexpression phenotypes indicate that they are required for abaxial cell identity. *KAN* genes belong to the GARP family of transcription factors (Kerstetter *et al.*, 2001).

The *KAN* family has four members in *Arabidopsis* (Kerstetter *et al.*, 2001; Eshed *et al.*, 2004). Due to genetic redundancy, loss of several genes is required to generate the most severe phenotypes (Eshed *et al.*, 1999; Eshed *et al.*, 2001; Kerstetter *et al.*, 2001). *kan1* and *kan1;kan2* mutant floral organs are adaxialised, and leaves are narrow with ectopic outgrowths on their abaxial

surface associated with patches of adaxial tissue (Eshed *et al.*, 2001; Kerstetter *et al.*, 2001). When *kan1*, 2 and 3 functions are lost, outgrowths are reduced and leaves are nearly radial. Vascular bundles in the stem are often radialised with xylem surrounding phloem (Emery *et al.*, 2003; Eshed *et al.*, 2004). Seedlings that overexpress *KAN* genes often lack a SAM and vascular tissue, and have a single abaxialised cotyledon. If leaves are produced, they are narrow or radial (Kerstetter *et al.*, 2001; Emery *et al.*, 2003).

KAN1, 2 and 3 are expressed in all lateral organs, while *KAN4* expression is limited to the ovules (Kerstetter *et al.*, 2001; Eshed *et al.*, 2004). *KAN* genes are initially expressed throughout the leaf anlagen, and become confined to the abaxial domain after emergence of the primordium (Kerstetter *et al.*, 2001). *KAN1*, 2 and 3 are expressed in developing vasculature and localise to the phloem (Emery *et al.*, 2003). *KANs* are expressed throughout the early globular stage embryo, before becoming confined to the peripheral region by the late globular stage (Kerstetter *et al.*, 2001).

Less is known about the *KAN* family in maize. There are at least 11 *KAN* family members in maize (pers. comm., Hector Candela and Sarah Hake). Therefore, there is likely to be a high level of functional redundancy. *ZmKAN2*, the maize homologue of *Arabidopsis KAN2*, is expressed on the abaxial side of young leaf primordia in a pattern complementary to *rd1*. It is also expressed in the peripheral zone of the SAM and in the stem at the base of the P1 primordium (Henderson *et al.*, 2006). The expression pattern in leaf primordia is similar to the *KAN* expression pattern in *Arabidopsis*. However, *Arabidopsis KANs* are not expressed in the SAM or the stem. Therefore, there may be functional differences in maize and *Arabidopsis*. Henderson *et al.* (2006) state that while the abaxial expression pattern is consistent with a role in promoting abaxial identity as in *Arabidopsis*, this is speculative as no mutant phenotypes have yet been analysed.

Recent data indicate that the *KAN* genes may act in a parallel pathway with the auxin response factors *ETTIN (ETT)* and *Auxin Response Factor4 (ARF4)* (Pekker *et al.*, 2005). These genes are expressed on the abaxial side of leaf primordia and in *kan1;kan2* outgrowths. *ett;arf4* loss-of-function mutants have

adaxialised leaves, similar to *kan* loss of function phenotypes. The data indicate that *ETT* and *ARF4* do not act downstream of *KAN*, but in a parallel pathway. It is proposed that these genes are expressed in the abaxial domain in response to auxin gradients in the primordium. Recent research has begun to elucidate many other interactions between plant hormones and genes that regulate organ development (Kepinski, 2006).

Interactions between *HD-ZIPIII* and *KANADI* genes

Genetic interactions indicate that *HD-ZIPIII* and *KAN* genes act antagonistically to establish adaxial and abaxial domains. *REV* gain-of-function alleles, and loss of *KAN* activity have similar phenotypes, characterised by adaxialised lateral organs and altered vascular patterning. Conversely, *phb;phv;rev* loss-of-function mutant embryos lack a SAM and, in severe cases, have a single radial, abaxialised cotyledon (Emery *et al.*, 2003). Overexpression of *KAN* causes a similar phenotype (Eshed *et al.*, 2001; Kerstetter *et al.*, 2001). *HD-ZIPIII* and *KAN* genes normally have complementary expression patterns. Loss of *KAN* activity results in expansion of the *HD-ZIPIII* expression domain (Eshed *et al.*, 2001). It is not clear whether the *KAN* genes specify abaxial cell types directly, or if their primary role is to repress *HD-ZIPIII* expression in abaxial domains (Emery *et al.*, 2003). Based on the complementary expression patterns and mutant phenotypes of *KAN* and *HD-ZIPIII* genes, it has been proposed that a common mechanism patterns the central-peripheral axis of the embryo and the adaxial-abaxial axis of lateral organs and vasculature (McConnell *et al.*, 2001; Emery *et al.*, 2003).

***leafbladeless1* is required for founder cell recruitment**

Analysis of recessive *leafbladeless1* (*lbl1*) mutants in maize suggests that adaxial-abaxial polarity is established within the SAM, and is required for the lateral propagation of founder cell recruitment (Timmermans *et al.*, 1998). Severe *lbl1* mutants have extremely narrow, abaxialised leaves. The needle-shaped leaves usually have a narrow ligular fringe and two rows of marginal hairs in close proximity, suggesting a severely reduced adaxial domain (Figure 1.4 C). Immunolocalisation of KN1 protein shows the region of KN1 downregulation is significantly reduced in severe *lbl1* mutants, implying that

founder cell recruitment is defective. A less severe phenotype involves the formation of ectopic laminae on the adaxial surface of the leaf blade (Figure 1.4 D). These ectopic outgrowths form at the boundary of adaxial tissue and abaxialised mutant sectors. The phenotypes suggest that the juxtaposition of adaxial and abaxial cell types is required for the lateral recruitment of founder cells within the SAM, and for subsequent lateral growth of the leaf blade.

The *Rld1* and *lbl1* phenotypes are mutually suppressive (Juarez *et al.*, 2004a). *rld1* expression is reduced in *lbl1* mutants, indicating that *lbl1* acts upstream of *rld1* (Juarez *et al.*, 2004a). It has emerged recently that *lbl1* acts in a pathway that produces a regulatory RNA which in turn regulates MiR166. Higher levels of MiR166 in *lbl1* mutants would account for the lower levels of *rld1* expression in these mutants (per. comm. Marja Timmermans).

YABBY genes promote lamina outgrowth

Members of the *YABBY* (*YAB*) gene family are associated with abaxial cell fate in *Arabidopsis*. Multiple lines of evidence support a role for the *YABs* in lamina outgrowth in maize and in dicot species.

The *Arabidopsis* *YABBY* family comprises 6 members (Bowman and Smyth, 1999; Eshed *et al.*, 1999; Sawa *et al.*, 1999; Siegfried *et al.*, 1999). *YAB* proteins have a zinc finger-like domain towards the amino terminus and a helix-loop-helix domain, known as the *YABBY* domain, near the C-terminus (Bowman and Smyth, 1999). Due to genetic redundancy, loss of several genes is required to see a loss-of-function phenotype. Overexpression causes the development of abaxialised lateral organs and meristem arrest, whereas loss of *YAB* function results in adaxialised organs (Alvarez and Smyth, 1999; Bowman and Smyth, 1999; Eshed *et al.*, 1999; Sawa *et al.*, 1999; Siegfried *et al.*, 1999; Villanueva *et al.*, 1999). Loss of *YAB* function is associated with misexpression of *KNOX* genes and the formation of ectopic meristems on the adaxial side of leaves and cotyledons, suggesting an additional role in repressing meristem initiation (Kumaran *et al.*, 2002).

Genetic and molecular data indicate that *YAB* function is downstream of *KAN* in *Arabidopsis*. *YAB* genes are expressed in a similar pattern to the *KAN*s. They are initially expressed throughout lateral organ anlagen, and become confined to the abaxial side of the primordium after emergence (Siegfried *et al.*, 1999). *FILAMENTOUS FLOWER (FIL)* is expressed throughout leaf primordia that ectopically express *KAN2*, although expression is transient (Eshed *et al.*, 2004). *YAB* activity is both necessary and sufficient for the development of abaxial cell types in a *kan* loss-of-function background (Eshed *et al.*, 2001; Eshed *et al.*, 2004).

GRAMINIFOLIA (GRAM) is the *Antirrhinum* orthologue of *FIL* (Golz *et al.*, 2004). *gram* leaves and petals are partially adaxialised, particularly at the margins, and are narrower than normal. In many cases, the corolla tube is unfused. *GRAM* appears to promote abaxial fate by excluding adaxial factors such as *AmPHB*, a function performed by *KAN* genes in *Arabidopsis*. In addition, there is evidence that *GRAM* promotes adaxial cell identity non-autonomously. Golz *et al.* (2004) propose that the primary function of *GRAM* may be to refine and maintain the boundary between adaxial and abaxial domains, and that this boundary is required for lateral growth. Unlike many other leaf polarity mutants, no outgrowths are seen at ectopic adaxial-abaxial boundaries in *gram* leaves.

The maize *Zea mays yabby (Zyb)* genes are expressed on the adaxial side of incipient and young leaf primordia, opposite to the pattern seen in *Arabidopsis* (Juarez *et al.*, 2004a). In older leaf primordia, expression persists at the margins and in the central layer. Expression of *Zyb9*, but not *Zyb14*, persists in the vasculature. *YAB* expression is increased in *Rld1-O*, suggesting that *YAB* genes are positively regulated by *rld1* in maize (Juarez *et al.*, 2004a).

Various lines of evidence suggest that the *YAB*s are required for lamina outgrowth. Loss of *YAB* function in *Arabidopsis* and *Antirrhinum* results in reduced lamina outgrowth, and ectopic outgrowths in *kan* mutants are dependant on *YAB* function (Siegfried *et al.*, 1999; Eshed *et al.*, 2004; Golz *et al.*, 2004). In *Arabidopsis*, *FIL* is expressed in *kan* outgrowths (Eshed *et al.*, 2004). It has been suggested that boundaries between *YAB*-expressing and

non-expressing cells promote outgrowth rather than absolute levels of *YAB* activity (Siegfried *et al.*, 1999; Eshed *et al.*, 2004; Golz *et al.*, 2004). This function appears to be conserved in maize leaf development (Juarez *et al.*, 2004a). In maize, *Zyb* expression is associated with abaxial outgrowths in *Rld1-O* leaves and adaxial outgrowths in *lbl1*. The *Rld1-O* outgrowths occur at the boundaries of *Zyb*-expressing and non-expressing cells of the central layer. It is suggested that polarised *YAB* expression may mediate founder cell recruitment in the maize SAM prior to emergence (Juarez *et al.*, 2004a).

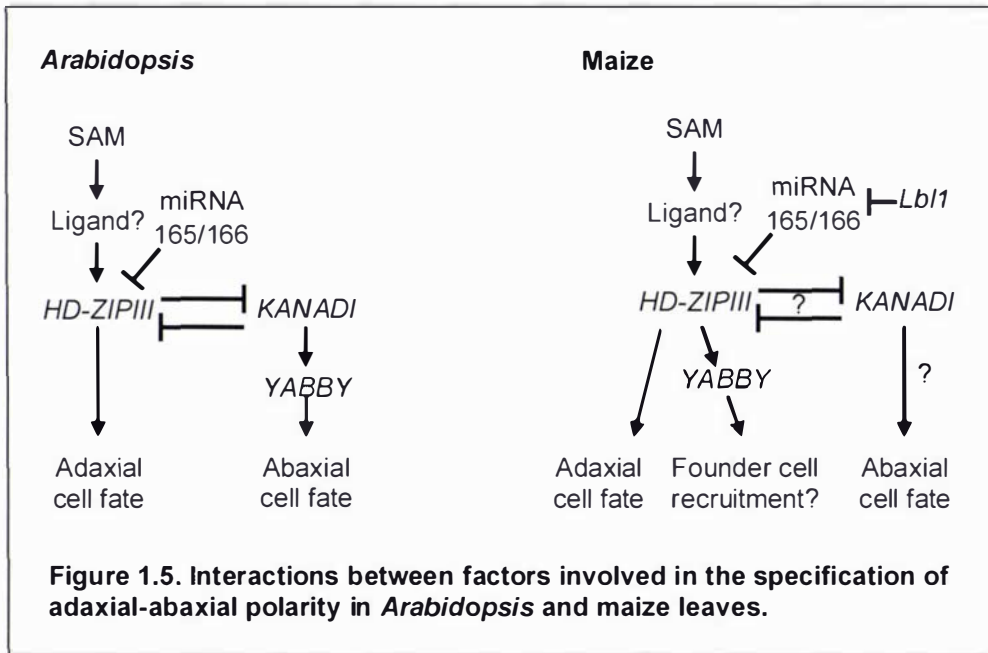
Genetic interactions that regulate adaxial-abaxial polarity

Figure 1.5 summarises interactions between leaf polarity genes discussed in this section. In *Arabidopsis*, *KAN* and *HD-ZIPIII* genes interact antagonistically to specify adaxial and abaxial domains in lateral organs. The expression pattern of *HD-ZIPIII* genes and a maize *KAN2* homologue suggests a similar mechanism exists in maize, but this has not been proven.

Based on surgical experiments, Sussex (1955) proposed that communication between the SAM and lateral organ primordia is required for adaxial cell identity. The *HD-ZIPIII* proteins are candidate receptors for such a signal, although a ligand has not been identified. In both maize and *Arabidopsis*, *HD-ZIPIII* genes are regulated by miRNAs. It has been suggested that the maize *HD-ZIPIII* gene *rld1* could integrate a signal from the SAM and miRNA signalling from below the leaf primordium (Juarez *et al.*, 2004a). Recent data indicate that miRNA166 in maize is regulated by a second miRNA, and that *lbl1* is involved in this pathway.

The *HD-ZIPIII* genes are associated with adaxial cell fate in both *Arabidopsis* and maize. A role for the maize *KAN* genes in promoting abaxial cell fate is speculative at this stage. The *Arabidopsis* *KAN* genes are associated with abaxial identity, but appear to act by promoting *YAB* expression, rather than specifying abaxial cell fate directly. In *Arabidopsis*, the *YABs* are expressed abaxially, downstream of the *KANs*, and specify abaxial cell identity. In contrast, the maize *YAB* genes are expressed adaxially and are downstream of *rld1*

(Juarez *et al.*, 2004a). In both maize and *Arabidopsis*, the YABs are implicated in lateral growth, and may promote founder cell recruitment in maize.



1.5.5 Medial-lateral patterning

***Narrow sheath* function is required for propagation of founder cell recruitment**

Analysis of *narrow sheath* (*ns*) mutants provides evidence for the existence of at least two lateral domains in the maize leaf – a marginal domain defined by *ns*, and a central domain. *NS1* and *NS2* are duplicate genes. Plants that are homozygous for both *ns1* and *ns2* have narrow leaves that lack the marginal characteristics of normal leaves (Figure 1.4 E). Cell lineage analysis indicates that a lateral domain is deleted. Albino sectors that in wild-type leaves would continue into the leaf margins are confined to the culm in *ns* plants (Scanlon and Freeling, 1997). Immunolocalisation of KN1 within the SAM has confirmed that KN1 is not downregulated in the domain that would normally give rise to the leaf margins (Scanlon *et al.*, 1996). In normal development, founder cell recruitment begins at the future midrib, and is propagated laterally to the marginal domains (Jackson *et al.*, 1994). A mosaic analysis has shown that loss of *NS* function at focal points on either side of the SAM results in the development of margin-less leaves (Scanlon, 2000). When *NS* is lost in other regions, leaves develop normally. *In situ* hybridisation has confirmed that *NS* is

expressed in two lateral foci in leaf founder cells, and also at the margin tips of leaf primordia (Nardmann *et al.*, 2004). These results suggest that NS function in lateral foci is required for the propagation of founder cell recruitment to the marginal domains. The central domain is initialised by another, as yet unknown, mechanism.

1.5.6 Summary of axial patterning

Analysis of leaf patterning mutants demonstrates that disruption of one axis affects specification of the other axes, indicating that the major axes of growth are not established independently. For example, disrupting adaxial-abaxial polarity affects establishment of the medial-lateral axis. The phenotypes of mutants that fail to establish either adaxial or abaxial cell identity support the hypothesis that the juxtaposition of these two compartments establishes the medial-lateral axis. There is evidence to support this hypothesis in both dicot and maize leaf development. However, there are also fundamental differences in leaf morphogenesis. In dicots, adaxial and abaxial domains are established after founder cell recruitment. In maize, adaxial and abaxial domains and the medial-lateral axis are established in the SAM, and are required for the lateral propagation of founder cell recruitment.

Members of the *KAN*, *YAB* and *HD-ZIPIII* families are found in monocots and dicots (Floyd and Bowman, 2007). However, their functions and interactions have diverged somewhat. The *Arabidopsis* *YABs* are expressed abaxially and are downstream of *KAN*, whereas the maize *YABs* are expressed adaxially and are regulated by *HD-ZIPIII*s. It has been suggested that the specification of abaxial identity that is fulfilled by *YAB* genes in *Arabidopsis* may be performed by *KAN* genes in maize (Juarez *et al.*, 2004a). A common function of *YAB* genes in *Arabidopsis*, *Antirrhinum* and maize appears to be promotion of lateral growth. In *Antirrhinum*, *YAB* genes may inhibit members of the *HD-ZIPIII* family, a role performed by the *KAN* genes in *Arabidopsis*. Thus, it is important not to assume orthologous functions without functional data.

1.6 Establishment and maintenance of developmental domains

During development, groups of cells are partitioned for particular fates. For example, cells that will be incorporated into a lateral organ must be distinguished from cells that will remain meristematic. Cells that will form the sheath or petiole must be distinguished from those that will form the leaf blade. However, to ensure coordinated development there must be continued communication between groups of cells. There is a network of transcriptional activators and repressors that control gene expression. The previous section focused on the importance of domains of gene expression in leaf patterning, and the consequences of disrupting this positional information. In addition to transcriptional regulation, there are post-transcriptional mechanisms that act to establish and maintain developmental domains. Two such mechanisms are the post-transcriptional regulation of gene expression by miRNAs, and the regulation of protein movement between cells.

1.6.1 MicroRNAs and gene regulation

Recent work has revealed the role of miRNAs as negative regulators of gene expression. miRNAs are short RNAs transcribed from non-protein coding genes that act as specificity determinants within complexes that target mRNAs for degradation (Carrington and Ambros, 2003). Information has come from studies of mutations that disrupt miRNA-mediated regulation, such as dominant *HD-ZIPIII* mutants, and from mutations to genes encoding proteins that form part of the miRNA processing machinery. MiRNA targets include families of transcription factors with roles in development in both plants and animals (Carrington and Ambros, 2003).

In plants, disruption of miRNA-mediated gene silencing produces a variety of defects, including leaf patterning defects that resemble dominant *HD-ZIPIII* mutations (Foster *et al.*, 2002). *ARGONAUTE1* (*AGO1*) functions in the miRNA pathway, and *ago1* mutants have leaf polarity defects (Carrington and Ambros, 2003; Kidner and Martienssen, 2004). In *ago1* mutants, *PHB* is expressed throughout the leaf primordia (Kidner and Martienssen, 2004).

The *HD-ZIPIII* genes *PHB*, *PHV* and *REV* contain a conserved complementary site for miRNA165/166 which can direct their cleavage *in vitro* (Tang *et al.*, 2003). Complementary sites overlap the sites of mutations in dominant alleles that are ectopically expressed. Experiments show that changing the *REV* mRNA sequence without changing the protein results in a gain-of-function phenotype. It was concluded that this phenotype results from interference with miRNA binding (Emery *et al.*, 2003). There is evidence that miRNAs also regulate *HD-ZIPIII* genes in differentiated cells by mediating chromatin methylation (Bao *et al.*, 2004).

1.6.2 Protein trafficking

Cells must communicate with their neighbours to ensure coordinated cell division and differentiation, necessitating the exchange of signalling molecules. The observation that cells differentiate according to position rather than lineage implies that positional information is communicated between neighbouring cells. One method is the movement of proteins from cell to cell through the plasmodesmata. Dynamic regulation of the plasmodesmata occurs during development. Evidence for symplastic domains included observations of the cell-to-cell trafficking of dyes, viral movement proteins and green fluorescent protein (GFP) (Gisel *et al.*, 1999; Crawford and Zambryski, 2000). It was found that proteins could move freely between some cells, but were excluded from others. Recent studies indicate that the passage of specific proteins is under developmental control (Kim *et al.*, 2003).

Mosaic analysis of a number of developmentally important genes indicates that they may act in a non cell-autonomous manner. A mosaic analysis of *Kn1* found that *Kn1* expression in the mesophyll was sufficient to condition the mutant phenotype in all cell layers, whereas expression in the L1 alone did not condition the mutant phenotype (Hake and Freeling, 1986). This result implied that either the gene product itself, or some downstream mediator(s), are able to move cell-to-cell. *In situ* hybridisation and immunolocalisation confirm that while *kn1* mRNA accumulates in the L2 and L3, but not the L1, KN1 protein accumulates in all cell layers (Smith *et al.*, 1992; Jackson *et al.*, 1994). Similarly, expression of the *Arabidopsis* floral meristem identity gene *LEAFY*

(*LFY*) in just the L1 of *lfy* mutants can rescue the *lfy* mutant phenotype in all cell layers. While *LFY* mRNA accumulated only in the L1, *LFY* protein was seen in all cell layers. This finding, as well as confirmation that transported *LFY* can activate downstream genes, indicates that the protein retains its biological activity (Sessions *et al.*, 2000).

Exclusion of *KN1* from incipient leaf primordia implies that protein movement within the SAM is developmentally regulated. Similarly, there is a sharp boundary of *LFY* protein between floral primordia and the inflorescence meristem, suggesting that protein movement across this boundary is blocked (Sessions *et al.*, 2000). The restriction of protein movement may function to partition groups of cells with different fates. Conversely, protein trafficking between cells with a common fate could ensure that all cells within a developmental field are synchronised to a given programme. For example, this could ensure that floral meristems undergo complete conversion to floral identity, and do not produce chimeric organs (Sessions *et al.*, 2000). *KN1* trafficking within the SAM may ensure that all cells retain their meristematic identity (Kim *et al.*, 2003).

The initiation of organs by the SAM is a dynamic process. It follows that the regulation of developmental domains must also be dynamic. Experiments using *KNOX* proteins fused to GFP (*GFP~KN1*) or viral movement proteins demonstrate that trafficking of *KNOX* proteins is developmentally regulated in *Arabidopsis* (Kim *et al.*, 2003). *GFP~KN1* could traffic from the inner layers of the leaf to the epidermis (L1), but not in the opposite direction, but could traffic out of the L1 in the SAM. Unlike the *GFP~KN1* fusion, *GFP~movement* protein could move out of the leaf epidermis, indicating that regulation was protein-specific. The mechanism is not yet known, but could be mediated by receptors within the plasmodesmata that recognise specific motifs, by post-translational protein modifications, or by a combination of mechanisms.

1.7 Homologies between lateral organs

1.7.1 Plants are comprised of repeated structural units

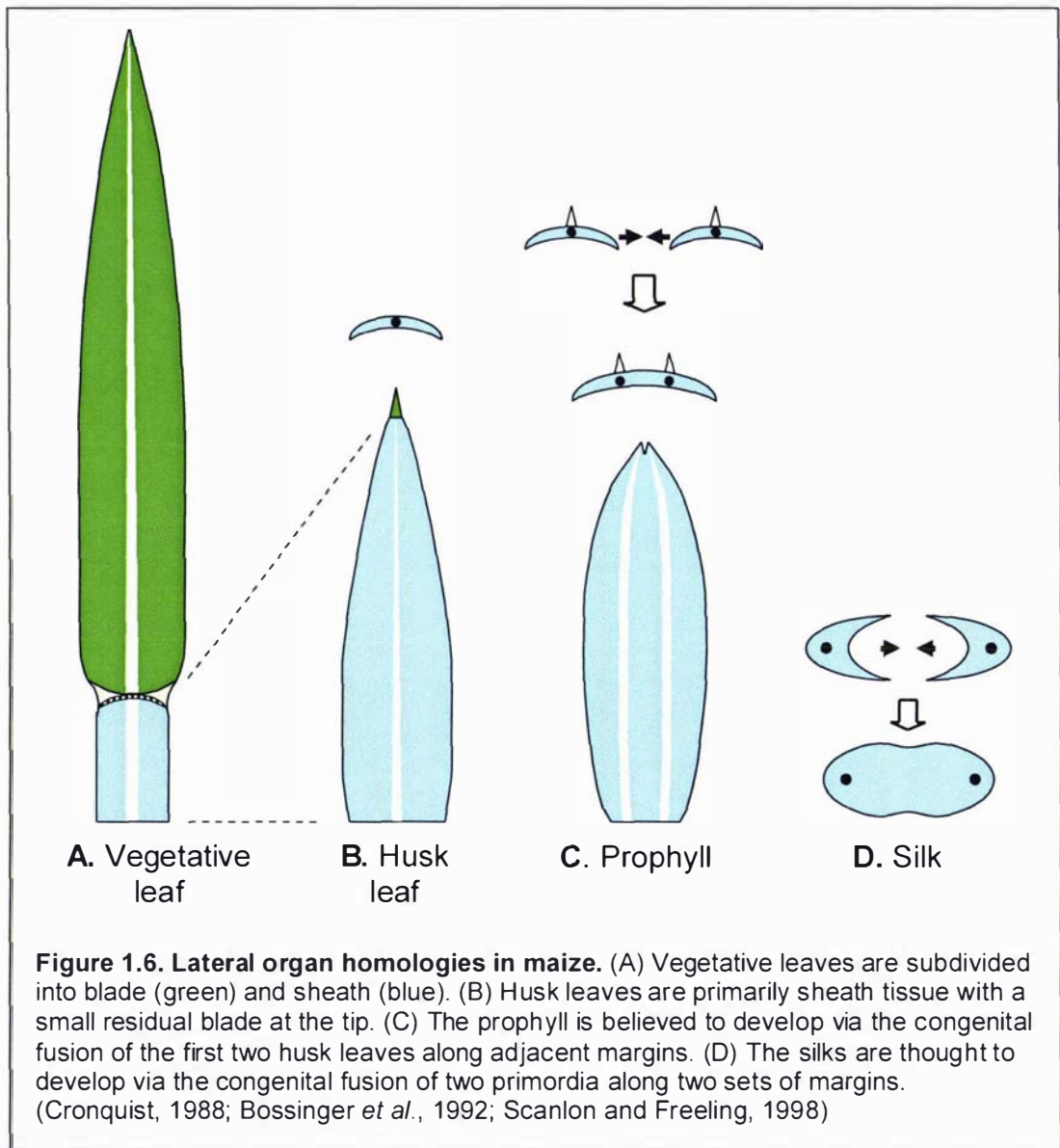
Plants have a metameric organisation, with the phytomer considered to be the basic structural unit. Each phytomer consists of a node, internode and leaf (Weatherwax, 1923; Sharman, 1942). In grasses, the leaves are subdivided into blade and sheath. Morphological diversity is achieved by the differential elaboration or repression of developmental compartments (Galinat, 1959). This is apparent in comparisons of different species, and when comparing vegetative and floral organs of the same plant. Analysis of developmental mutants reveals that leaves and homologous organs are patterned by common genetic programmes, as well as organ-specific programmes (Bossinger *et al.*, 1992).

According to the leaf zonation hypothesis, leaves are comprised of two morphological compartments along the proximal-distal axis – the upper and lower leaf zones (Figure 1.7) (Troll, 1955; Kaplan, 1973). Dicot leaves are derived mainly from the upper leaf zone, whereas, maize leaves are almost entirely lower leaf zone. Maize vegetative and husk leaves differ in the relative contributions of the blade and sheath (Figure 1.6 A, B). The blade is the dominant part in vegetative leaves, whereas the husk leaves are mainly sheath tissue.

One conserved element of phytomer organisation in the grasses is the production of fused organs by newly initiated meristems. Bossinger *et al.* (1992) termed the first phytomer produced by a newly initiated meristem a "type 2 phytomer". Subsequent phytomers each have a single leaf primordium and are termed "type 1 phytomers". The type 2 phytomer is typified by the prophyll which subtends the female inflorescence (the ear). The prophyll is believed to develop via the congenital fusion of the first two husk leaves along adjacent margins (Figure 1.6 C) (Bossinger *et al.*, 1992; Scanlon and Freeling, 1998). Other organs that may be classed as type 2 phytomers are the coleoptile, palea, lodicules and stamens (Bossinger *et al.*, 1992). The glumes are the first organs to be initiated by the spikelet axis. However, in maize and barley they are not fused organs. Bossinger *et al.* suggest that the two glumes may be

considered together to correspond to a type two phytomer, a suggestion that is supported by the finding that in some species the two glumes are fused.

The silks (gynoecia) are thought to represent a different form of phytomer fusion. According to one model, the silks develop via the congenital fusion of two carpels along two sets of margins (Cronquist, 1988; Scanlon and Freeling, 1998) (Figure 1.6 D).



1.7.2 Mutant phenotypes provide a tool for detecting organ homologies within a species

Mutant phenotypes provide a useful tool for investigating homologies between lateral organs. For example, analysis of the *ns* phenotype provides support for the hypothesis that the maize prophyll is derived from two fused leaves (Scanlon and Freeling, 1998). The prophyll is the first organ to be produced by the newly initiated lateral meristem. It has two midribs (keels) separated by membranous tissue. In the *ns* mutant, the distance between the two keels is reduced, and the membranous tissue between the keels is replaced by thicker tissue. In addition, the outer margins are replaced by thick, blunt margins. Scanlon and Freeling (1998) propose that this is due to the deletion of the margins of each of the leaves that comprise the prophyll. The *ns* phenotype is consistent with the hypothesis that the prophyll is derived from two leaves fused along their inner margins, with each keel representing the midrib of a single leaf. In contrast, the palea (another organ with two midribs) is only affected at the margins while the distance between the midribs is not affected. Therefore, the *ns* phenotype provides no evidence that the palea is formed by phytomer fusion. The fused organ theory implies that the prophyll is derived from two founder cell populations. One way to test this would be to observe KNOX downregulation in lateral meristems during the earliest stages of prophyll initiation. Downregulation of KNOX proteins in two discrete spots would support the two phytomer theory.

1.7.3 Mutations to orthologous genes in diverse species

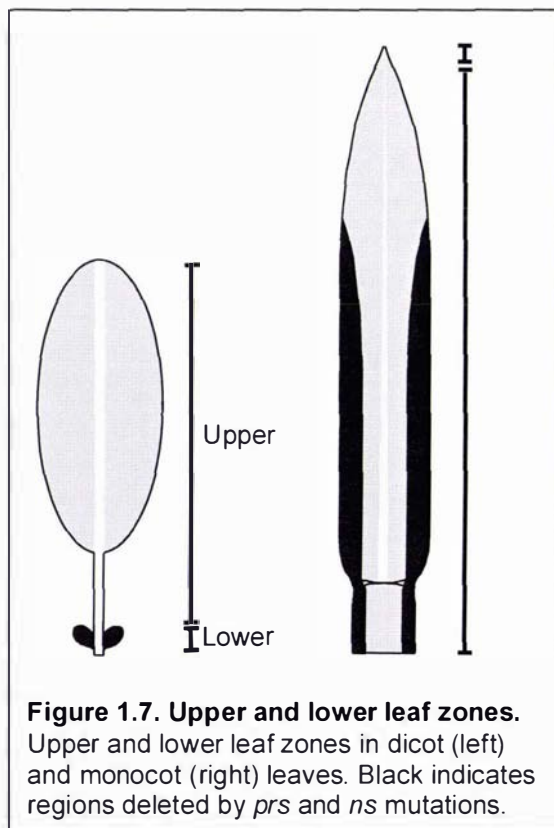
rough sheath2* and *phantastica

The homologous genes *PHAN* in *Antirrhinum*, and *Rs2* in maize negatively regulate *Knox* expression in lateral organ primordia and have loss-of-function phenotypes that are similar to overexpression of *Knox* genes (Waites and Hudson, 1995; Schneeberger *et al.*, 1998). Loss of *Knox* regulation in *rs2* mutants causes proximal-to-distal tissue displacement (Schneeberger *et al.*, 1998). Loss of function of *PHAN*, the homologous gene in *Antirrhinum*, causes upper leaves and floral organs to develop as radial, abaxialised structures (Waites and Hudson, 1995). This phenotype was originally interpreted as a defect in adaxial-abaxial patterning. However, in light of homology between *Rs2*

and *PHAN*, the *phan* phenotype has been interpreted by some authors as primarily a defect in proximal-distal patterning ("petiolization" of the leaf) rather than a defect in establishing adaxial-abaxial polarity (Tsiantis *et al.*, 1999). In this interpretation, radialised *phan* leaves result from extension of the largely unifacial petiole region, equivalent to the extension of sheath tissue seen in *rs2* mutants. The fact that *PHAN* is not restricted to the adaxial domain, but is transcribed throughout the leaf primordium, is consistent with this model (Waites *et al.*, 1998). This interpretation suggests that *PHAN* is the functional orthologue of *Rs2*.

narrow sheath and pressed flower

The leaf zonation hypothesis proposes that diverse leaf morphologies have evolved by the differential elaboration of upper and lower leaf zones (Troll, 1955; Kaplan, 1973). According to this model, bifacial monocot leaves such as maize are derived almost entirely from the lower leaf zone, whereas dicot



leaves are derived mainly from the upper leaf zone (Figure 1.7). In maize, the lower leaf zone is highly elaborated, comprising the sheath and most of the blade, whereas the upper leaf zone is represented by only a small unifacial tip. In *Arabidopsis*, the lower leaf zone consists of the leaf base and stipules while the rest of the leaf is upper leaf zone. A comparison of the loss-of-function phenotypes of the homologous genes *ns* in maize, and *pressed flower (prs)* in *Arabidopsis* support this model (Nardmann *et al.*, 2004).

NS1, *NS2* and *PRS* encode *WUSCHEL*-like homeobox genes (Matsumoto and Okada, 2001; Nardmann *et al.*, 2004). *NS1* and *NS2* are expressed at two foci in the SAM, where they are required for recruitment of leaf founder cells in a lateral domain of the SAM. It is proposed that *NS* function is confined to the

lower leaf zone. Sequence identity, expression patterns, and mutant phenotypes suggest that *ns* and *PRS* are functional orthologues (Matsumoto and Okada, 2001; Nardmann *et al.*, 2004). *ns* mutant leaves lack a marginal domain that encompasses most of the sheath and the lower leaf blade, whereas the leaf phenotype in *Arabidopsis* is restricted to deletion of the stipules at the base of the leaf (Figure 1.7) (Scanlon, 2000; Nardmann *et al.*, 2004). It is suggested that the different phenotypes reflect differences in leaf morphogenesis in maize and *Arabidopsis*, specifically the different contributions of the upper and lower leaf zones, and the portion of the SAM that contributes founder cells to the leaf primordium (Scanlon, 2000). In maize, the lower leaf zone is highly elaborated and *ns* affects a large portion of the leaf. In contrast, the lower leaf zone is much reduced in dicot leaves and *prs* only affects the leaf base and stipules. The maize leaf founder cell population encompasses the entire circumference of the SAM. Therefore, the failure to initialise cells in a lateral portion of the SAM would be expected to delete a significant portion of the leaf. In contrast, *Arabidopsis* leaf founder cells occupy only a fraction of the circumference of the SAM and, as predicted, only a small portion of the leaf is deleted.

1.8 Genome duplication and subfunctionalisation

Polyploidy (whole genome duplication) is believed to have played an important role in plant evolution, particularly of flowering plants (Blanc and Wolfe, 2004; de Bodt *et al.*, 2005; Duarte *et al.*, 2006). There is evidence that maize is the descendant of an allotetraploid event that occurred around 4.8 million years ago (Gaut and Doebley, 1997; Swigonova *et al.*, 2004). High levels of genetic redundancy are seen in maize as there are duplicate copies of most genes. It has been proposed that genome duplication provides opportunities for subfunctionalisation and neofunctionalisation (Lynch and Conery, 2000). A duplicated gene can have three possible fates – nonfunctionalisation (one copy becomes nonfunctional), neofunctionalisation (gain of a novel function) or subfunctionalisation (partitioning of the ancestral expression pattern between the two copies). Duplication events, followed by neofunctionalisation or subfunctionalisation, are believed to have contributed substantially to the evolution of morphological complexity (de Bodt *et al.*, 2005).

Numerous examples of subfunctionalisation are evident in the families of transcription factors that regulate plant development. One example is the role of *KAN* genes in *Arabidopsis* ovule development (McAbee *et al.*, 2006).

ABERRANT TESTA SHAPE (*ATS*, also known as *KAN4*) is expressed in the abaxial layer of the inner integument and is required for normal development of the inner integument. *KAN1* and *KAN2* act redundantly to provide a homologous function in the outer integument. The expression pattern parallels the expression of *KAN* genes in leaves. Thus, *KAN* family members have become specialised for very specific roles in ovule development.

1.9 Maize inbred lines

Maize is genetically very diverse, with a genome complexity comparable to that of humans (Tenaillon *et al.*, 2001). Inbred lines are highly homogeneous, homozygous lines that have been created by multiple rounds of self-pollination and selection. They provide an array of uniform, reproducible genotypes that samples from this genetic diversity (Lee, 1994). Comparisons of inbred lines show high levels of sequence polymorphisms (Tenaillon *et al.*, 2001; Fu and Donner, 2002; Song and Messing, 2003; Brunner *et al.*, 2005). Much of this polymorphism is attributable to the activity of transposable elements (Lai *et al.*, 2005; Morgante *et al.*, 2005).

Studies have found differences in expression levels of homologous genes in different inbred lines (Song and Messing, 2003; Guo *et al.*, 2004). A comparison of allelic chromosomal regions in two inbred line, Mo17 and B73, found extensive regions of non-homology (Brunner *et al.*, 2005). It is proposed that the different sequence environment of conserved genes may affect their expression. Flanking sequences could influence gene expression by acting as enhancers, producing antisense transcripts, or by influencing chromatin state. These non-genic sequences could affect expression level, tissue specificity or temporal regulation of active genes.

It is useful to introgress into different inbred lines when characterising a mutant phenotype. Firstly, inbred lines provide uniform backgrounds in which to assess

the phenotype and, secondly, expression of many morphological traits varies greatly depending on background (Coe, 1994; Freeling and Fowler, 1994). This is due to the variability of modifying genetic factors in different backgrounds and differences such as developmental rate. Thus, introgressing into a range of inbreds can provide a spectrum of phenotypes for analysis. Suppression or alterations to mutant phenotypes in different genetic backgrounds can provide clues as to the function of the gene.

1.10 Aims and objectives

The overall aim of the project was to determine the roles of *wab1* and *Mwp1* in maize leaf development, and thus gain a better understanding of leaf axial patterning in grasses. Specific aims were as follows:

- I. In order to test the hypothesis that *Wab1-R* acts cell-autonomously, and to extricate interactions between *Wab1-R* and *Lg1*, a mosaic analysis of *Wab1-R* was carried out in *Lg1* and *lg1-R* backgrounds. To test the hypothesis that *Lg1* acts cell-autonomously to condition ectopic auricle tissue in *Wab1-R* leaves and to promote lateral growth, a mosaic analysis of *lg1-R* was conducted in *Wab1-R* and *wab1* backgrounds.
- II. In order to gain a better understanding of the mechanisms controlling lateral growth of the maize leaf, the timing and location of the *Wab1-R* lateral growth defect were investigated by an analysis of vascular development in *Wab1-R* leaf primordia and a cell lineage analysis of *Wab1-R* leaves.
- III. Characterisation of the *mwp1-R* phenotype and *in situ* hybridisation of known polarity genes were carried out in order to ascertain the role of *Mwp1* in leaf development and to test the hypothesis that the *mwp1-R* mutation disrupts adaxial-abaxial polarity in lateral organs. To determine if *mwp1-R* affects lateral and proximal-distal growth of lateral organs, wild-type and *mwp1-R* leaves and floral organs were measured.

IV. In order to better understand the genetic control of axis specification in maize lateral organs with diverse morphologies, the polarity of *mwp1-R* and wild-type floral organs and prophylls were investigated by scanning electron microscopy (SEM) and light microscopy. Early prophyll development was characterised by SEM, and by *in situ* hybridisation of known polarity genes.

2. General Materials and Methods

2.1 Maize nomenclature

Symbols used to designate genes referred to in this study are in accordance with standard maize nomenclature (Burr *et al.*, 1995).

Gene loci are represented by lower case italic characters. Where a mutant allele is recessive, it is designated by a lower case, italicised symbol. The symbol for dominant wild-type alleles is the same three letter symbol as for mutant alleles, but with the first letter capitalised. Where the mutant allele is dominant, the first letter of the symbol is capitalised. The symbol for the corresponding wild-type allele then has all lower case letters.

In maize, the first mutant allele discovered is referred to as the reference allele. Reference alleles are designated by "-R" after the three letter symbol. All mutant alleles used in this study were reference alleles. Thus, in this text the recessive reference allele at the *mwp1* locus is referred to as *mwp1-R* and the wild-type allele is referred to as *Mwp1*. The dominant reference allele at the *wab1* locus is referred to as *Wab1-R*, and the wild-type allele is referred to as *wab1*. The recessive reference allele at the *lg1* locus is referred to as *lg1-R*, and the wild-type allele is referred to as *Lg1*.

Four marker genes were used for clonal and mosaic analyses. Recessive alleles of *white seedling3-R* (*w3-R*), *lemon white-R* (*lw-R*) and *albescens-R* (*al-R*) cause chlorophyll deficiencies and condition albino leaf phenotypes. The recessive allele *virescent4-R* (*v4-R*) delays chlorophyll accumulation and conditions a yellow or virescent leaf phenotype.

2.2 Inbred lines

A number of standard maize inbred lines were used in this work. These were; A188, W23 and B73. These stocks were obtained from the Maize Genetics Coop.

2.3 Growth conditions

Field

The plants used in this study were grown in fields at the Institute of Developmental Phenomenology, Raunaki, New Zealand and at the Massey University Plant Growth Unit, Palmerston North, New Zealand. Seeds were hand planted into cultivated soil in late November and grown to maturity.

Glasshouse

Seedlings for histology and SEM were grown in glasshouses at HortResearch, Palmerston North, New Zealand. Glasshouse temperature was maintained at between 23°C and 25°C and photoperiodic extension lighting was used over the winter months. Plants were watered by hand once per day.

2.4 Stereomicroscope and light microscopy

A Leica (MZFLIII) stereomicroscope equipped with a DC200 digital camera was used in the course of this research. It is referred to in the following text as the stereomicroscope. The light microscope used in the course of this research was an Axioplan microscope equipped with an Axiophot camera (Zeiss, Jena, Germany).

2.5 Scanning electron microscopy

2.5.1 Preparation of specimens

For scanning electron microscopy (SEM) of mature tissue, entire leaves and inflorescences were harvested in the field, placed in water and taken to the lab where small samples (less than 4 mm x 4 mm) were excised with a razor blade and fixed. Mature leaf tissue was fixed in 3% (w/v) glutaraldehyde and 2% (w/v) paraformaldehyde in 0.1 M phosphate buffer (pH 7.2) overnight at room temperature.

For analysis of younger tissues, seedlings were grown in the glasshouse and entire seedlings were taken to the lab, dissected under the stereomicroscope and fixed. Meristematic tissue was fixed in 3% glutaraldehyde and 2%

paraformaldehyde in 0.05 M phosphate buffer (pH 7.2) overnight at room temperature.

Samples for SEM were dehydrated in a graded ethanol series, critical-point dried in liquid CO₂ (Polaron E 3000 critical point dryer) and sputter coated with 25 nm gold (SCD-050 sputter coater; Bal-Tec, Balzers, Liechtenstein).

2.5.2 Preparation of replicas

Resin replicas of epidermal surfaces and developing prophylls were made using a dental impression media method (Williams *et al.*, 1987). Leaf tissue was flattened onto double-sided tape on a glass microscope slide. Developing axillary buds were dissected on glass microscope slides under the dissecting microscope. Fresh dental impression media (Coltene® President light body dental impression media, NJ, USA) was mixed on a parafilm strip and the specimen was immediately pressed into it to create a mould. For more 3-dimensional specimens, such as axillary buds, segments of plastic drinking straw were cut to make small cylindrical containers. Dental impression media was transferred to the straw segment immediately after mixing, and the specimen was pressed into the centre. The media was allowed to set for five minutes or longer.

Tissue was gently removed from the mould once the media was set. Casts were then made by filling the mould with resin (Araldite super strength liquid epoxy resin, Selleys) and applying a vacuum to remove air bubbles. These were left to set overnight then replicas were gently removed and mounted on SEM stubs. Replicas were sputter coated as described above.

2.5.3 Viewing and photography

Specimens were examined on a Cambridge 250 Mark III scanning electron microscope (Cambridge Instruments, Cambridge, UK) operated at 20 kV, and images were captured on 35 mm film.

2.6 Histology

2.6.1 Paraffin sections

Fixation

Tissue for paraffin embedding was fixed in FAA (3.5% formaldehyde, 5% acetic acid, 50% ethanol (v/v)). Excess tissue was removed under the stereomicroscope, and samples were transferred to vials containing FAA. These were then put into a desiccator and a vacuum was applied. Care was taken not to allow the fixative to boil. Samples were held under vacuum for 2-5 min, and then the vacuum was released slowly. FAA was replaced and the vials were left at room temperature for 2-3 h.

Dehydration

Dehydration steps were carried out at 4°C. Fix was removed by pouring or pipetting and samples were rinsed with 50% ethanol (v/v). Samples were run through a graded ethanol series (50%, 70%, 85%, 95% + 0.1% eosin, 100%, 100% for 90 min each), then left in 100% ethanol overnight.

Histoclear infiltration

Histoclear (National Diagnostics) infiltration was carried out at room temperature. Samples were treated with 100% ethanol for 2 h, 50% histoclear: 50% ethanol for 1 h and three changes of 100% histoclear for 1 h each.

Paraffin infiltration

Paraplast chips (McCormick Scientific) were added to approximately half the volume of histoclear. Vials were transferred to a 55°C oven and left overnight. The following morning, the molten paraffin and histoclear solution was poured off. Molten paraplast was then replaced twice per day for three days or three times per day for two days.

Casting blocks

Paraffin blocks were cast in foil candy cups (Home Style Chocolates). Foil cups were placed on a 55°C hot plate and filled with fresh molten paraffin. Tissue samples were transferred to candy cups using clean forceps and positioned in the correct orientation. Cups were then transferred to a cool surface such as an

inverted petri dish in an ice box to set. Paraffin blocks were stored at 4°C until required.

Sectioning paraffin embedded material

5-10 µm sections were cut on a microtome (Leica model Jung RM 2045). Wax ribbons were transferred to a 42°C water bath (Leica model HI 1210) to relax any creases in the ribbon. Ribbons were floated onto microscope slides (ProbeOn Plus, Fisher Scientific) and positioned using toothpicks. Slides were held vertically to drain, and excess water was removed by blotting with a Kim wipe (Kimberly-Clark). Slides were then placed on a 42°C hot plate (Leica model HI 1220) and allowed to dry overnight.

2.6.2 Staining

Toluidine Blue

The protocol used for toluidine blue staining of paraffin sections is adapted from Ruzin (1999). Paraffin sections were stained in 0.05% (w/v) toluidine in water for 30 min before removal of the paraffin. Slides were rinsed in water and air dried. Paraffin was removed with histoclear (first rinse 10 min, second rinse 5 min). Coverslips were mounted with DPX (dibutylphthalate (10 ml) + polystyrene (25 g) + xylene (70 ml)) (Ruzin, 1999).

Safranin and fast green

The protocol for safranin and fast green staining of paraffin sections is adapted from Johansen (1940). Slides were placed in metal slide racks, and all steps were carried out at room temperature. Slides were dewaxed by immersing in histoclear for 10 min and then in fresh histoclear for a further 10 min. Slides were run through a graded ethanol series and then stained in safranin solution (1% (w/v) safranin in 2:1:1 methyl cellosolve : 95% ethanol : water) for 24 - 48 h. Slides were rinsed in distilled water until the water ran clean, immersed in 70% ethanol for 5 min and then destained in picric acid (0.5% (w/v) picric acid in 95% ethanol) for 10 s. Slides were rinsed in 95% ethanol for 1 min, then in a second solution of 95% ethanol for 10 s, stained in fast green solution (0.15% (w/v) fast green in 1:1:1 methyl cellosolve : ethanol : clove oil) for 10 - 15 s, then immediately rinsed in clove oil. Slides were then treated with the following

solutions; clove oil : histoclear for 10 s, histoclear : ethanol for 5 min, and two changes of histoclear for 5 min each. Coverslips were mounted with DPX.

2.6.3 Resin sections

Leaf tissue was fixed in 3% glutaraldehyde and 2% paraformaldehyde in 0.1 M phosphate buffer (pH 7.2) for 3 h at room temperature. Samples were infiltrated and embedded in Procure 812 (ProSciTech, Kelso, Australia). Sections (1µm) were cut, heat mounted and stained with 0.05% toluidine blue in water and photographed under the light microscope.

2.6.4 Distinguishing xylem and phloem in sectioned material

The vessel elements of the xylem have lignified cell wall thickenings and lack protoplasts. Helical thickenings of vessel elements can be identified by examining serial sections. In tissue that has been stained with toluidine blue, lignified cell wall thickenings stain a lighter colour than other cell walls. In tissue stained with safranin and fast green, the lignified cell walls of the vessel elements stain bright red (Ruzin, 1999). Cytoplasm and non-lignified cell walls stain green. The phloem is comprised of smaller, non-lignified sieve tube elements with companion cells.

3. *Wavy auricle in blade1-R*

3.1 Introduction

Wab1-R is a dominant mutation characterised by ectopic auricle and sheath-like tissue in the leaf blade. *Wab1-R* leaf blades are narrow and have fewer lateral veins than wild-type leaves (Hay and Hake, 2004). The *Wab1-R* allele used in the current study arose in androgenous tissue culture and was recovered by James Wassom (Hake *et al.*, 1999).

Initial characterisation of the *Wab1-R* phenotype was undertaken by Angela Hay as part of a PhD project supervised by Sarah Hake (Plant Gene Expression Center, Albany, CA). This work has subsequently been published in *Plant Physiology* (Hay and Hake, 2004). A second publication in *Development* details a mosaic analysis of *Wab1-R* and an analysis of *Ig1-R* leaf shape undertaken by Toshi Foster, Sarah Hake and myself (Foster *et al.*, 2004). *Lg1* expression data provided by Angela Hay is also included in the *Development* publication.

The liguleless mutants, *Ig1* and *Ig2*, delete ligule and auricle tissues (Emerson, 1912; Brink, 1933). Genetic analysis indicates that these genes act in a common pathway to specify ligule and auricle development (Harper and Freeling, 1996). *Lg1* is expressed at low levels in the ligular region of developing leaf primordia and acts cell-autonomously to specify ligule and auricle tissues, whereas, *Lg2* acts non-autonomously (Becraft *et al.*, 1990; Harper and Freeling, 1996; Moreno *et al.*, 1997). A mosaic analysis of *Ig1-R* found that the ligule and auricle reinitiate in a more basal position on the marginal side of *Ig1-R/-* sectors (Becraft and Freeling, 1991). This analysis supports a model in which *Lg1* function is required for the transmission of an inductive signal.

Crossing *Wab1-R* to *Ig1-R* mutants revealed a novel phenotype. Unlike *Ig1-R* mutants, which have distinct regions of blade and sheath, the blade-sheath boundary of *Ig1-R;Wab1-R* double mutants is severely disrupted, with strips of sheath-like tissue extending along the length of the blade (Hay and Hake, 2004). The leaf blade of *Ig1-R;Wab1-R* double mutants is much narrower than

either of the single mutants. *Lg1* is expressed earlier and more distally in *Wab1-R* mutant leaf primordia, further suggesting an interaction between the two genes (Foster *et al.*, 2004). To further elucidate interactions between *Lg1* and *Wab1-R*, mosaic analyses of *Wab1-R* in *Lg1* and *lg1-R* backgrounds and of *lg1-R* in a *Wab1-R* background were conducted. To better understand the nature of the *Wab1-R* narrow leaf phenotype, an analysis of vascular development and a cell lineage analysis in *Wab1-R* leaves were conducted.

3.2 Specific materials and methods

3.2.1 Phenotypic analysis of *Wab1-R* and *lg1-R;Wab1-R* plants

F3 families segregating 1:1 for *lg1-R : lg1-R;Wab1-R/wab1* were used for phenotypic analyses. Tissue samples from specific regions of the blade and sheath (see Figure 3.4) were fixed for SEM and light microscopy.

3.2.2 Mosaic and clonal analyses

Genetic stocks

Crosses for the mosaic and clonal analyses were carried out by Sarah Hake. Introgressed material was provided by Sarah Hake and Angela Hay.

Mosaic analysis of Wab1-R and clonal analysis of lg1-R leaves

For the mosaic analysis of *Wab1-R*, heterozygous *Wab1-R/wab1* plants were crossed to Maize Genetics Coop stocks heterozygous for *white seedling3-R* (*w3-R*). For the mosaic analysis of *Wab1-R* in a *lg1-R* background, *lg1-R/lg1-R;Wab1-R/wab1* plants were crossed to *lg1-R/lg1-R; v4-R w3-R/v4-R W3* stocks from the Maize Genetics Coop (Figure 3.1).

The same stock (*lg1-R* and *Lg1* plants) was also used for the clonal analysis of *lg1-R* leaves, as the *w3-R* marker gene is on the opposite chromosome arm to *lg1* and is therefore considered to be unlinked to *lg1*.

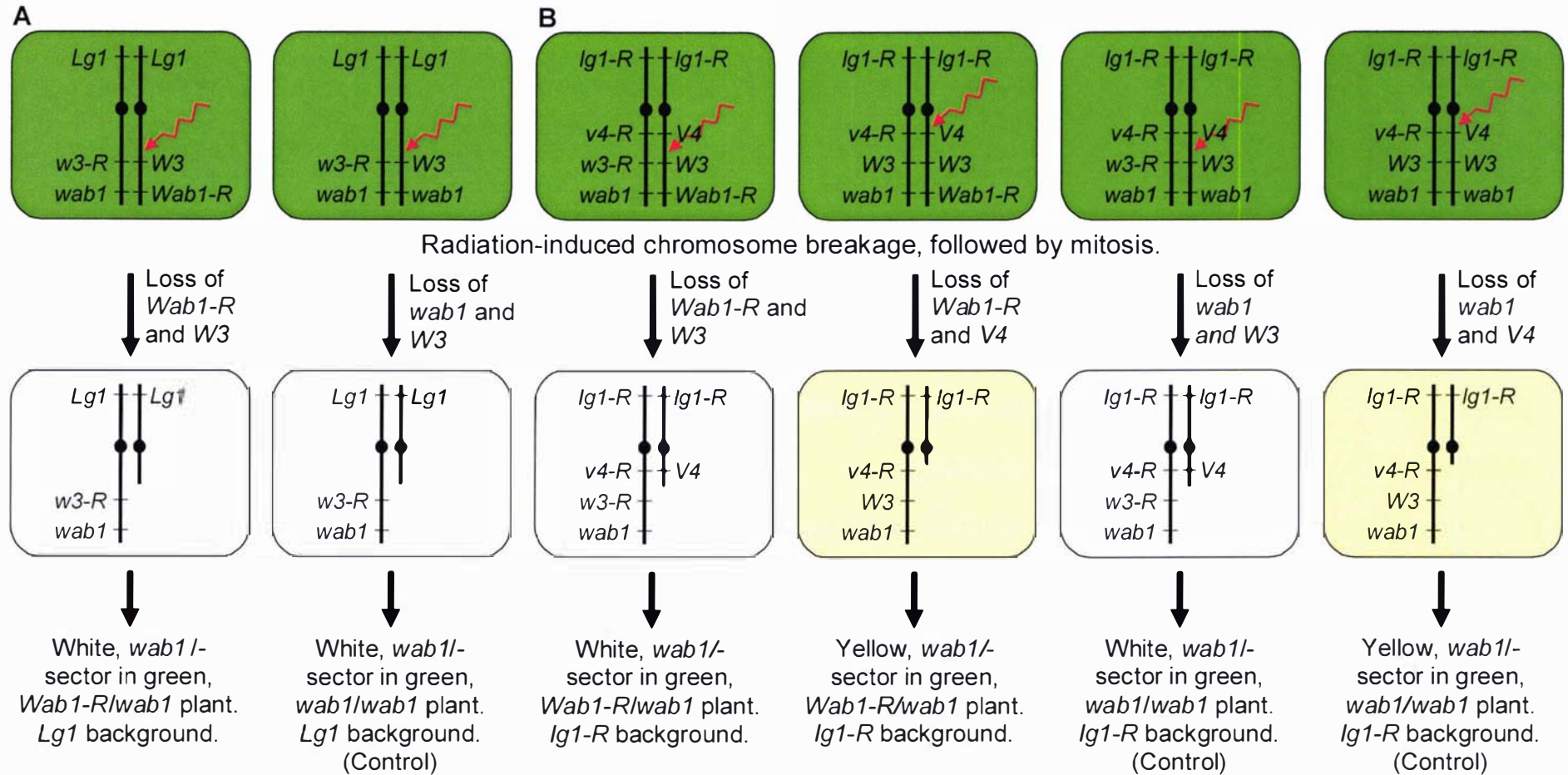
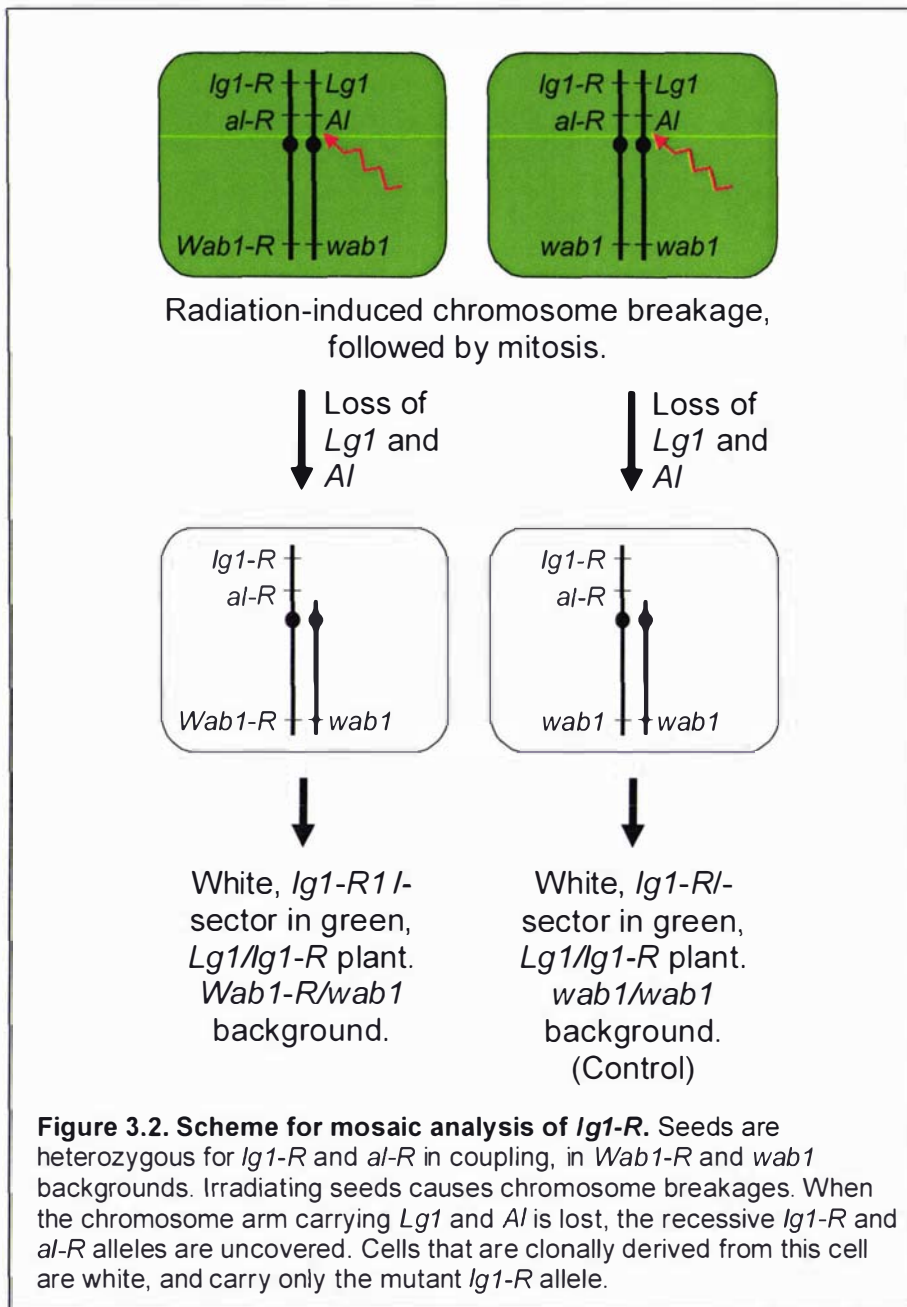


Figure 3.1. Scheme for mosaic analysis of *Wab1-R*. (A) Seeds are heterozygous for *W3* and *Wab1-R* in coupling, in a *Lg1* background. *w3-R* is an albino marker gene. Irradiating seeds causes chromosome breakages. When the chromosome arm carrying *W3* and *Wab1-R* is lost, the recessive *w3-R* and *wab1* alleles are uncovered in that cell. Cells that are clonally derived from this cell are albino and carry only the non-mutant *wab1* allele. Control plants are heterozygous for *W3* and homozygous for the wild-type *wab1* allele. (B) Seeds are heterozygous for *W3*, *V4* and *Wab1-R* in coupling, or heterozygous for *V4* and *Wab1-R* and homozygous for *W3*, in a *Ig1-R* background. Loss of the chromosome arm carrying *W3* and *Wab1-R* results in white, *wab1*⁻ sectors. Loss of *V4* and *Wab1-R* results in yellow *wab1*⁻ sectors.

Mosaic analysis of *Ig1-R* in *Wab1-R* background

For the mosaic analysis of *Ig1-R* in *Wab1-R* and *wab1* backgrounds, heterozygous *Wab1-R* plants were crossed to Maize Genetics Coop stocks heterozygous for *Ig1-R* and the linked marker gene *albescent-R* (*al-R*) (Figure 3.2).



Clonal analysis of *Wab1-R* leaves

For the clonal analysis of *Wab1-R* leaves, heterozygous *Wab1-R/wab1* plants were crossed to Maize Genetics Coop stocks heterozygous for the unlinked marker gene *lemon white-R* (*lw-R*).

Irradiation conditions

Seeds were imbibed for 48 hours at 25°C then irradiated with approximately 1,500 rads. The irradiation utilised a 6 MV photon (X-ray) beam generated by a linear accelerator at the Palmerston North Hospital Radiotherapy Unit, Palmerston North, New Zealand.

Sector analysis

Plants were grown to maturity and screened for albino (*w3-R/-* or *lw-R/-* or *al-R/-*), and yellow (*v4-R/-*) sectors throughout development. All sectored leaves were harvested at maturity and photographed and/or photocopied. Leaf number, sector width and the lateral position of the sector within the blade and sheath were recorded.

Transverse hand sections of freshly harvested sectored leaves were examined by epifluorescence microscopy using a Leica (MZFLIII) stereomicroscope equipped with a 395-440 nm excitation filter and a 470 nm observation filter. All sections were photographed using a DC200 digital camera (Wetzlar, Germany). Under these conditions, normal chloroplasts fluoresce bright red and cell walls appear blue-green. No chlorophyll autofluorescence is detected in *w3-R/-* or *al-R/-* cells. The presence or absence of chlorophyll in epidermal layers was scored by inspecting guard cells, the only chloroplast-containing cell-type in the epidermis.

Sectors of *v4-R/-* appear yellow due to a delay in the accumulation of chlorophyll, but eventually become green. Sector boundaries of *v4-R/-* sectors were marked with a pen. Samples of leaf tissue that spanned sector boundaries were fixed for SEM. Prior to fixation, a small notch was made at the sector boundary.

Measurements of mosaic leaves

For the mosaic analyses, the sectored and non-sectored sides of each leaf were measured from midrib to margin at three points along the leaf: blade midpoint, blade-sheath boundary, and sheath midpoint. The width of the non-sectored leaf-half was subtracted from that of the sectored half to give an absolute difference in leaf-half width. For each genotype and measurement position, data were analysed using a non-parametric 1-sign test to determine if

the median values were significantly different than 0. This test was used because data from *Wab1-R* and *Ig1-R;Wab1-R* leaves are not normally distributed. For the mosaic analysis of *Wab1-R*, the lateral position of each sector was represented as the distance from the midrib to the closest sector border, divided by the width of the entire leaf-half (see Table 3.5). Statistical analysis was performed using Origin 6.0 (Microcal Software, Inc., Northampton, MA, USA) and MINITAB (State College, PA, USA).

Clonal analysis of *Ig1-R* leaves

For the comparison of clonal, *w3-R*-marked sectors in wild-type and *Ig1-R* plants, sector widths were measured at the blade-sheath boundary. To minimise variation in leaf shape, only leaves 9-17 were included in this analysis. The median sector width was calculated separately for sectors near the midrib (lateral position 0-0.29) and in lateral plus margin domains (0.3-1.0). Data from wild-type and *Ig1-R* plants were compared using a Kruskal-Wallis test. This test was used because the data from *Ig1-R* plants are not normally distributed.

Clonal analysis of *Wab1-R* leaves

To investigate the nature of the *Wab1-R* narrow leaf phenotype, a clonal analysis was undertaken. Half-leaf width (from midrib to margin) and sector width were measured at the blade midpoint, at the base of the blade, and in the culm. The mean sector width was calculated separately for sectors near the midrib (lateral position 0-0.29), in the lateral domain (0.3-0.59), and near the margin (0.6-1.0). Means were compared by Student's t-test to determine if they were significantly different at the 0.05 confidence level. Data were analysed using Microsoft Office Excel 2003.

The position of a sector within the culm was used to approximate the radial position of the sector within the SAM from which that phytomer arose. This method is similar to that employed by Scanlon (2000) in the mosaic analysis of *ns*. The radial point of the culm corresponding to the midrib of the leaf above was designated as 0°. Measurements were made from 0° to the inner boundary of the sector, from 0° to the outer sector boundary, and of the entire culm circumference. The radial position of each sector in the culm was calculated in degrees from the midrib (see Figure 3.8) using the following equations:

Position of inner sector boundary= $S_i/C \times 360$

Position of outer sector boundary= $S_o/C \times 360$

Where;

S_i =distance from midrib to inner sector boundary

C=circumference of culm

S_o =distance from midrib to outer sector boundary

Thus, for a sector that begins 8 mm from the midrib, in a culm with a circumference of 60 mm, the position of the inner sector boundary is calculated as $8/60 \times 360=48^\circ$.

3.2.3 *Ig1-R* leaf measurements

The *Ig1-R* mutation was introgressed at least four times into the W23 inbred background and plants were grown to maturity in the Gill Tract nursery, Albany, CA. The 9th, 10th, and 11th leaves down from the tassel were measured from *Ig1-R* and *Lg1/Ig1-R* siblings. Leaf width was measured at the blade-sheath boundary, and blade and sheath length were measured along the midrib. Data were compared by one-way ANOVA.

3.2.4 Lateral vein count in *Wab1-R* leaf primordia

Wab1-R leaves have fewer lateral veins than wild-type leaves (Hay and Hake, 2004). To determine when this defect is first apparent, lateral veins were counted in early stage leaf primordia. This analysis was done in B73 stock and *Wab1-R* introgressed seven times into a B73 background. *Wab1-R* homozygotes were used, as the phenotype is more severe in homozygotes than in heterozygotes (Hay and Hake, 2004). Seedlings were harvested at 12 to 16 d after germination. Outer leaves were removed and the apices were fixed in FAA and paraffin embedded. 10 μm transverse sections were cut, mounted on slides and stained with toluidine blue. Leaf primordia 9-12 were examined. Developing lateral veins were counted in sections 20 μm above the base of the primordium. Developing procambial strands were identified by cell divisions at angles that disrupt the parallel arrangement of cells (Sharman, 1942; Esau, 1960).

The mean number of lateral veins was calculated separately for *Wab1-R* and wild-type leaf primordia at each plastochron stage (P1- P6). The means for each plastochron were compared by Student's t-test to determine if they were significantly different at the 0.05 confidence level. Data were analysed using Microsoft Office Excel 2003.

3.3 Results

3.3.1 *lg1-R* enhances the *Wab1-R* mutant phenotype

Four distinct tissue types demarcate the proximal-distal axis of the maize leaf, the proximal sheath and distal blade are separated by ligule and auricle tissues (Figure 3.3 A, E). The ligule is an epidermally-derived fringe, and the auricles are thickened wedges of tissue that act as a hinge between blade and sheath (Sharman, 1941; Becraft *et al.*, 1990). Each of these tissue types has characteristic epidermal features and histological organisation, which have been well characterised by scanning electron and light microscopy (Sharman, 1942; Esau, 1977; Russell and Evert, 1985; Langdale *et al.*, 1989; Sylvester *et al.*, 1990).

The *Wab1-R* mutation disrupts normal patterning of the leaf and results in patches of ectopic auricle, sheath and ligule in the leaf blade (Figure 3.3 F; Hay and Hake, 2004). Often a localised increase in blade width occurs immediately distal to patches of ectopic auricle. In addition, the normally placed auricle is more extensive, spreading distally into the leaf blade. Long strips of thickened auricle tissue and the reduced lamina width give *Wab1-R* plants an unusual appearance; narrow, rigid leaves extend from the main axis at a more obtuse angle than wild-type leaves (Figure 3.3 B). Examination of histological and epidermal features reveals that the *Wab1-R* blade contains cells with auricle and sheath identity (Figure 3.4 I, J, L). In both ectopic sheath and auricle tissue, intermediate veins fuse into lateral veins, and normal bundle sheath anatomy is absent or incomplete (arrowheads in Figure 3.4 I, J).

We constructed double mutants between *Wab1-R* and *lg1-R* to analyse the effect that loss of auricle tissue would have on the *Wab1-R* phenotype. Recessive *lg1* mutations remove ligule and auricle, giving the mutant leaves a

more upright appearance (Figure 3.3 D) (Emerson, 1912). Despite the lack of ligule and auricle, *lg1-R* leaves have separate blade and sheath domains (Figure 3.3 H). *lg1-R;Wab1-R* double mutants exhibit a striking, narrow leaf phenotype (Figure 3.3 C, G). Both the normal and ectopic auricle tissue is absent in the double mutant, most of the proximal blade is deleted, and sheath-like tissue extends along the margins of the residual blade.

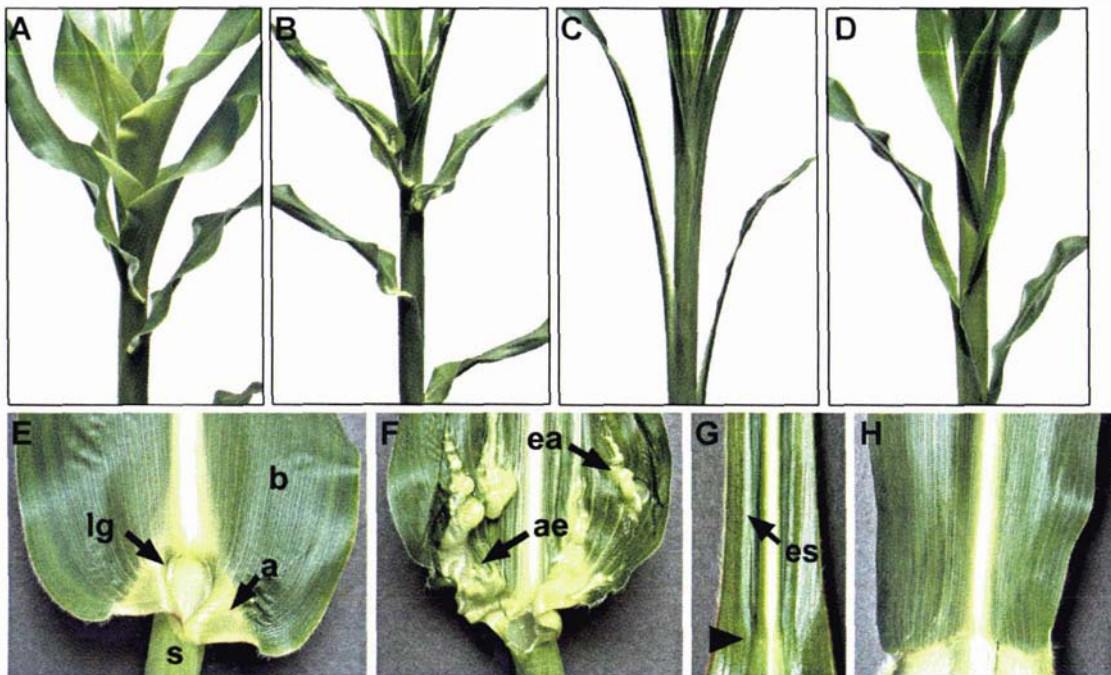


Figure 3.3. Leaf and whole plant phenotypes. (A) Wild-type, (B) *Wab1-R*, (C) *lg1-R;Wab1-R*, and (D) *lg1-R* plants 8 weeks after planting. Adaxial view of blade-sheath boundary of (E) wild-type, (F) *Wab1-R*, (G) *lg1-R;Wab1-R*, and (H) *lg1-R* leaves. b=blade, s=sheath, lg=ligule, a=auricle, ea=ectopic auricle, ae=auricle extension, es=ectopic sheath. Arrowhead in (G) indicates presumptive blade-sheath boundary in *lg1-R;Wab1-R* leaf.

The ectopic tissue in *lg1-R;Wab1-R* leaf blades has histological and epidermal features similar to sheath tissue. The adaxial surface is hairless and cells are long with smooth cell wall junctions (Figure 3.4 M), while the abaxial surface is covered with hairs specific to abaxial sheath tissue (not shown). *lg1-R;Wab1-R* sheath-like tissue is very thin in the transverse dimension (Figure 3.4 K) and the intervascular spacing and prominent transverse veins resemble those normally found in marginal sheath tissue (Figure 3.4 G). In distal positions and near the midrib, *lg1-R;Wab1-R* leaves have normal blade tissue (not shown). Sheath tissue identity is not affected by the *lg1-R* or *Wab1-R* mutations.

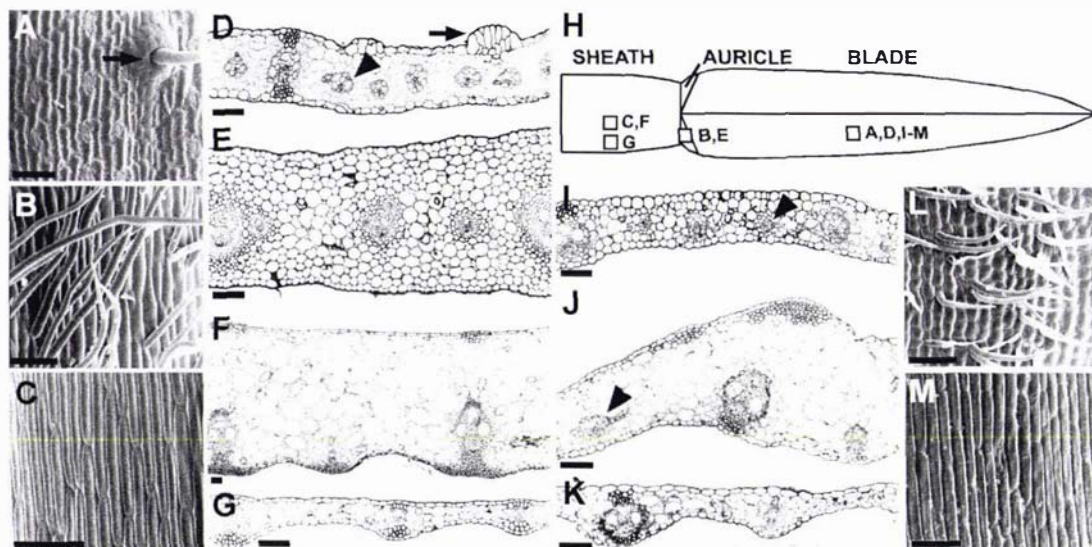


Figure 3.4. Epidermal and histological features of wild-type, *Wab1-R* and *lg1-R;Wab1-R* leaves. SEM of adaxial surface of wild-type (A) blade, (B) auricle and (C) sheath. Transverse section through wild-type (D) blade, (E) auricle, (F) internal sheath and (G) marginal sheath tissue. (H) Cartoon depicting regions where tissue was sampled. Transverse sections through (I) ectopic auricle in *Wab1-R* blade, (J) ectopic sheath in *Wab1-R* blade and (K) ectopic sheath in *lg1-R;Wab1-R* blade. SEM of adaxial surface of (L) *Wab1-R* ectopic auricle and (M) *lg1-R;Wab1-R* ectopic sheath. All sections are oriented with the adaxial surface upwards. Arrows in (A) and (D) indicate multicellular base of macrohair. Normal bundle-sheath anatomy indicated by arrowhead in (D), abnormal bundle-sheath anatomy indicated by arrowheads in (I) and (J). Scale bars = 100 μm .

3.3.2 *lg1-R* alters leaf shape

Although the *lg1* ligule defect has been well described by others, the altered shape of *lg1* leaves has not been reported. We found that *lg1-R* leaves are significantly narrower at the blade-sheath boundary than *Lg1/lg1-R* siblings (Table 3.1). The mean width of the ninth leaf counting down from the tassel was 76 mm for *lg1-R* plants, whereas, the mean width was 102 mm for wild-type siblings. A similar trend was seen for the tenth and eleventh leaves down from the tassel. We also noted that while the overall lengths of *lg1-R* and *Lg1/lg1-R* leaves are the same, *lg1-R* blades are shorter and *lg1-R* sheaths are longer than those of *Lg1/lg1-R* siblings (Table 3.1). This finding indicates that the blade-sheath boundary is established in a more distal position in the *lg1-R* mutant.

Table 3.1. Comparison of *lg1-R* and wild-type (*Lg1/lg1-R*) leaf shape. Sheath length, blade length, and leaf width at the blade-sheath boundary were measured for *lg1-R/lg1-R* and *Lg1/lg1-R* siblings. Data were compared by one-way ANOVA. Means of all measurements are in mm. Leaves were numbered counting down from the tassel. Sample sizes are as follows; *lg1-R/lg1-R* (N=21), *Lg1/lg1-R* (N=13). * indicates values that are significantly different at the 0.05 confidence level. SE = standard error. The schematic shows measurement positions and illustrates *lg1-R/lg1-R* and *Lg1/lg1-R* leaf shape. W = width.

A

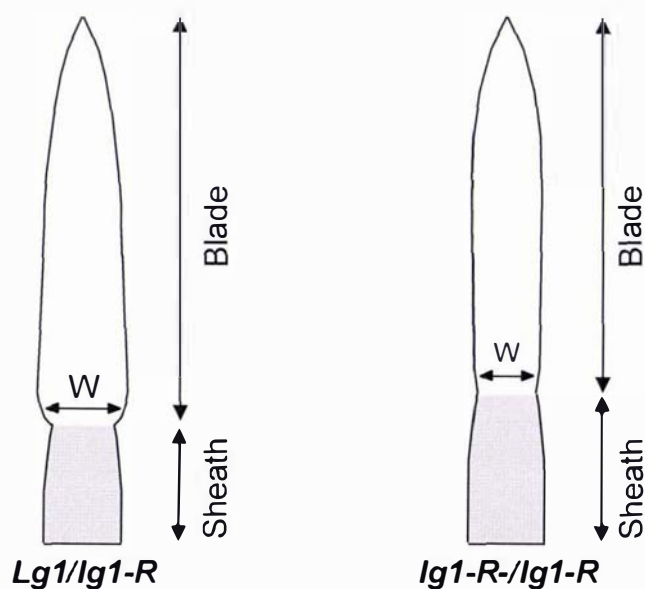
Ninth leaf down		<i>Lg1/lg1-R</i>	<i>lg1-R/lg1-R</i>	P-value
Total leaf length	Mean	903	893	0.607
	SE	17.4	10.5	
Blade length	Mean	697	649	0.006*
	SE	15.2	8.6	
Sheath length	Mean	206	243	<0.001*
	SE	3.7	3.7	
Blade width	Mean	102	76	<0.001*
	SE	2.9	2.2	

B

Tenth leaf down		<i>Lg1/lg1-R</i>	<i>lg1-R/lg1-R</i>	P-value
Total leaf length	Mean	874	846	0.346
	SE	33.3	17.7	
Blade length	Mean	660	605	0.029*
	SE	21.0	13.6	
Sheath length	Mean	202	243	<0.001*
	SE	4.3	4.0	
Blade width	Mean	92	65	<0.001*
	SE	2.3	2.3	

C

Eleventh leaf down		<i>Lg1/lg1-R</i>	<i>lg1-R/lg1-R</i>	P-value
Total leaf length	Mean	789	762	0.537
	SE	38.7	22.6	
Blade length	Mean	575	521	0.155
	SE	35.4	18.5	
Sheath length	Mean	212	242	<0.001*
	SE	3.9	3.1	
Blade width	Mean	76	54	<0.001*
	SE	2.5	2.1	



We compared the width of *w3-R*-marked clonal sectors in wild-type (*Lg1/lg1-R*) and *lg1-R* plants. Sectors were measured at the base of the blade. Sectors located near the midrib had similar median widths in wild-type and *lg1-R* blades. However, sectors in lateral and marginal regions were significantly narrower in *lg1-R* mutants than in wild-type leaves (Table 3.2). These data indicate that the *lg1-R* lateral growth defect is localised to lateral and marginal domains at the base of the blade.

Table 3.2. Median width of clonal sectors in *Lg1/lg1-R* and *lg1-R/lg1-R* plants, measured at the blade-sheath boundary. Median sector widths were calculated separately for sectors near the midrib (0-0.29) and sectors in lateral and marginal positions (0.3-1.0). Data were compared by the Kruskal-Wallis test for non-parametric distribution of data. * indicates values that are significantly different at the 0.05 confidence level.

Genotype	N	Lateral position of sector	Median sector width (mm)	P-value
<i>Lg1/lg1-R</i>	22	0-0.29	1.0	0.453
<i>lg1-R/lg1-R</i>	40	0-0.29	1.0	
<i>Lg1/lg1-R</i>	18	0.3-1.0	5.0	0.007*
<i>lg1-R/lg1-R</i>	45	0.3-1.0	2.0	

3.3.3 Mosaic analysis of *Wab1-R*

Sectors of tissue lacking the dominant *Wab1-R* allele (*wab1/-*) were created in both *Wab1-R* and *lg1-R;Wab1-R* mutants to determine if *Wab1-R* disrupts leaf patterning in a cell-autonomous manner (Figure 3.1). Stocks carrying *Wab1-R* in repulsion to *w3-R* were X-irradiated to induce random chromosome breaks. Radiation-induced breaks proximal to *W3* resulted in albino, non-*Wab1* (*w3-R wab1/-*) sectors in otherwise green, *Wab1-R* or *lg1-R;Wab1-R* plants. In *lg1-R;Wab1-R* plants, chromosome breaks proximal to *V4* created yellow, *lg1-R* (*v4-R wab1/-;lg1-R/lg1-R*) sectors. The loss of *W3* in normal plants, and either *W3* or *V4* in *lg1-R* plants, provided control sectors that were hemizygous for chromosome 2L.

Out of 1681 irradiated seeds, 93 *w3-R wab1/-* sectored leaves were identified in 42 *Wab1-R/wab1* plants and 51 sectored leaves were identified in 32

wab1/wab1 control plants. In the second experiment, 4,608 seeds were irradiated; 115 *w3-R wab1/-* sectors and 65 *v4-R wab1/-* sectors were identified in 81 *Ig1-R/Ig1-R*; *Wab1-R/wab1* plants. In 46 *Ig1-R/Ig1-R*; *wab1/wab1* control plants, 90 *w3-R wab1/-* and 50 *v4-R wab1/-* sectors were analysed.

To ensure that the chromosome arm carrying *Wab1-R* was lost early in leaf development, only sectors that extended through both the sheath and blade were analysed. Given the variability of the *Wab1-R* phenotype, only sectors adjacent to tissue displaying a mutant phenotype could be scored. Thus, of 273 total sectors, only 77 were scorable for tissue identity. Sectors adjacent to ectopic auricle and sheath tissue were analysed for phenotypic expression (mutant or wild-type) and cell layer composition (green or albino) (Table 3.3). Because *v4-R* sectors eventually accumulate normal amounts of chlorophyll, it was difficult to determine the internal layer composition of yellow, *v4-R* sectors in mature leaves. Thus, only *w3-R* sectors were scored for albino versus green mesophyll and epidermal layers. We predicted that white or yellow (*wab1/-*) sectors would have normal blade tissue if *Wab1-R* functions cell autonomously, whereas the sectors would have the same mutant phenotype as the adjacent green tissue if *Wab1-R* acts in a non-autonomous manner.

Ectopic auricle and auricle extension phenotypes in *Wab1-R* mutants

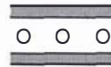
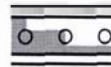
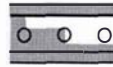
Sectors were examined using SEM and handsections to determine the phenotype of *wab1/-* tissue. In 77% (24/31) of scorable sectors, *wab1/-* cells exhibited normal blade characteristics whereas adjacent *Wab1-R* tissue displayed either ectopic auricle or extension of auricle phenotypes (Table 3.3, Figure 3.5 A-F). These results indicate that *Wab1-R* generally acts in a cell-autonomous manner in the lateral dimension to condition ectopic auricle and auricle extension phenotypes.

Figure 3.5 F is a SEM of the adaxial epidermis of the boxed region shown in Figure 3.5 C. There is a clear transition from albino *wab1/-* tissue, which has blade characteristics such as macrohairs (left of arrowhead), to green, hairless *Wab1-R/wab1* tissue with unexpanded dovetailed cells typical of immature auricle (right of arrowhead, Figure 3.5 F). Green, *Wab1-R/wab1* tissue fluoresces red under UV illumination while albino *wab1/-* tissue appears blue-

green. When sectored tissue is viewed in transverse section, abrupt changes in histology are apparent at the sector boundaries. For example, in Figure 3.5 G, the albino *wab1*⁻ tissue has characteristics of blade tissue, whereas the adjacent *Wab1-R/wab1* tissue is thicker and auricle-like. The SEM in Figure 3.5 H shows the same sector boundary, with albino tissue to the left of the arrowhead and green tissue to the right. The green *Wab1-R/wab1* tissue has larger mesophyll cells and is densely covered by long hairs without multicellular bases; these cells are characteristics of mature auricle tissue. The albino *wab1*⁻ tissue has prickly hairs, macrohairs and cell types typical of blade tissue.

Of the seven sectors that displayed auricle characteristics through all or part of the sector, six had one or more inner layers of green, *Wab1-R* cells (Table 3.3). These results indicate that *Wab1-R* generally acts cell-autonomously in the lateral dimension, but may act non-cell autonomously between cell layers.

Table 3.3. Summary of *wab1*⁻ sector phenotypes. Sectors were scored as “+” if they displayed characteristics of blade tissue, and “W” if they exhibited auricle or sheath characteristics. Mixed layer sectors that spanned fewer than three veins were included as part of the larger adjacent sector. If adjacent sector types displayed different phenotypes then both were scored. Otherwise, only the sector composition adjacent to green, *Wab1-R* tissue was scored. *Four yellow (*v4-R*) sectors were not included in sector subtypes due to difficulties in determining the exact layer composition of *wab1 v4-R*⁻ sectors.

Phenotype	Scorable sectors	All sector types				
			white L1/ white L2	green L1/ white L2	white L1/ mixed L2	green L1/ mixed L2
<i>Wab1</i>						
Ectopic auricle/ Auricle extension	31	24 + (77%) 7 W (23%)	4 1	17 2	1 0	2 4
<i>Wab1</i>						
Ectopic sheath	20	15 + (75%) 5 W (25%)	0 1	14 3	0 0	1 1
<i>Ig1-R;Wab1</i>						
Ectopic sheath	26*	26 + (100%) 0 W (0%)	10 0	11 0	0 0	1 0

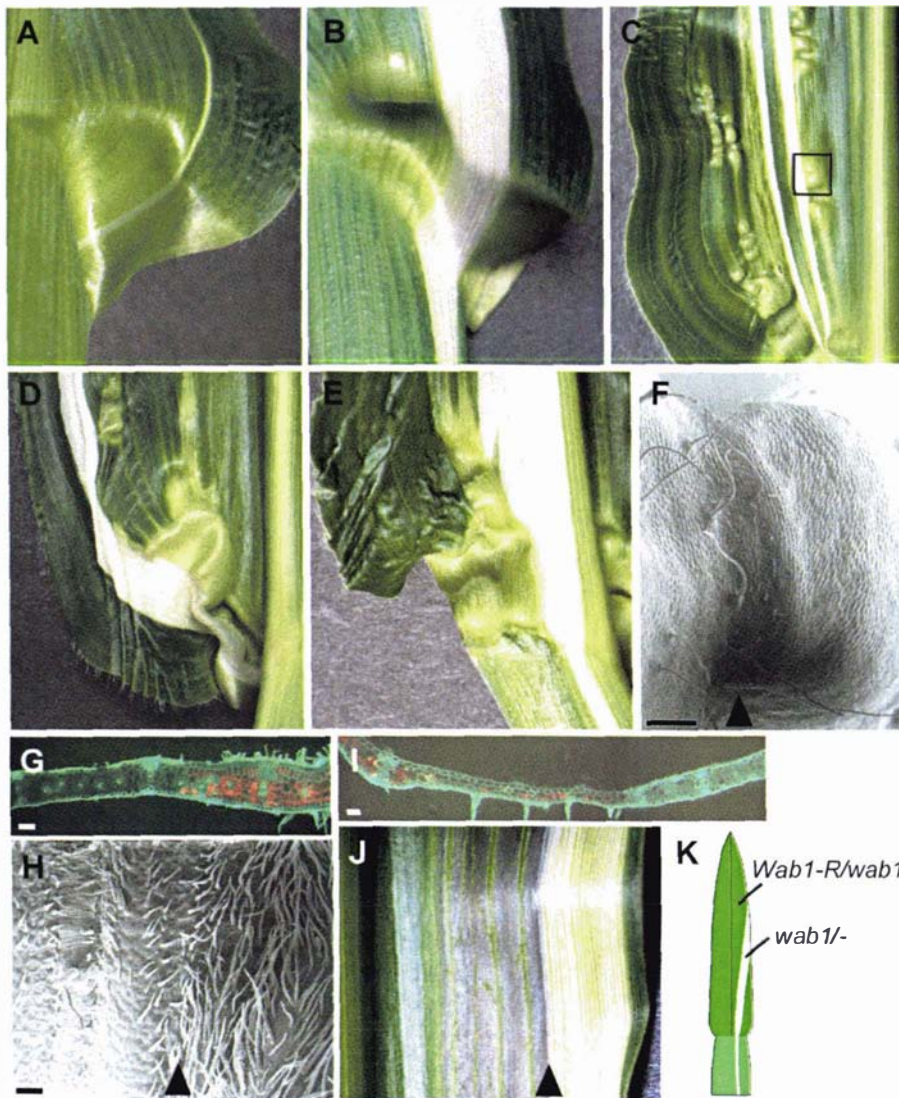


Figure 3.5. Phenotypes of *wab1*⁻ sectors in *Wab1-R* leaves. (A-E) Abaxial view of *Wab1-R* leaves exhibiting auricle extension and/or ectopic auricle phenotypes with albino *wab1*⁻ sectors exhibiting normal blade characteristics. (F) Scanning electron micrograph of adaxial surface of boxed region shown in (C), illustrating unexpanded, dovetailed auricle-like cells in *Wab1-R/wab1* ectopic auricle tissue (right of arrowhead), and normal blade epidermal characteristics such as macrohairs in the *wab1*⁻ sector (left of arrowhead). (G) Fluorescence micrograph of a transverse section through a sector adjacent to auricle extension, illustrating a sharp boundary between green, *Wab1-R/wab1* auricle-like tissue (fluoresces red), and albino, *wab1*⁻ tissue (appears blue-green). (H) SEM of adaxial surface of sector boundary shown in (G), exhibiting hairy, fully expanded auricle-like cells in *Wab1-R/wab1* tissue (right of arrowhead) and normal blade cells including prickle hairs and macrohairs in *wab1*⁻ tissue (left of arrowhead). (I) Fluorescence micrograph of a transverse section through the sector shown in (J). Green, *Wab1-R/wab1* tissue is very thin with widely spaced veins, a hairless adaxial surface and abaxial hairs characteristic of marginal sheath tissue. Albino *wab1*⁻ tissue has the histological organization of normal blade tissue. (J) Abaxial view of sector adjacent to ectopic sheath tissue, arrowhead marks sector boundary. (K) Cartoon depicting an albino wild-type (*wab1*⁻) sector in a green *Wab1-R/wab1* leaf. Scale bar = 500 μ m in F, and 100 μ m in G-I.

An interesting pattern was observed in *Wab1-R* plants with mild auricle extension phenotypes. In most cases, sectors in these plants had auricle extension to the midrib side of the sector, but recovered normal tissue identity both within the sector and on the marginal side of the sector (e.g. Figure 3.5 A, B). In plants exhibiting more severe phenotypes such as ectopic auricle and sheath, sectors with normal tissue identity were flanked by mutant tissue on both sides. These results suggest that normal (*wab1*) cells may have a directional effect on adjacent *Wab1-R* cells. There was no obvious relationship between recovery of tissue identity and sector size.

Ectopic sheath tissue in *Wab1-R* and *Lg1-R;Wab1-R* mutants

In *Wab1-R* mutants, 75% (15/20) of the sectors adjacent to ectopic sheath-like tissue exhibited normal blade characteristics (Table 3.3). These results also indicate that *Wab1-R* generally disrupts tissue patterning in a cell-autonomous manner. Figure 3.5 J shows an albino sector adjacent to a region of ectopic marginal sheath tissue, and Figure 3.5 I is a transverse section through this sector boundary. The green, *Wab1-R/wab1* mutant tissue has characteristics of marginal sheath tissue; it is thin, has widely spaced veins, the adaxial surface is hairless, and the abaxial surface has long hairs without multicellular bases (Figure 3.5 I). In contrast, the adjacent albino *wab1/-* tissue exhibits histological organisation and epidermal features specific to normal blade tissue (Figure 3.4 D).

In *Lg1-R;Wab1-R* double mutants, all (26/26) scorable *wab1/-* sectors exhibited normal blade characteristics, indicating that *Wab1-R* acts completely autonomously in the absence of *Lg1* (Table 3.3). The widest sectors were located at the margin, and restored the leaf half to a more normal shape and width (Figure 3.6 A, B). Figure 3.6 A shows a yellow *wab1 v4-R/-* sector that occurred at the margin. The yellow blade tissue has almost doubled the width of the leaf base. The sector shown in Figure 3.6 C was sectioned and examined by SEM (Figure 3.6 D, E). In transverse section, there is a sharp boundary between albino *wab1/-* blade tissue and green *Wab1-R/wab1* tissue with veins appressed against the abaxial surface, typical of sheath (Figure 3.6 D). The SEM shows crenulated blade cells to the left of the sector boundary (arrowhead), and smooth-walled, elongated sheath-like cells to the right (Figure

3.6 E). Figure 3.6 F is a transverse section through another sector boundary, illustrating the abrupt transition between albino blade tissue and green tissue with long abaxial hairs and other characteristics typical of marginal sheath.

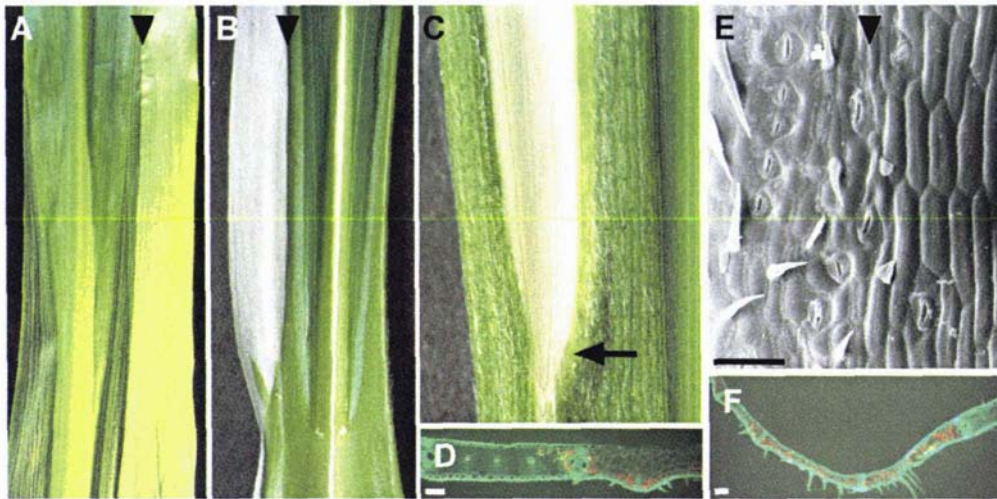


Figure 3.6. Phenotypes of *wab1*^{-/-} sectors in *Ig1-R;Wab1-R* leaves. (A) Abaxial view of yellow *v4-R wab1*^{-/-} sector, and (B) adaxial and (C) abaxial view of white, *w3-R wab1*^{-/-} sectors adjacent to ectopic sheath tissue. Arrowheads in (A) and (B) mark sector borders. (D) Fluorescence micrograph of a transverse section through the inner sector boundary of leaf shown in (C). Green *Ig1-R;Wab1-R* tissue has histological organisation of sheath, and albino *wab1*^{-/-} tissue exhibits blade histology. (E) SEM of adaxial surface of sector boundary shown in (C) and (D), illustrating the sharp boundary between epidermal cell types in *Ig1-R;Wab1-R/wab1*^{-/-} tissue (right of arrowhead) and *Ig1-R;wab1*^{-/-} tissue (left of arrowhead). (F) Fluorescence micrograph of a transverse section through another sector adjacent to marginal sheath-like tissue. The adaxial surface of green sheath-like tissue in (D) and (F) is hairless, whereas the albino tissue has hairs specific to blade. Scale bar = 100µm in (D-F).

In summary, mixed layer sectors behaved differently in *Wab1-R* and *Ig1-R;Wab1-R* plants. In *Wab1-R* plants, some mixed layer sectors exhibited the *Wab1-R* phenotype, whereas none of the mixed layer sectors in *Ig1-R;Wab1-R* plants exhibited the *Wab1-R* phenotype. Thus, *Wab1-R* may act non-autonomously between layers or laterally, but only in a *Lg1* background.

Effect of *wab1*^{-/-} sectors on leaf width

The leaf blades of *Wab1-R* and especially *Ig1-R;Wab1-R* mutants are significantly narrower than those of wild-type siblings (Hay and Hake, 2004). To investigate the effect of *wab1*^{-/-} sectors on *Wab1-R* and *Ig1-R;Wab1-R* leaf width, the width of sectored and non-sectored halves of each leaf were measured and compared. In both *Wab1-R* and *Ig1-R;Wab1-R* plants, there is a small but significant increase in the median width of the sectored half of the blade relative to the non-sectored half (Table 3.4). Measurements made at the

sheath midpoint show no significant difference in width between leaf-halves, indicating that *Wab1-R* specifically disrupts lateral growth of blade tissue (Table 3.4). No difference between the widths of sector and non-sector leaf-halves was found in wild-type and *Ig1-R* control plants.

Table 3.4. Median differences in the width of *wab1l*-sector and non-sector leaf-halves at the blade-sheath boundary and sheath midpoint. The sector and non-sector sides of each leaf were measured from midrib to margin at the blade-sheath boundary and sheath midpoint. The width of the non-sector leaf-half was subtracted from that of the sector half to give an absolute difference in leaf-half widths. A value greater than 0 indicates that the sector half of the leaf is wider than the non-sector half. The data were analysed using a non-parametric 1-sign test to determine if the median values were significantly different from 0. * indicates values that are significantly different from 0 at the 0.05 confidence level.

Position of measurement	Genotype	N	Median difference (mm)	P-value
Blade-sheath	Wild-type	51	0.0	1.000
	<i>Wab1-R</i>	93	1.0	0.013*
	<i>Ig1-R</i>	118	0.0	0.146
	<i>Ig1-R;Wab1-R</i>	164	0.5	0.001*
Mid-sheath	Wild-type	29	0.0	0.189
	<i>Wab1-R</i>	33	0.0	0.690
	<i>Ig1-R</i>	48	0.0	0.324
	<i>Ig1-R;Wab1-R</i>	67	0.0	0.672

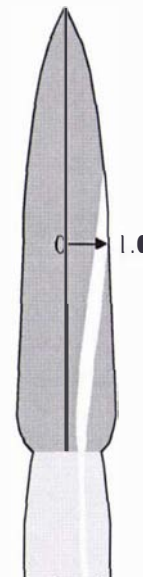
Analysis of the data suggested a relationship between sector position and effect on leaf width. In both *Wab1-R* and *Ig1-R;Wab1-R* plants, sectors near the midrib were not associated with a significant difference in leaf-half width, whereas leaf-halves with sectors in lateral and marginal positions were significantly wider than non-sector leaf halves (Table 3.5 A).

Many of the widest sectors in *Ig1-R;Wab1-R* plants were yellow, *v4-R* sectors. To test if there is a difference in behaviour between *v4-R* and *w3-R* sectors, the median difference in leaf-half widths was evaluated separately for yellow and white sectors in *Ig1-R;Wab1-R* and *Ig1-R* plants. Sectors near the midrib were not included in this analysis as we had previously determined that they have no significant effect on leaf width. Surprisingly, yellow sectors had a significantly greater effect on leaf width than the white sectors (Table 3.5 B). No difference was detected between yellow and white sectors in *Ig1-R* controls, indicating that

this effect is not inherent to *v4-R* sectors, but only occurs in a *Wab1-R* background.

Table 3.5. Median differences in *wab1*-sectored and non-sectored leaf-half widths, and effect of sector position. The sectored and non-sectored sides of each leaf were measured from midrib to margin at the blade midpoint. The width of the non-sectored leaf-half was subtracted from that of the sectored half to give an absolute difference in leaf-half width. Differences in leaf-half widths were analysed using a non-parametric 1-sign test to determine if the median values were significantly different than 0 at the 0.05 confidence level. (A) The relative lateral position of each sector is represented as the distance from the midrib to the closest sector border, divided by the width of the entire leaf-half. Values range from 0 for sectors at the midrib to near 1.0 for sectors at the margin. (B) Median differences were calculated separately for white (*w3-R*) and yellow (*v4-R*) sectors in *Ig1-R* and *Ig1-R;Wab1-R* leaves. * indicates values that are significantly different from 0 at the 0.05 confidence level.

Genotype	Lateral position of sector	N	Median difference (mm)	P value
A.				
Wild-type	0-1.0	50	0.0	1.000
<i>Wab1-R</i>	0-1.0	83	1.0	0.004*
	0-0.29	19	0.0	1.000
	0.3-1.0	64	1.0	0.001*
<i>Ig1-R</i>	0-1.0	140	0.0	0.440
<i>Ig1-R;Wab1-R</i>	0-1.0	180	1.0	<0.001*
	0-0.29	64	0.0	0.390
	0.3-1.0	116	2.0	<0.001*
B.				
<i>Ig1-R;w3</i>	0.3-1.0	44	0.0	1.000
<i>Ig1-R;v4</i>	0.3-1.0	18	-0.5	0.424
<i>Ig1-R;Wab1-R w3</i>	0.3-1.0	77	1.5	<0.001*
<i>Ig1-R;Wab1-R v4</i>	0.3-1.0	39	3.5	<0.001*



3.3.4 Mosaic analysis of *Ig1-R*

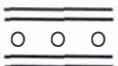
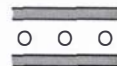
Previous mosaic analyses indicate that *Lg1* acts cell-autonomously to specify ligule and auricle tissues (Becraft *et al.*, 1990). My results indicate that *Lg1* has a role in positioning of the blade-sheath boundary and promotes lateral growth at the base of the blade. To determine if these effects are cell-autonomous or non-autonomous and to test the hypothesis that *Lg1* conditions ectopic auricle tissue in *Wab1-R* leaves, sectors of albino *Ig1-R* tissue were induced in *Lg1;wab1* and *Lg1;Wab1-R* plants (Figure 3.2). From this mosaic analysis, a

total of 66 *al Ig1-R/-* sectored leaves were identified in 31 *Lg1;wab1* plants and 98 sectored leaves were identified in 44 *Lg1;Wab1-R* plants.

Effects of *Ig1-R/-* sectors on normal and *Wab1-R* ectopic auricle tissue

Sectors of white, *Ig1-R/-* tissue in *Lg1;wab1* and *Lg1;Wab1-R* plants were scored for their effects on normal ligule and auricle tissues (Table 3.6). Sectors in *Lg1;Wab1-R* plants were also scored for their effects on ectopic auricle and sheath tissue. Sectors through the auricle had either auricle or blade characteristics. Sectors through the ligule were scored as normal, missing or reduced. Missing ligules were completely deleted within sectors. Reduced ligules were present, but the ligule was shorter within the sector than in surrounding tissue.

Table 3.6. Summary of *Ig1-R/-* sector phenotypes. *Ig1-R/-* sectors in *wab1* (A) and *Wab1-R* (B) leaves were scored for layer composition and tissue identity. Sectors were scored as "Bl" if they displayed characteristics of blade tissue, "Aur" if they exhibited auricle characteristics and "Sh" if they exhibited sheath characteristics. Sectors through the ligule were scored as "N" if the ligule appeared normal, "R" if the ligule was reduced in height within the sector and "M" if the ligule was completely missing within the sector.

	Number of scorable sectors	Sector phenotype	All sector types				
				white L1/ white L2	green L1/ white L2	white L1/ mixed L2	green L1/ mixed L2
A. <i>wab1</i>							
Auricle	31	Aur	22 (71%)	1	13	0	8
		Bl	9 (29%)	1	7	1	0
Ligule	33	N	15 (46%)	1	9	0	5
		R	6 (18%)	0	5	0	1
		M	12 (36%)	2	7	1	2
B. <i>Wab1-R</i>							
Auricle	67	Aur	21 (31%)	3	6	0	12
		Bl	46 (69%)	14	27	1	4
Ligule	74	N	24 (32%)	5	9	2	8
		R	13 (18%)	3	7	0	3
		M	37 (50%)	9	24	0	4
Ect auricle	35	Aur	7 (20%)	0	3	1	3
		Bl	28 (80%)	10	18	0	0
Ect sheath	9	Sh	5 (56%)	1	4	-	-
		Bl	4 (44%)	1	3	-	-

In *wab1* plants, 71% (22/31) of *Ig1-R/-* sectors that passed through the auricle had normal auricle characteristics (Table 3.6 A). Fourteen of these sectors had all white, *Ig1-R/-* mesophyll layers. This result differs from the findings of Becraft *et al.* (1990), who found that sectors with all white *Ig1-R/-* mesophyll layers developed blade characteristics in all (251/251) cases. Four sectors that had white epidermis were scorable for ligule characteristics. In three cases the ligule was missing within the sector, while in one case the ligule appeared normal. Surprisingly, the about half (14/29) of the sectors with green epidermis had ligules that were reduced or missing. This differs from the results of Becraft *et al.* (1990), who found that green, *Lg1* epidermal tissue was strictly correlated with the development of a normal-looking ligule.

In *Wab1-R* plants, 67 *Ig1-R/-* sectors were scorable for their effect on normal auricle tissue (Table 3.6 B). Of these, 31% (21/67) had auricle characteristics and 69% (46/67) had blade characteristics. The majority (41/50) of sectors with white mesophyll had blade characteristics, whereas, the majority (12/17) of sectors with some green mesophyll had auricle characteristics. In *Wab1-R* plants, 74 sectors were scorable for ligule characteristics. The majority of these (50/74) had ligules that were reduced or missing.

Only *Ig1-R/-* sectors that traversed ectopic auricle tissue in *Wab1-R* leaves could be scored for their effect on this mutant phenotype. Thus, only 35 sectors were scorable for ectopic auricle identity. Sectors adjacent to ectopic auricle tissue were analysed for phenotypic expression (blade or auricle identity) and cell layer composition (green *Lg1/Ig1-R* or albino *Ig1-R/-*) (Table 3.6 B). Of the sectors that were scorable for ectopic auricle, most (80%) showed normal blade characteristics within the sector. An example of a *Ig1-R/-* sector with blade characteristics is shown in Figure 3.7. The sectored tissue is thinner than the surrounding ectopic auricle tissue, causing buckling of the leaf (Figure 3.7 A). Sections through the sectored region show that the surrounding green *Lg1/Ig1-R* tissue has large cells and long hairs without multicellular bases characteristic of auricle tissue. White *Ig1-R/-* tissue is thinner and blade-like (Figure 3.7 B, C).

All (10/10) of the sectors that had all white cell layers, and most (18/21) of the sectors with white mesophyll and green epidermis, had normal blade identity

(Figure 3.7 B). In contrast, all (4/4) of the sectors with green mesophyll layers had auricle characteristics. No examples of conversion of ectopic auricle to sheath tissue were observed.

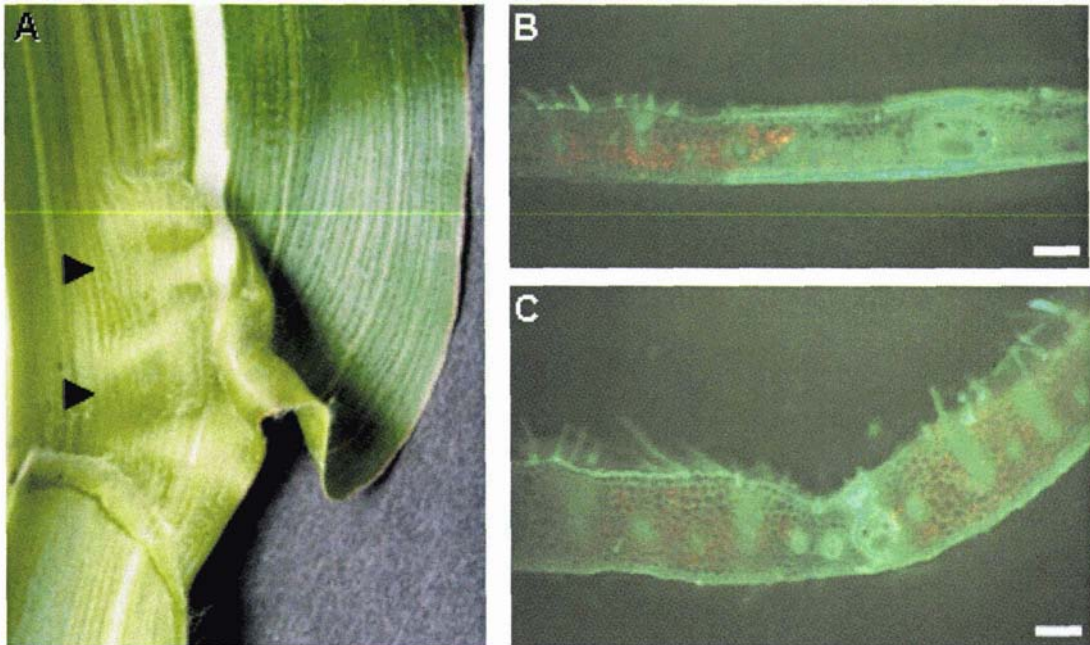


Figure 3.7. Phenotype of *Ig1-R/-* sector in *Lg1;Wab1-R* leaf. (A) *Wab1-R* leaf with white, *Ig1-R/-* sector that traverses ectopic auricle tissue. (B) Hand-section through sector boundary at position indicated by upper arrowhead. Green *Lg1* tissue has long hairs without multicellular bases characteristic of auricle tissue. White *Ig1-R/-* tissue has bulliform cells and prickly hairs characteristic of blade tissue. (C) Hand-section through sector region indicated by lower arrowhead. Green tissue is thick and auricle-like, with large cells and long hairs. White *Ig1-R/-* tissue is thinner, with smaller cells. Scale bars = 200 μ m.

Effects of *Ig1-R/-* sectors on *Wab1-R* ectopic sheath tissue

In *Wab1-R* plants, only *Ig1-R/-* sectors that traversed ectopic sheath tissue were scorable for this characteristic. Sectors were analysed for phenotypic expression and cell layer composition. Of the nine scorable sectors, 5 (56%) sectors had sheath identity and 4 had blade identity (Table 3.6B). Only two completely white (*Ig1-R/-*) sectors were obtained. One of these had sheath-like characteristics, while the other had normal blade characteristics. Of the seven sectors with green epidermis and white internal layers, 4 had sheath-like characteristics, while 3 had the characteristics of blade tissue. No sectors were obtained that were scorable for ectopic sheath and had green internal cell layers.

Effects of *lg1-R/-* sectors on leaf width

We hypothesised that if *Lg1* promotes lateral growth in a cell-autonomous manner, then *lg1-R/-* sectors should undergo less lateral growth than surrounding green tissue. Therefore, leaf halves with sectors should be narrower than non-sectored leaf-halves. The sectored and non-sectored halves of each leaf were measured from midrib to margin at the blade-sheath boundary and at the blade mid-point. Measurements were made of 66 *wab1* leaves with *lg1-R/-* sectors and 96 *Wab1-R* leaves with *lg1-R/-* sectors. Fewer leaves were measured at the blade midpoint than at the base of the blade, as some sectors intersect the margin of the leaf before they reach the blade midpoint. No significant difference was found in the width of sectored and non-sectored leaf-halves in either the *wab1* or *Wab1-R* backgrounds (Table 3.7).

Table 3.7. Median differences in the width of *lg1-R/-* sectored and non-sectored leaf-halves. The sectored and non-sectored sides of each leaf were measured from midrib to margin at the blade midpoint and the base of the blade. The width of the non-sectored leaf-half was subtracted from that of the sectored half to give an absolute difference in leaf-half widths. A value greater than 0 indicates that the sectored half of the leaf is wider than the non-sectored half. The data were analysed using a non-parametric 1-sign test to determine if the median values were significantly different than 0 at the 0.05 confidence level.

Position of measurement	Genotype	N	Median difference (mm)	P-value
Mid-blade	<i>wab1</i>	63	0.0	0.775
	<i>Wab1-R</i>	91	0.0	0.289
Base blade	<i>wab1</i>	66	0.0	0.890
	<i>Wab1-R</i>	96	0.0	0.320

3.3.5 Clonal analysis of *Wab1-R* leaves

Wab1-R leaves are narrower than wild-type leaves (Hay and Hake, 2004). To investigate the nature of the narrow leaf phenotype, a cell lineage analysis was undertaken. Clonal sectors of white (*lw-R/-*) cells were induced in *Wab1-R* plants and wild-type (*wab1*) controls. 37 sectored leaves were obtained in 23 wild-type plants and 81 sectored leaves were obtained in 32 *Wab1-R* plants. Eleven sectors were recorded in the culm of wild-type plants, and 28 sectors in *Wab1-R* plants.

Leaves were measured from midrib to margin at the blade midpoint and at the base of the blade. *Wab1-R* leaves were significantly narrower than wild-type leaves (Table 3.8). The difference in width was more pronounced at the blade midpoint than at the base of the blade.

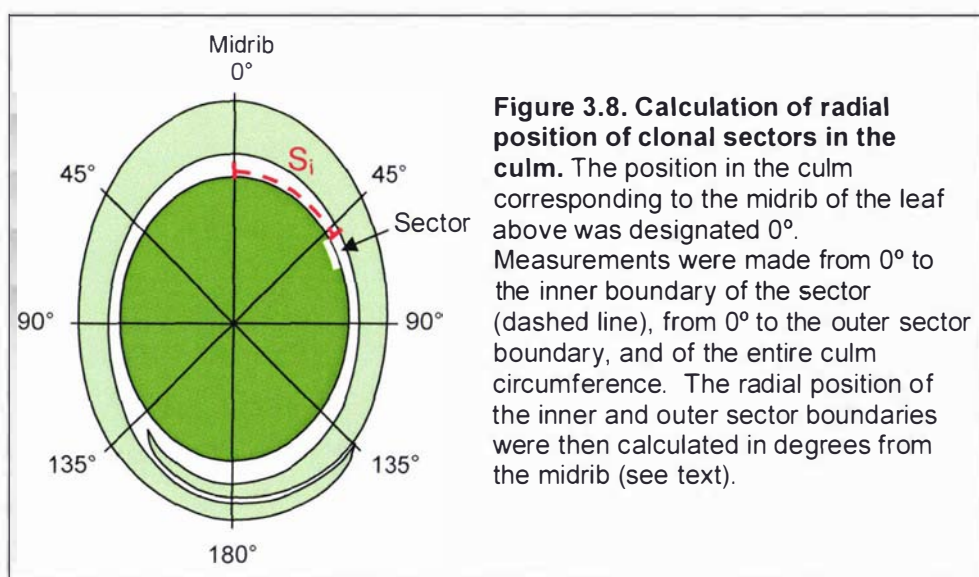
Sectors were assigned to one of three lateral positions within the leaf blade; midrib (0-0.29), lateral (0.3-0.59) or marginal (0.6-1.0). Mean sector widths in *Wab1-R* and wild-type leaves were compared separately for sectors in each lateral position (Table 3.8). At the blade midpoint, mean sector widths in midrib and lateral domains were not significantly different for *Wab1-R* and wild-type leaves. However, only three lateral position sectors were obtained in wild-type leaves and these were notably wider than sectors in *Wab1-R* leaves. Sectors in the marginal part of the leaf were significantly wider in wild-type leaves than in *Wab1-R* leaves. At the base of the blade, midrib domain sectors were significantly wider in *Wab1-R* leaves than in wild-type leaves. There was no significant difference in the width of *Wab1-R* and wild-type lateral or marginal domain sectors measured at the base of the blade.

Table 3.8. Mean widths of clonal sectors in *Wab1-R* and wild-type leaves. Sector width and leaf-half width were measured at the blade midpoint and the base of the blade. Mean sector widths were calculated separately for sectors near the midrib (sector position 0-0.29), in the lateral domain (0.3-0.59), and near the margin (0.6-1.0). Wild-type and *Wab1-R* means were compared by Student's T-test to determine if they are significantly different at the 0.05 confidence level. * indicates values that are significantly different. Sample sizes for each category are indicated in brackets. SE = standard error.

		Sector position		Wild-type	<i>Wab1-R</i>	P-value
Mid-blade	Half-leaf width (mm)		Mean SE	34.2 (N=35) 1.6	19.7 (N=66) 0.2	<0.001*
	Sector width (mm)	0-0.29	Mean SE	1.9 (N=13) 0.3	2.0 (N=17) 0.6	0.873
		0.3-0.59	Mean SE	4.5 (N=3) 0.3	2.9 (N=11) 0.4	0.057
		0.6-1.0	Mean SE	3.1 (N=19) 0.6	1.9 (N=38) 0.3	0.048*
Base blade	Half-leaf width (mm)		Mean SE	34.8 (N=37) 2.0	29.5 (N=81) 1.3	0.020*
	Sector width (mm)	0-0.29	Mean SE	1.3 (N=18) 0.2	2.3 (N=37) 0.3	0.036*
		0.3-0.59	Mean SE	4.0 (N=13) 1.0	4.1 (N=28) 0.7	0.940
		0.6-1.0	Mean SE	3.5 (N=6) 1.3	2.9 (N=16) 0.6	0.670

Hay and Hake (2004) hypothesised that the narrowness of *Wab1-R* leaves is due to the deletion of a lateral domain. If this hypothesis is correct, then we would predict that sectors that originate in this particular region of the SAM would not extend into the leaf blade. The culm is not affected by *Wab1-R* and, since it is a radial structure, the position of clonal sectors in the culm approximates the position of sectors in the SAM from which it is derived (Scanlon, 2000). Therefore, to determine if a lateral domain is deleted in *Wab1-R* leaves, the position of each clonal sector in the culm was recorded and its position calculated in degrees from the midrib (Figure 3.8). It was then noted whether the sector continued into the leaf above.

From the *Wab1-R* clonal analysis, sectors were obtained that covered all radial positions of the culm except the region between 0° and 31°. All sectors that were observed in the culm continued into the blade of the leaf above. These results do not support the hypothesis that the *Wab1-R* narrow leaf phenotype is caused by the deletion of a lateral domain.

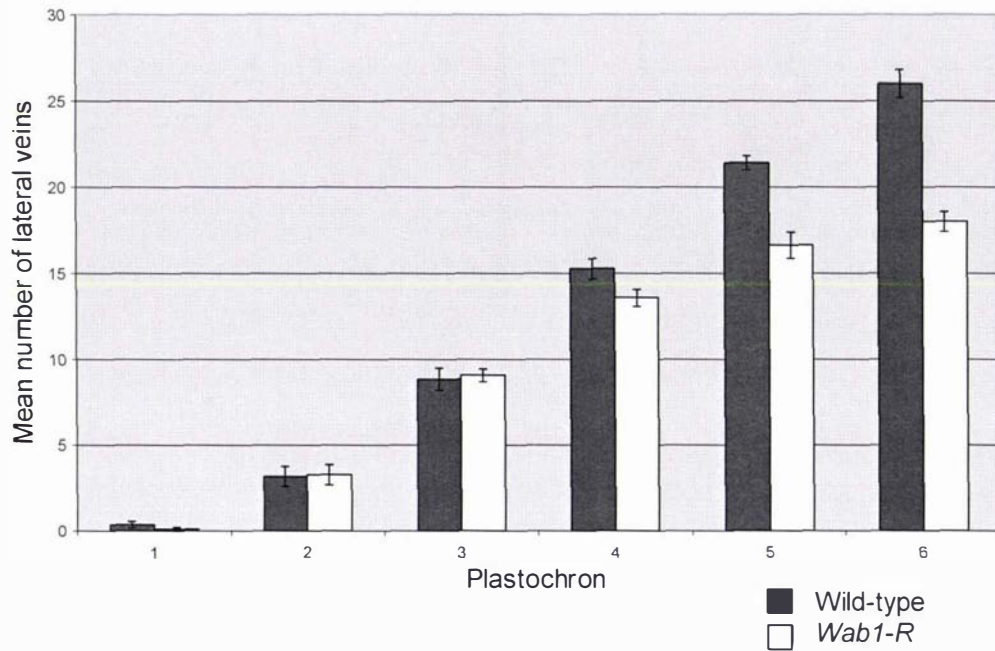


3.3.6 *Wab1-R* leaves have fewer lateral veins by plastochron 4

Hay and Hake (2004) found that *Wab1-R* leaves are narrower and have fewer lateral veins than wild-type leaves. To determine when the reduction in lateral veins is first apparent, lateral veins were counted in transverse sections of

Wab1-R and wild-type (B73) leaf primordia. My data show no significant difference in the number of lateral veins in *Wab1-R* and wild-type leaf primordia at stages P1, P2 or P3 (Figure 3.9). At P4, there was a significant difference in the number of lateral veins in *Wab1-R* and wild-type leaf primordia. Wild-type leaf primordia at P4 had an average of 15.3 lateral veins, whereas *Wab1-R* leaf primordia at the same stage had an average of 13.4 lateral veins. At P5 the difference was even more pronounced – wild-type leaf primordia had an average of 21.4 lateral veins, whereas *Wab1-R* leaf primordia had an average of 16.6 lateral veins.

A. Lateral vein number in wild-type and *Wab1-R* leaf primordia



B.

Plastochron		Wild-type (B73)	<i>Wab1-R</i>	P-value
P1	Mean	0.4	0.1	0.225
	SE	0.2 (N=8)	0.1 (N=9)	
P2	Mean	3.2	3.3	0.878
	SE	0.6 (N=12)	0.6 (N=11)	
P3	Mean	8.8	9.1	0.752
	SE	0.7 (N=12)	0.4 (N=16)	
P4	Mean	15.3	13.4	0.031*
	SE	0.6 (N=8)	0.5 (N=14)	
P5	Mean	21.4	16.6	<0.001*
	SE	0.4 (N=5)	0.8 (N=8)	
P6	Mean	26	18	<0.001*
	SE	0.8 (N=4)	0.6 (N=3)	

Figure 3.9. Lateral vein number in wild-type and *Wab1-R* leaf primordia.

(A) Lateral veins were counted in wild-type (B73) and *Wab1-R* leaf primordia at stages P1-P6. The mean number of lateral veins was calculated separately for wild-type and *Wab1-R* leaf primordia at each plastochron. Mean number of lateral veins in wild-type and *Wab1-R* leaf primordia is plotted against plastochron number. Bars represent standard error.

(B) The wild-type and *Wab1-R* means for each plastochron were compared by Student's t-test to determine if they are significantly different at the 0.05 confidence level. * indicates values that are significantly different. SE = standard error.

3.4 Discussion

In the maize leaf, ligule and auricle form at the boundary between the blade and sheath. *Lg1* has been implicated in the propagation of a signal that correctly positions this boundary, and is necessary for the development of ligule and auricle tissues. The dominant *Wab1-R* mutation affects medial-lateral and proximal-distal patterning, resulting in narrow leaves and inappropriate cell differentiation. The recessive *Ig1-R* mutation exacerbates the *Wab1-R* phenotype. *Lg1* expression is activated precociously in *Wab1-R* leaves and may counteract some effects of the *Wab1-R* mutation (Foster *et al.*, 2004). A mosaic analysis of *Wab1-R* was conducted in *Lg1* and *Ig1-R* backgrounds to determine if *Wab1-R* affects leaf development in a cell-autonomous manner. This analysis showed that *Wab1-R* generally acts cell-autonomously to disrupt proximal-distal patterning. Examples of *Wab1-R* non-autonomy were only observed in a *Lg1* background, supporting a role for *Lg1* in signal propagation. A mosaic analysis of *Ig1-R* in a *Wab1-R* background indicated that *Wab1-R* ectopic auricle tissue is conditioned by *Lg1*. The mosaic analyses and comparison of mutant leaf shapes revealed previously unreported functions of *Lg1* in both normal leaf development and in the dominant *Wab1-R* mutant. A detailed discussion of these results is presented below.

3.4.1 *Lg1* influences cell-autonomy of the *Wab1-R* phenotype

In the majority of *Wab1-R* leaves and in all *Ig1-R;Wab1-R* leaves, scorable *wab1/-* sectors exhibited characteristics of normal blade tissue, whereas adjacent tissue differentiated inappropriately as sheath or auricle. The sharp boundaries between tissue types were coincident with sector boundaries, indicating that *Wab1-R* generally acts cell autonomously in the lateral dimension to disrupt normal proximal-distal patterning.

Twelve of the 51 scorable sectors showed some aspect of the *Wab1-R* mutant phenotype and thus are exceptions to the general rule of cell-autonomy. Of these 12, two were completely albino and therefore had no layer with *Wab1-R*. Of the 10 remaining sectors, half carried *Wab1-R* only in the epidermis, and half carried *Wab1-R* in the epidermis and/or one mesophyll layer. Thus, *Wab1-R*

may act non-autonomously in the lateral dimension and/or between cell layers to influence cell identity in *wab1/-* tissue.

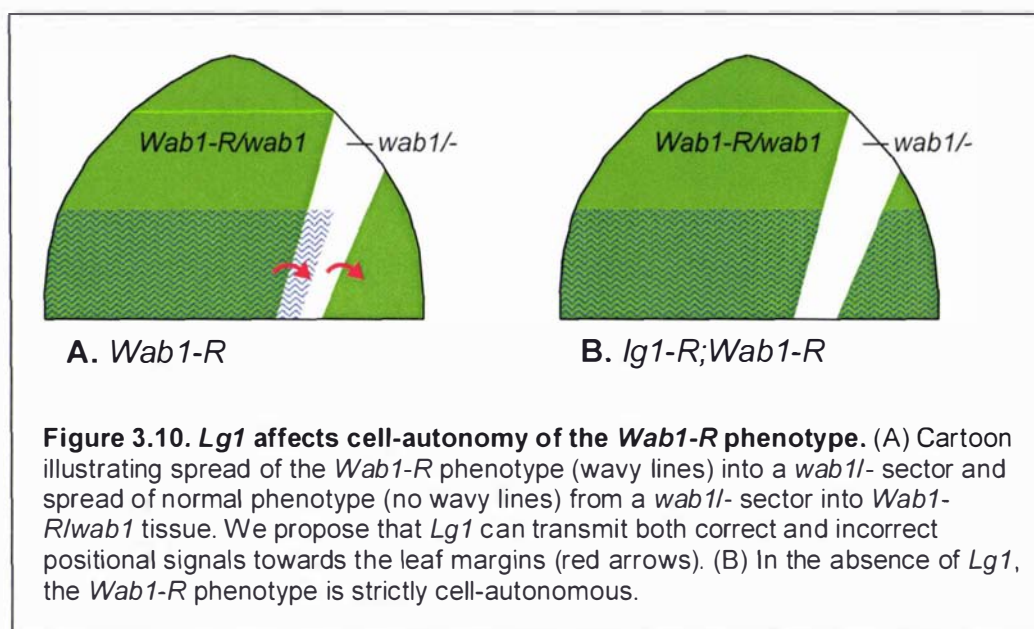
In contrast, all *wab1/-* sectors in *lg1-R;Wab1-R* plants had normal cell types. *Wab1-R* in either the epidermis or a single mesophyll layer did not condition the mutant phenotype (12 of 26 sectors). These results suggest that normal *Lg1* function is required for *Wab1-R* to act non-autonomously.

A few cases of non-autonomy were observed in which the normal blade phenotype (*wab1*) was seen on the margin side of the sector as well as within the sector (Figure 3.5 A, B). The extension of the normal phenotype from the sector into genetically *Wab1-R* cells was only seen in mildly affected plants. This pattern could reflect the fact that the *Wab1-R* phenotype is most severe in the lateral domain. Alternatively, it may be that once correct proximal-distal patterning is established within *wab1/-* tissue, this information can be propagated towards the margins into *Wab1-R/wab1* tissue, but only if *Wab1-R* activity is low. Interestingly, non-autonomy was never documented in *lg1-R;Wab1-R* plants. Cells in *lg1-R;wab1/-* sectors always had blade identity and cells outside of these sectors always had sheath identity. Thus, *Lg1* may affect the autonomy of *Wab1-R* in both lateral and transverse dimensions.

Previous mosaic analyses of *lg1-R* have indicated that *Lg1* is involved in signal propagation, while also acting cell-autonomously to induce ligule and auricle (Becraft *et al*, 1990; Becraft and Freeling, 1991). One of the key findings of this work was the observation that ligule and auricle reinitiated immediately within *Lg1/lg1-R* tissue on the margin side of *lg1-R/-* sectors, but was displaced proximally. The authors interpreted this as evidence that *Lg1* is involved in the propagation of a “make ligule and auricle” signal, and that this signal moves from the midrib towards the margins. Observations from the current analysis support this hypothesis.

These data suggest that *Wab1-R* alters positional information in a cell-autonomous manner, resulting in inappropriate cell differentiation. We speculate that *Lg1* is responsible for the non-autonomous effects of *Wab1-R* that were observed in our mosaic analysis. According to this model, *Lg1* may occasionally

transmit the signal to initiate ectopic auricle from *Wab1-R* tissue into *wab1/-* sectors (Figure 3.10 A). Similarly, *Lg1* may relay correct positioning of the auricle and ligule from *wab1/-* sectors into adjacent *Wab1-R* tissue. In the absence of *Lg1*, there is no lateral signalling from *Wab1-R* tissue into *wab1/-* sectors, or from sectors into *Wab1-R* tissue (Figure 3.10 B).



3.4.2 Loss of *Wab1-R* is associated with an increase in leaf width

A significant difference was found between the widths of sectored (i.e. cells that have lost *Wab1-R*) and non-sectored leaf-halves in *Wab1-R* and *lg1-R;Wab1-R* plants, but not in wild-type or *lg1-R* control plants. No obvious differences in cell width were seen between similar cell types in sectored and non-sectored tissue (data not shown). Therefore, it can be inferred that the increase in lateral growth associated with *wab1/-* sectors was the result of increased longitudinal cell divisions. It is difficult to determine if increased cell division was confined to the sectored tissue or occurred throughout the sectored leaf-half. The fact that a significant difference was recorded between sectored and non-sectored leaf-half widths suggests that *Wab1-R* restricts lateral growth with at least some degree of autonomy. If *Wab1-R* were entirely non-autonomous, then the presence of a *wab1/-* sector would have no effect on leaf-half width. A mosaic analysis of the *tangled* mutation in maize found that the cell division defect is autonomous in both the lateral and transverse dimensions (Walker and Smith,

2002). Thus, there is precedence for strict autonomy of cell division patterns in chimeric tissues.

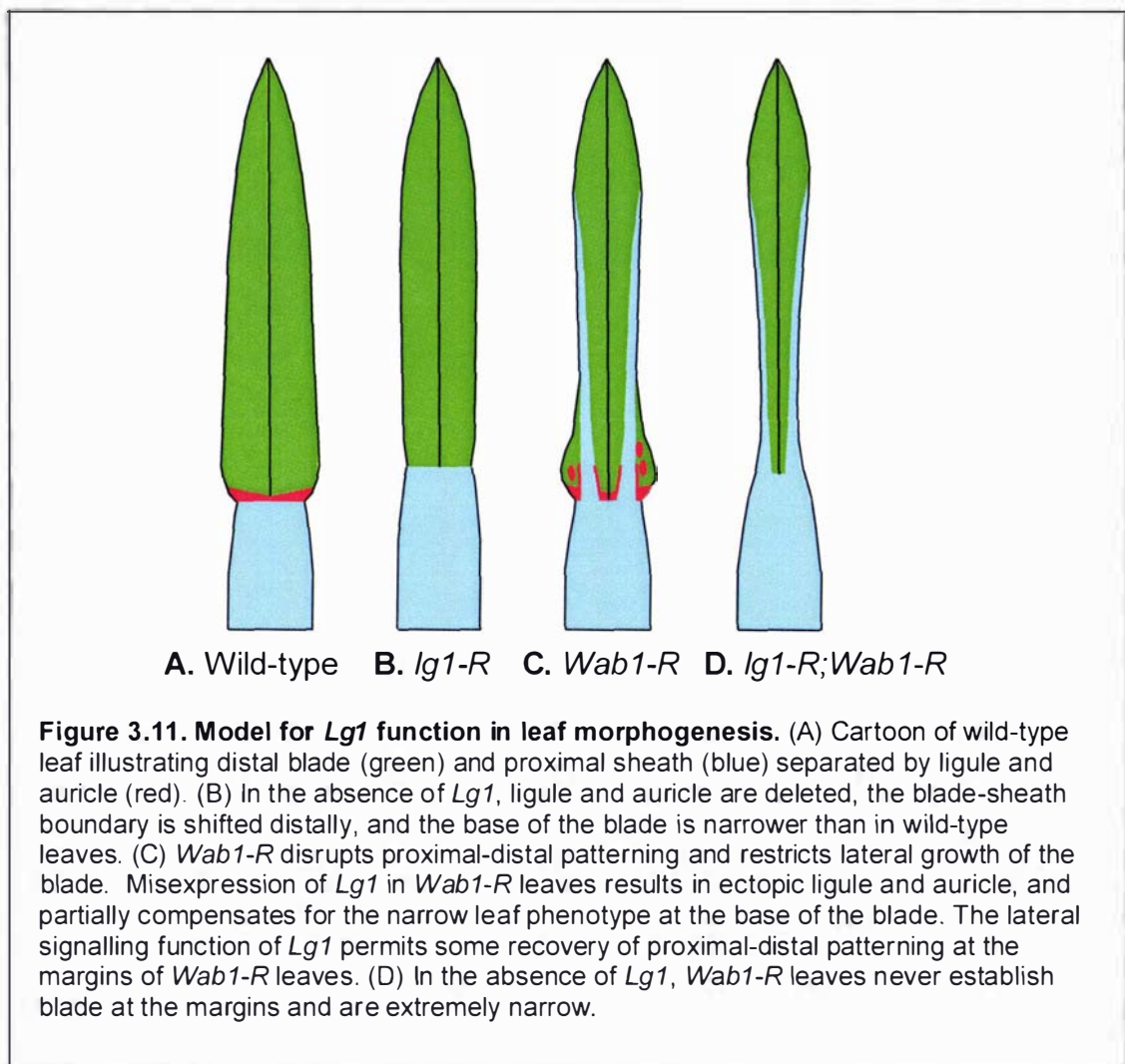
In both *Ig1-R;Wab1-R* and *Wab1-R* leaves, sectors positioned near the midrib had no significant effect on leaf-half width, whereas sectors in the outer two thirds of the leaf-half were associated with significant differences between sectored and non-sectored leaf-half widths. This result could reflect the fact that sectors near the midrib tend to be very narrow, and hence have a minimal effect on lateral growth. Alternatively, it may reflect the fact that the *Wab1-R* phenotype primarily affects regions outside the midrib domain (Hay and Hake, 2004).

3.4.3 The role of *Lg1* in leaf morphogenesis

This study provides evidence of previously unreported functions of *Lg1* in leaf morphogenesis. *Ig1-R* leaves were found to have longer sheaths and shorter blades than wild-type (*Lg1//Ig1-R*) siblings, although overall leaf length was not significantly different. Thus, the blade-sheath boundary was shifted distally in *Ig1-R* leaves (Figure 3.11 B). These results suggest that *Lg1* is required for correct positioning of the blade-sheath boundary.

It was also determined that *Ig1-R* leaves were narrower at the base of the blade than wild-type siblings (Figure 3.11 B). A comparison of clonal sectors in *Ig1-R* and wild-type control plants indicated that margin and lateral sectors were significantly narrower in *Ig1-R* mutants than in wild-type leaves. These results imply that *Lg1* promotes lateral growth at the base of the blade. Sylvester and co-workers (1990) showed that a localised increase in both longitudinal and transverse anticlinal divisions generates a band of small cells across the base of the leaf primordium. This preligule band is a necessary prerequisite for the formation of ligule and auricle. *Ig1-R* mutants are specifically defective in longitudinal divisions in the preligule region and at the base of the blade. *Lg1* may promote lateral growth via a direct effect on the rate and orientation of cell divisions. Alternatively, the development of the auricle itself may drive lateral growth of the lower leaf blade, ensuring the coordinated expansion of the leaf.

We suggest that misexpression of *Lg1* is responsible for the ectopic auricle and much of the lateral growth at the base of *Wab1-R* leaf blades. This is reflected in the shape of *Wab1-R* leaves, which are relatively wide at the base of the blade, but narrow in more distal areas (Figure 3.11 C). We speculate that the lateral signalling function of *Lg1* permits some recovery of proximal-distal patterning at the margins of *Wab1-R* leaves (Figure 3.11 C). In the absence of *Lg1*, *Wab1-R* leaves never establish blade in this region, and are extremely narrow (Figure 3.11 D).



3.4.4 Ectopic auricle tissue in *Wab1-R* leaves is conditioned by *Lg1*

To further investigate interactions between *Lg1* and *Wab1-R*, a mosaic analysis of *lg1-R* was conducted in a *Wab1-R* background. *lg1-R/-* sectors were analysed for their effects on ectopic auricle and sheath tissue. The majority

(28/35) of *lg1-R/-* sectors in *Wab1-R* leaves that were scorable for ectopic auricle tissue exhibited normal blade characteristics. In these cases, ectopic auricle tissue ended abruptly at sector boundaries (Figure 3.7). The results of this analysis suggest that *Lg1* acts cell-autonomously in the lateral dimension to specify ectopic auricle tissue in *Wab1-R* mutants and supports the hypothesis that misexpression of *Lg1* is responsible for the ectopic auricle tissue in *Wab1-R* leaf blades.

All (10/10) of the sectors that were completely white and traversed ectopic auricle tissue had blade identity (Table 3.6 B). This result suggests that *Lg1* acts strictly cell-autonomously in the lateral dimension to condition ectopic auricle in *Wab1-R* leaves. Where *Lg1* was present only in the epidermis, the majority (18/21) of sectors that traversed ectopic auricle tissue had blade identity. The observation that a small number (3/21) of such sectors exhibited auricle characteristics may indicate that there is some *Lg1*-mediated signalling between the epidermis and internal cell layers. However, there are alternative explanations. The *lg1-R* phenotype varies in expressivity, thus these sectors may reflect a lack of expressivity rather than non-autonomy by *Lg1* (Becraft *et al.*, 1990). Alternatively, they could be a result of recombination events between *Lg1* and *al-R*. Becraft *et al.* (1990) estimated that there may be 7% recombination between *lg1-R* and *al-R*. The current data do not allow these possibilities to be distinguished.

Only four sectors with internal layers of green, *Lg1* cells were obtained that were scorable for the ectopic auricle phenotype (Table 3.6 B). All of these sectors had auricle identity. This result suggests that *Lg1* in internal cell layers may act non-autonomously to condition the *Wab1-R* ectopic auricle phenotype in overlying cell layers. However, more sectors would need to be analysed to confirm this. The result is consistent with the work of Becraft *et al.* (1990), who found that *Lg1* in any cell layer is sufficient to induce the development of normal auricle in all layers.

The *Wab1-R* mutation causes distal tissues to differentiate as more proximal tissue types (Hay and Hake, 2004). In a *Lg1* background, ectopic auricle and sheath-like tissues develop in the leaf blade. In the absence of *Lg1* most of the

blade is converted to sheath-like tissue. *Lg1* has previously been shown to specify auricle tissue (Becraft *et al.*, 1990). We hypothesised that the primary *Wab1-R* defect is the "proximalisation" of distal tissues, and that ectopic auricle tissue in *Wab1-R* mutants is conditioned through ectopic expression of *Lg1*. If this hypothesis is correct, then, in the absence of *Lg1*, sheath would be the "default" tissue type. This hypothesis predicts that *lg1-R/-* sectors that traverse regions of ectopic auricle will have sheath identity.

In the mosaic analysis of *lg1-R* in *Wab1-R* plants, the majority (28/35) of sectors that passed through ectopic auricle tissue had blade identity, the remainder were auricle-like (Table 3.6 B). No examples of conversion of ectopic auricle to sheath tissue were observed. These data are consistent with the hypothesis that ectopic auricle in *Wab1-R* mutants is conditioned through *Lg1*. However, they do not support the hypothesis that sheath tissue is the default tissue type in the absence of *Lg1* function.

The results of this mosaic analysis of *lg1-R* in *wab1* leaves differed from those of previous analyses (Becraft *et al.*, 1990). Becraft *et al.* (1990) found that sectors with all white (*lg1-R/-*) mesophyll layers had blade characteristics in all (251/251) cases. In our experiment, 14/22 sectors with all white mesophyll layers had auricle characteristics (Table 3.6 A). There are a number of possible explanations for this result. Firstly, there may have been a recombination event between *al-R* and *Lg1*, such that white sectors in these leaves were *Lg1 al-R/-* rather than *lg1-R al-R/-*. Secondly, the genetic stock may have been heterozygous for a second, unlinked albino marker gene. This second marker may have been uncovered in some plants, thus creating albino sectors that were *Lg1/lg1-R*. Finally, white sectors with auricle characteristics may reflect the variable expressivity of the *lg1-R* phenotype. Vestiges of ligule and auricle often occur on upper leaves of *lg1-R* plants (Becraft *et al.*, 1990; Sylvester *et al.*, 1990). Five of the sectors we observed with auricle characteristics occurred on leaf ten or lower, suggesting that these were not the result of incomplete expressivity of the *lg1-R* phenotype. The results of this analysis also differed from those of Becraft *et al.* in that about half (14/29) of the sectors with green (*Lg1/lg1-R*) epidermis had ligules that were reduced or missing. Becraft *et al.* (1990) found that green, *Lg1* epidermal tissue was strictly correlated with the

development of a normal-looking ligule. It is not clear why our result differed from this analysis.

3.4.5 Effects of *Ig1-Rl-* sectors on *Wab1-R* ectopic sheath tissue

Nine sectors were obtained that were scorable for ectopic sheath-like tissue (Table 3.6 B). Seven had white (*Ig1-Rl-*) mesophyll with green (*Lg1/Ig1-R*) epidermis and two were entirely white. Of these, four had blade identity and five had sheath-like characteristics. *Ig1-R* leaves have a less defined blade-sheath boundary than wild-type leaves, and *Ig1-R;Wab1-R* double mutants have more extensive regions of sheath tissue extending into the leaf blade than *Wab1-R* single mutants (Becraft *et al.*, 1990). Therefore, it was not predicted that *Ig1-Rl-* sectors would restore blade-like characteristics. The fact that half of the observed sectors had sheath-like identity indicates that ectopic sheath tissue is not dependent on *Lg1* function. Some areas of ectopic sheath tissue did end at *Ig1-Rl-* sector boundaries. This may reflect the fact that clonal sectors in maize leaves and regions of cleared tissue in *Wab1-R* leaves both tend to be bordered by lateral veins (Cerioli *et al.*, 1994). Thus, it is likely that clonal sectors were simply coincident with boundaries of ectopic sheath tissue.

3.4.6 *Lg1* promotes lateral growth in a non-cell autonomous manner

The analysis of *Ig1-R* leaf shape indicates that *Lg1* promotes lateral growth of leaves in both *wab1* and *Wab1-R* backgrounds. To determine if *Lg1* promotes lateral growth in a cell-autonomous manner, *Lg1;Wab1-R* and *Lg1;wab1* leaves with *Ig1-Rl-* sectors were measured at the blade midpoint and the base of the blade.

It was predicted that if *Lg1* promotes lateral growth cell-autonomously, then leaf-halves with *Ig1-Rl-* sectors should be narrower than non-sectored halves of the same leaves. Analysis of measurement data showed no significant difference in the width of sectored and non-sectored leaf-halves in either the *wab1* or *Wab1-R* backgrounds (Table 3.7). Thus, the data do not support the hypothesis that *Lg1* promotes lateral growth in a cell-autonomous manner, suggesting that *Lg1* acts non-autonomously to promote lateral growth.

3.4.7 *Lg1* has both cell-autonomous and non-autonomous functions

Previous mosaic analyses have shown that *Lg1* acts cell-autonomously to specify auricle and ligule (Becraft *et al.*, 1990; Becraft and Freeling, 1991). The current study indicates that *Lg1* also conditions *Wab1-R* ectopic auricle tissue in a cell-autonomous manner. However, our data suggest that *Lg1* promotes lateral growth in a non-autonomous manner. Thus, *Lg1* has both cell-autonomous and non-autonomous functions. In addition to specifying ligule and auricle tissue, there is evidence that *Lg1* is required for correct positioning of the blade-sheath boundary. The blade-sheath boundary of *Lg1* leaves is less defined and is shifted distally (Becraft *et al.*, 1990). These results point to multiple roles for *Lg1* in leaf morphogenesis and tissue specification, which may be mediated by multiple downstream pathways.

3.4.8 *Wab1-R* leaf primordia are narrower and initiate fewer lateral veins than wild-type leaf primordia

Hay and Hake (2004) found that *Wab1-R* leaf blades are much narrower than wild-type and have fewer lateral veins. Sheath width is not affected by *Wab1-R*. The lateral growth defect was seen in leaf primordia as young as P3. Wild-type P3 leaf primordia completely enclosed the SAM and younger leaf primordia, whereas, *Wab1-R* leaf primordia at the same stage did not fully enclose the apex (Hay and Hake, 2004). To determine when the reduction in lateral vein number is first apparent, lateral veins were counted in early leaf primordia of *Wab1-R* and wild-type plants. My results show no significant difference in *Wab1-R* and wild-type lateral vein number in P3 stage primordia (Figure 3.9). At P4, *Wab1-R* leaf primordia have fewer lateral veins than wild-type. Thus, the difference in lateral vein number is apparent one plastochron later than the visible reduction in width. This finding is consistent with a model in which primordium size governs the number of veins that are initiated. It has been proposed that vascular pattern is determined by a self-organising system involving auxin transport (Scarpella *et al.*, 2006).

Hay and Hake (2004) hypothesised that the *Wab1-R* narrow leaf phenotype is due to the deletion of a lateral domain in the leaf blade. To test this hypothesis, a clonal analysis was conducted in *Wab1-R* and wild-type leaves. A similar clonal analysis of *ns* leaves found that sectors derived from a specific region of the *ns* meristem did not extend into the leaf above (Scanlon and Freeling, 1997). This study provided evidence that a lateral domain encompassing the leaf margins is not initialised in *ns* mutants.

It was predicted that if *Wab1-R* causes the deletion of a specific lateral domain in the leaf, then sectors that are present in the corresponding radial position in the SAM would not extend into the leaf blade. The position of sectors within the culm was used to approximate their radial position within the SAM (Figure 3.8). Overlapping sectors that covered almost all positions of the culm were obtained. All of these sectors continued into the leaf blade. Thus, these results do not support the hypothesis that *Wab1-R* causes the deletion of a lateral domain. No culm sectors were obtained in the region nearest the midrib. Therefore, the possibility that this region is affected by *Wab1-R* cannot be ruled out. This seems unlikely, however, as the cells immediately adjacent to the midrib contribute little to the overall width of the leaf (Poethig and Szymkowiak, 1995), and *Wab1-R* has no obvious effect on tissue identity in this region.

We suggest that *Wab1-R* causes a reduction in lateral growth, rather than the deletion of a specific domain. A comparison of clonal sector width in *Wab1-R* and wild-type leaves provides support for this hypothesis, although the experiment did not generate enough sectorised leaves to undertake a detailed comparison of cell fate in *Wab1-R* and wild-type leaves. The greatest difference in the width of *Wab1-R* and wild-type leaves was seen at the blade midpoint (Table 3.8). Sectors in the marginal domain of *Wab1-R* leaves were significantly narrower than sectors in the marginal domain of wild-type leaves. There was also a notable difference in the width of lateral domain sectors measured at the blade midpoint in *Wab1-R* and wild-type leaves, although this difference was not found to be statistically significant. This is likely to reflect the small number of sectors obtained in this region.

At the base of the blade, sectors in the midrib domain of *Wab1-R* leaves were wider than sectors in the equivalent position in wild-type leaves. This result was surprising, as *Wab1-R* leaves are slightly narrower than wild-type leaves at this point, although the reduction is less severe than at the blade midpoint. No significant difference was found in the width of *Wab1-R* and wild-type lateral and marginal domain sectors measured at the base of the blade. This may reflect the fact that the narrow leaf phenotype is much less severe at the base of the blade than at the blade midpoint (Hay and Hake, 2004). This finding is consistent with the hypothesis that ectopic *Lg1* expression in *Wab1-R* leaves promotes lateral growth at the base of the blade and partially compensates for the *Wab1-R* narrow leaf defect.

4. *milkweed pod1-R*

4.1 Introduction

milkweed pod1-R (*mwp1-R*) is a recessive mutation that was first identified by ectopic outgrowths on the abaxial surface of the husk leaves. The mutant was discovered by Oliver Nelson and is believed to be a spontaneous mutation (pers. comm., Hector Candela and Sarah Hake). The *Mwp1* gene has recently been cloned by Hector Candela, a postdoctoral fellow in Sarah Hake's lab. *Mwp1* is a member of the *KANADI* gene family, and *mwp1-R* is the first *kan* loss-of-function mutant to be reported in maize (pers. comm., Hector Candela and Sarah Hake).

The various maize lateral organs exhibit morphological differences which may be viewed as differential elaboration of a common pattern. The vegetative leaf is subdivided into blade and sheath, with the blade being the dominant part, whereas the husk leaves are mainly sheath tissue with a small residual blade at the tip. The prophyll and gynoecium are each thought to be derived from the fusion of two phytomers. The prophyll is believed to form via the fusion of two primordia along adjacent margins. Each of the midrib regions develops a prominent keel. The *mwp1-R* phenotypes observed in different lateral organs reflect their diverse morphologies.

In order to elucidate the role of *Mwp1* in normal leaf development, a detailed analysis of the *mwp1-R* phenotype and characterisation of the expression patterns of known polarity genes in *mwp1-R* lateral organs were undertaken. In addition, prophyll development was investigated in *mwp1-R* and wild-type backgrounds in order to gain a better understanding of axial patterning in lateral organs with diverse morphologies.

4.2 Specific Materials and Methods

4.2.1 Material for SEM and histology

Detailed protocols for SEM and histology are provided in Sections 2.5 and 2.6.

Tissue from *mwp1-R* and wild-type husk leaves was fixed for SEM and sectioning. Samples were taken from a point midway between the base and tip and midway between the centre and margin of the leaf.

Samples of *mwp1-R* and wild-type prophyll tissue were fixed for SEM and sectioning. Tissue was taken from the keel region, midway between the base and tip of the prophyll.

Tissue from unfused *mwp1-R* prophylls displaying the "tab" phenotype was fixed for SEM and sectioning. Tissue was taken from the "tabs" of *mwp1-R* prophylls and from the central membrane of wild-type prophylls at a point midway between the base and tip of the prophyll.

Tissue from *mwp1-R* and wild-type vegetative leaf sheath margins was fixed for SEM and sectioning. Tissue was taken from a point midway between the base of the leaf and the blade-sheath boundary.

Segments of *mwp1-R* and wild-type silk tissue were fixed for SEM and sectioning. Samples for SEM were taken from the base of the silk. Samples for sectioning were taken at a point midway between the base and tip of the silk.

Tissue from *mwp1-R;Wab1-R* leaves was fixed for SEM and sectioning. Samples were taken from regions where ectopic sheath-like tissue extended into the leaf blade in *mwp1-R;Wab1-R* leaves and equivalent positions in wild-type leaves.

4.2.2 Measurements of *mwp1-R* and wild-type lateral organs

Measurements were all made on mature field grown W23 and A188 inbred plants, and on *mwp1-R* introgressed into either W23 or A188 five times. Introgressed material was supplied by Sarah Hake and Hector Candela. Husk leaf, prophyll and vegetative leaf measurements were made using a ruler and a flexible dressmakers' measuring tape. Each data set comprised eight or more individuals (exact sample sizes are given in results tables).

Prophylls and husk leaves

The prophyll and husk leaves 1, 4 and 8 (numbered from outer to inner) from the upper ear of each plant were measured. Prophyll and husk leaf length were measured from the base of the leaf to the blade-sheath boundary. Width was measured from margin to margin at a point midway between the base of the leaf and the blade-sheath boundary. For prophylls, the distance between the keels was measured at a point midway between the base and tip of the leaf (see Table 4.1).

Vegetative leaves

Vegetative leaves 8, 9 and 10 (counting down from the tassel) were measured. Blade length was measured from the blade-sheath boundary to the tip of the leaf. Sheath length was measured from the base of the leaf to the blade-sheath boundary. Half-leaf width was measured from midrib to margin. Blade width was measured at the widest part at the base of the blade. Sheath width was measured at a point midway between the base of the leaf and the blade-sheath boundary.

Silks

Sectioned material was photographed under the stereomicroscope. Measurements were made from calibrated digital photographs. Measurements were made of the distance between the veins and of the distance from one vein to the outer edge of the silk (see Table 4.6).

Paleae and glumes

Paleae and glumes were dissected from male florets and flattened onto double sided tape attached to glass microscope slides. They were photographed under

the stereomicroscope. Measurements were made from calibrated digital photographs. Length was measured from base to tip. Width was measured from margin to margin at the widest point. For each palea, the distance between the veins was measured.

Statistical analysis

Mean values for each measurement point were calculated separately for *mwp1-R* and wild-type. Means were compared by Student's t-test to determine if they were significantly different at the 0.05 confidence level. Data were analysed using Microsoft Office Excel 2003.

4.2.3 SEM of developing prophylls

Replicas of axillary buds were created using the method described in Section 2.5.2. Axillary buds were taken from reproductive nodes. Axillary buds are suppressed in nodes above the ear, so the most distal nodes that contained axillary buds were selected (Poethig, 1988). Subtending leaves were removed to expose axillary buds. Buds at the earliest stages were cast while still attached to the main axis. Later stage buds were detached from the main axis using a razor blade before casting. This allowed the side of the prophyll adjacent to the culm to be viewed.

4.2.4 Measurements of developing prophylls

Developing prophylls were measured from electron micrographs. Overall length was measured from base to tip. When the tips were curled over, a piece of thread was used to trace the line of the prophyll and the length of the straightened thread was measured. The length of the fused region was measured from the base of the prophyll to the cleft where the two prophyll tips join, or to the top of the strip of tissue connecting the two prongs in unfused *mwp1-R* prophylls (see Figure 4.11).

4.2.5 *In situ* hybridisation

The *in situ* hybridisation protocol used is a modified version of the one described by Jackson (1991).

Probe synthesis

Clones of the *rld1* and *zyb9* genes in the vector pBluescript (Stratagene) were kindly provided by Marja Timmermans (Cold Spring Harbour Laboratory, New York). The *rld1* clone encompassed nucleotides 619-1674 of the *rld1* coding sequence (Juarez *et al.*, 2004b). The *zyb9* clone comprised the 5' region, including the Zn-finger domain (Juarez *et al.*, 2004a). GenBank accession numbers are: *rld1* AY501430; *zyb9* AY313903.

Clones were transformed into DH5 α cells, selected on ampicillin plates and cells were grown in 10 ml overnight cultures. Plasmid DNA was extracted using the QIAprep® Spin Miniprep Kit (QIAGEN) and eluted in 50 μ l of water. Plasmid DNA was sequenced by the Alan Wilson Centre Genome Sequencing Service to confirm that the correct sequence had been obtained.

Plasmid was digested with the appropriate restriction enzyme to give a linear template for the transcription reaction. For the *zyb9* antisense probe, plasmid was linearised with BamHI and the T7 RNA polymerase (Roche) was used in the transcription reaction. For the *rld1* antisense probe, plasmid was linearised with XhoI and the T3 RNA polymerase (Roche) was used in the transcription reaction. Protein was removed from the linearised plasmid by phenol chloroform extraction.

DIG-labelled probe was synthesised by *in vitro* transcription using 1 μ g of the linearised plasmid as a template, DIG RNA labelling mix (Roche) and the supplied buffer in a final volume of 20 μ l. The transcription reaction was carried out at 37°C for 1 h. An aliquot was saved to run on a gel after DNase treatment.

The DNA template was degraded by DNase treatment. Water and 5 μ l RNase free DNase (Roche) were added to the transcription reaction to make a final volume of 100 μ l and incubated at 37°C for 10 min. An aliquot was run on a gel alongside the reserved aliquot from the transcription reaction to ensure that the template was degraded. Probe was ethanol precipitated, then resuspended in 50 μ l of water and 50 μ l of formamide to create the stock probe.

RNase treatment of solutions and equipment

Precautions were taken to prevent RNase contamination during the *in situ* hybridisation procedure. All solutions were made using DEPC-treated water (1 ml of DEPC was added to 1 L of milli-Q water, incubated overnight with occasional shaking, and then autoclaved). All glassware, slide racks and forceps were baked at 250°C for 6-8 h. Plastic containers were soaked in H₂O₂ overnight and then rinsed in RNase-free water. Benches were cleaned with RNase away (Molecular BioProducts). Latex gloves were worn for all steps and changed regularly.

Prehybridisation treatments

Slides were placed in metal slide racks and all prehybridisation treatments were carried out at room temperature.

Dewaxing

Slides were dewaxed in two changes of Histoclear for 10 min each.

Hydration

Slides were hydrated through a graded ethanol series (2 x 100% for 2 min, 95%, 85%, 70%, 50%, 30% for 1 min each, 0.85% NaCl for 2 min), then immersed in 0.1 M HCl for 20 min, water for 5 min and 1xPBS for 2 min.

Pronase treatment

Pronase was prepared by predigesting 50mg/ml pronase (Roche) at 37°C for 4 h to remove nucleases. 1 ml aliquots were stored at -20°C.

Pronase solution was prepared immediately before use by adding 1 ml of 50 mg/ml predigested pronase to 400 ml of 37°C pronase buffer (50 mM Tris pH 7.5, 5 mM EDTA). Slides were incubated in pronase solution for 20 min at 37°C. Pronase digestion was stopped by immersing slides in 0.2% (w/v) glycine in 1xPBS for 2 min, then rinsing in 1xPBS for 2 min.

Acetic anhydride

A 400 ml container of 0.1 M triethanolamine was placed on a stir plate and the slide rack was suspended in this solution. 2 ml of acetic anhydride was added

while the triethanolamine solution was being stirred. Slides were incubated for 10 min with continued stirring then rinsed in PBS for 2 min.

Dehydration

Slides were dehydrated in a graded ethanol series using the same ethanol series as before, but with fresh 100% ethanol for the final step. Slides were left to dry for 30 min or more.

Hybridisation

Working probe was made by diluting 1 μ l of stock probe to 19 μ l of 50% formamide per slide. The working probe was heated at 80°C for 2 min to relax secondary structures then cooled on ice before adding to the hybridisation buffer.

The following hybridisation buffer was used;

1 ml 10% (w/v) Boehringer blocking reagent (Roche)

1.125 ml 20xSSPE

1 g dextran sulfate

50 μ l 100 mM DDT

100 μ l 10 mg/ml tRNA

4 ml deionised formamide

Water to 8 ml

20 μ l of the working probe, 80 μ l of hybridisation buffer and 1 μ l of RNase OUT (Invitrogen) were used for each slide.

Hybridisation solution (100 μ l) was pipetted onto each slide and covered with a glass coverslip, taking care to remove bubbles. Slides were transferred to a sealable plastic box lined with paper towels soaked in 50% (v/v) formamide. Sealed boxes were placed in a 50-55°C incubator and left to hybridise overnight.

Washes

The following morning the coverslips were removed, slides were returned to the rack and washed in 0.2% SSC for 1 h at 55°C and in fresh 0.2% SSC for a further hour. Slides were then immersed in 1xPBS for 10 min.

Blocks and antibody incubation

Blocking steps were carried out at room temperature. Slides were placed in plastic trays on a rocking platform and treated with a series of blocking solutions: Block A (1% Boehringer block in 1xTBS) for 45 min, Block A for 20 min, Block B (1% BSA, 0.3% Triton x-100 (Sigma) in 1xTBS) for 45 min.

Anti-DIG conjugated antibody (Roche) was diluted 1:1250 in Block B. 150 µl of antibody solution was pipetted onto each slide and slides were covered with glass coverslips. Slides were transferred to a sealable plastic box lined with damp paper towels, and incubated at room temperature for 2 h. Coverslips were removed and slides were returned to plastic trays. Slides were treated with four changes of Block B for 20 min each.

Slides were returned to the rack and immersed in Buffer C (100 mM Tris pH 9.5, 50 mM MgCl₂, 100 mM NaCl) for 15 min then in fresh Buffer C for a further 15 min.

Digoxygenin detection

100 µl of NBT/BCIP (Roche) was diluted in 5 ml of Buffer C just before use. 100 µl of solution was pipetted onto each slide and covered with a glass coverslip. Slides were transferred to a sealable plastic box lined with damp paper towels, and incubated at room temperature in complete darkness for 15 - 48 h. Staining intensity was checked under the stereomicroscope.

To stop the staining reaction, slides were returned to the rack and rinsed for 10 min in TE. Slides were allowed to air dry before mounting coverslips with immunomount (Shandon).

4.2.6 Husk leaf and prophyll material for *in situ* hybridisation

To determine the expression patterns of adaxially expressed genes in developing prophylls, husk leaves and vegetative leaves, tissue was fixed and probed for *zyb9* and *rld1* expression.

For husk leaves and prophylls, seedlings were harvested at 28 to 50 days after planting. Approximately seven outer leaves were removed from each, leaving lateral buds in upper nodes and their subtending leaves intact.

To facilitate comparisons of mutant and wild-type development, buds at similar developmental stages, and sections from equivalent positions within the bud were compared. Buds at similar developmental stages were identified by counting the number of leaves that had been initiated by the lateral meristem. Sections from equivalent positions were selected by counting the number of sections from the base of the bud.

For analysis of sheath margins, seedlings were harvested at 24-28 days after planting. The outer four leaves and the distal part of the shoot were removed.

Genetic material was chosen from backgrounds that exhibit the particular trait being studied. Husk leaf outgrowths and the subdivided keel phenotype were examined in *mwp1-R* introgressed into the W23 background, with wild-type W23 plants as a control. The unfused prophyll phenotype was studied in a non-inbred line that consistently showed this phenotype. Sheath margin outgrowths were examined in *mwp1-R* introgressed into the A188 background, with wild-type A188 as a control.

4.3 Results

4.3.1 Husk leaf phenotype

mwp1-R and wild-type husk leaves were examined by SEM and light microscopy of sectioned tissue (Figure 4.1, Figure 4.2). In transverse section the wild-type husk leaf has a ribbed appearance and the vascular bundles are oriented with xylem at the adaxial pole (false coloured pink) and phloem at the

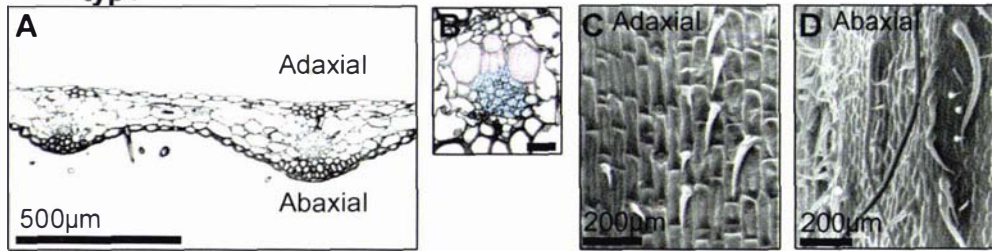
abaxial pole (false coloured blue) (Figure 4.2 A, B). Wild-type husk leaves are relatively smooth on the adaxial surface, with brick-shaped cells and shorter prickle-like hairs (Figure 4.2 C). The abaxial surface is hairier, particularly near the margins, and the cells are more rounded (Figure 4.2 D).

Outgrowths on *mwp1-R* husk leaves generally occur in pairs on the abaxial surface (Figure 4.1 D, Figure 4.2 E, F). The outer surfaces of ectopic flaps are hairy and have rounded cells, similar to abaxial margin tissue (Figure 4.2 F). The epidermis between outgrowth pairs is smoother, with brick-like cells and only shorter prickle-like hairs, similar to adaxial epidermis (Figure 4.2 J). Vascular bundles are oriented with xylem to the inner side of ectopic flaps (Figure 4.2 G). Vascular bundles at junctions between outgrowths and the main lamina are often partially or fully radialised, with xylem surrounding phloem tissue (Figure 4.2 H, I).



Figure 4.1. Wild-type and *mwp1-R* ears. (A) Wild-type ear. (B) Abaxial surface of wild-type husk leaf. (C) *mwp1-R* ear. (D) Abaxial surface of *mwp1-R* husk leaf with ectopic outgrowths.

Wild-type



milkweed pod1-R

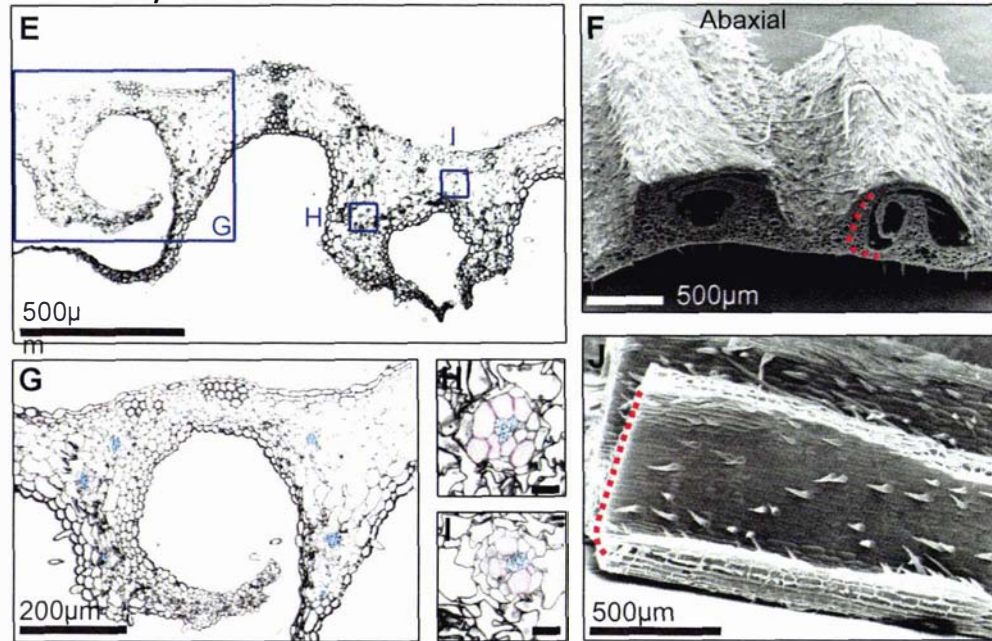


Figure 4.2. Ectopic outgrowths on *mwp1-R* husk leaves are associated with adaxialised tissue.

(A-D) Wild-type husk leaves have a polarised arrangement of vascular tissue and epidermal characteristics. (A) Transverse section of wild-type husk leaf. (B) The vascular bundles of wild-type husk leaves are oriented with xylem (false coloured pink) on the adaxial side and phloem (false coloured blue) on the abaxial side. (C) The adaxial epidermis is relatively smooth, has only shorter hairs, and the cells are brick-like. (D) The abaxial epidermis has a variety of hair types with long hairs near the margins, and more rounded cells.

(E-J) *mwp1-R* husk leaves develop pairs of ectopic outgrowths on the abaxial surface. (G) Vascular bundles are oriented with xylem to the inner side of tissue flaps. (H, I) Vascular bundles at outgrowth junctions are often partially radialised. (F) The outer epidermis of these outgrowths has long hairs characteristic of abaxial marginal tissue. (J) The epidermis between pairs of outgrowths is smooth with only shorter hairs and is more similar to adaxial epidermis. (J) is a piece of tissue adjacent to (F) that has been cut away to reveal the epidermis between tissue flaps. Red dotted lines indicate equivalent positions. Scale bars in (B), (H) and (I) = 20µm.

Expression of *rld1* and *zyb9* in husk leaves

To determine if genes that are normally expressed adaxially are misexpressed in *mwp1-R* husk leaves, developing husk leaves were probed with *zyb9* and *rld1* (Figure 4.3, Figure 4.4). Juarez *et al.* (2004b) found that *zyb9* and *zyb14* have similar expression patterns in vegetative leaf primordia, and my preliminary results indicated that they also have similar expression patterns in developing husk leaves. Therefore, it was decided to use *zyb9* as a probe representative of the *YABBY* family. Transverse sections from the basal part of lateral buds are shown. In the centre of each is the ear axis (asterisks). Husk leaf primordia surround the ear axes.

rld1 is expressed on the adaxial side of wild-type husk leaf primordia (Figure 4.3 A-C). Ectopic outgrowths on *mwp1-R* husk leaves are associated with *rld1* misexpression (Figure 4.3 D-F). Figure 4.3 D shows paired outgrowths on the abaxial side of husk leaves two and three (arrowheads). In the region between the outgrowths, *rld1* is expressed both adaxially and abaxially. Expression is particularly strong on the abaxial side between outgrowths (Figure 4.3 E, F).

zyb9 is expressed on the adaxial side of young husk leaf primordia (data not shown). In older husk leaf primordia, *zyb9* expression does not appear strongly polarised (Figure 4.4 A, B). *zyb9* expression persists at the margins and in developing vascular bundles, but fades from medial regions.

Ectopic outgrowths on *mwp1-R* husk leaves are associated with *zyb9* expression (Figure 4.4 C, D). Figure 4.4 C shows paired outgrowths on the abaxial side of husk leaves three and four (arrowheads). These outgrowths occur in the medial region of each husk leaf. *zyb9* is expressed in each outgrowth (Figure 4.4 D), whereas *zyb9* is not expressed in the medial region of wild-type husk leaves at similar stages (Figure 4.4 B).

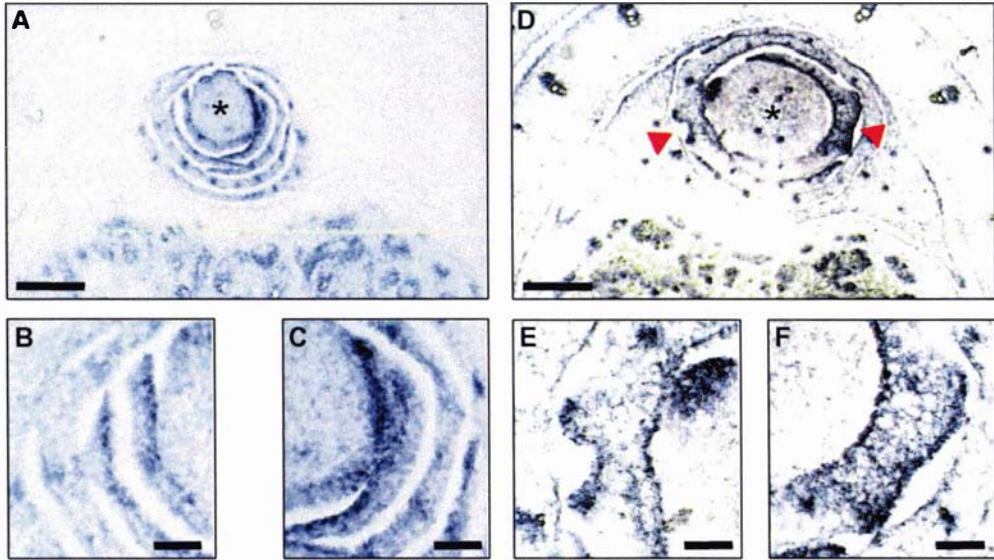
Wild-type***milkweed pod1-R***

Figure 4.3. *rld1* is misexpressed in *mwp1-R* husk leaf primordia. (A-C) *rld1* is expressed on the adaxial side of wild-type husk leaves. (A) Transverse section through wild-type lateral bud. The ear axis can be seen at the centre (asterisk), the culm is below and the subtending vegetative leaf is above. Developing husk leaves and the prophyll surround the ear axis. (B, C) Close-ups of wild-type husk leaves showing *rld1* expression on the adaxial side. Expression persists at the margins and in developing vascular bundles, but fades from the medial region.

(D-F) *rld1* expression in *mwp1-R* husk leaves. (D) Transverse section through *mwp1-R* lateral bud. Husk leaf primordia have ectopic outgrowths (arrowheads). *rld1* is expressed on the abaxial side, between pairs of ectopic outgrowths. (E, F) Close-ups of ectopic outgrowths in (D). Scale bars in (A) and (D) = 200 μ m. Scale bars in (B), (C), (E) and (F) = 50 μ m.

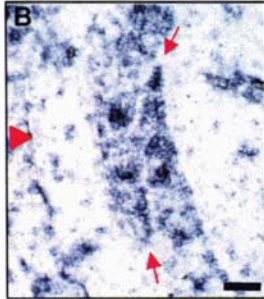
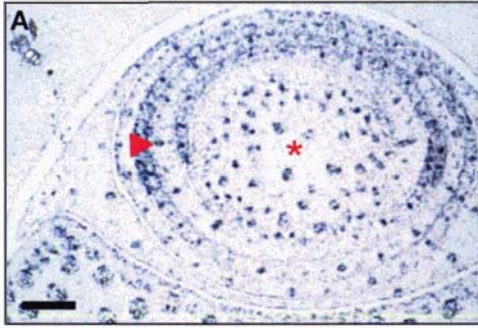
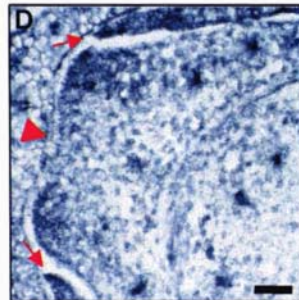
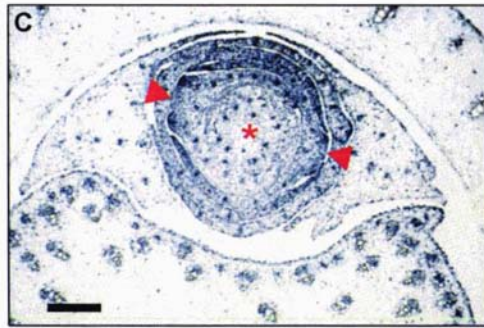
Wild-type***milkweed pod1-R***

Figure 4.4. *zyb9* is misexpressed in *mwp1-R* husk leaf primordia. (A, B) *zyb9* expression in wild-type husk leaf primordia. (A) Transverse section through wild-type lateral bud. The ear axis can be seen at the centre (asterisk), the culm is below and the subtending vegetative leaf is above. Husk leaf primordia surround the ear axis. *zyb9* expression persists at the margins and in developing vascular bundles of older wild-type husk leaves. Expression fades from the medial region. (B) is a close-up of the medial region (arrowhead) of husk leaf three and margins (arrows) of husk leaf four.

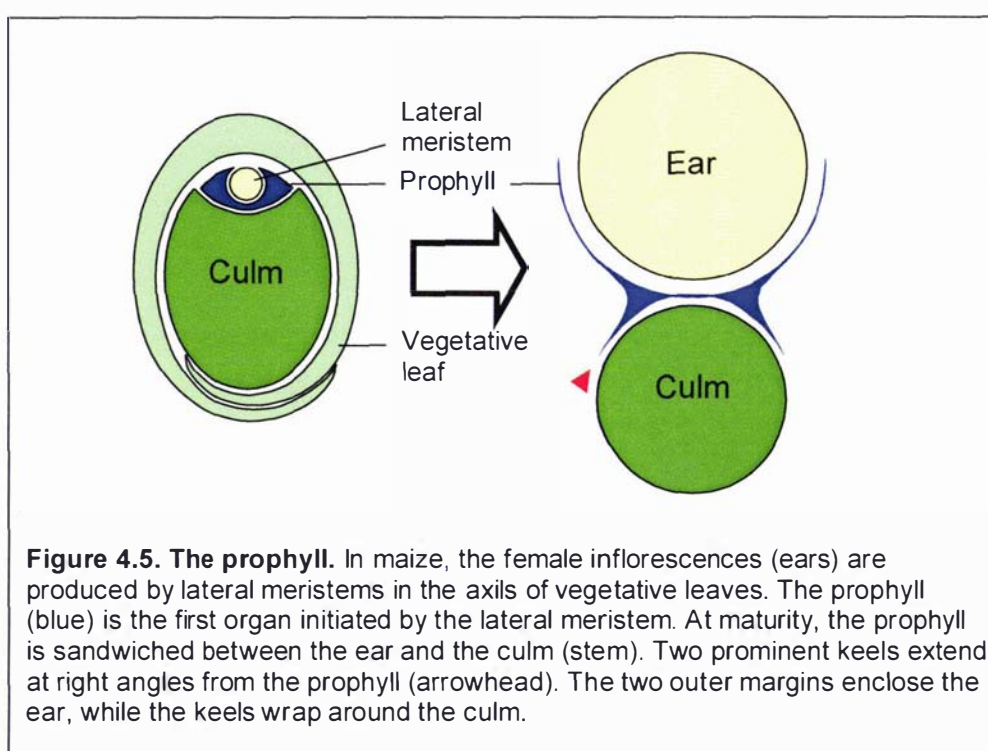
(C, D) *zyb9* expression in *mwp1-R* husk leaf primordia. (C) Transverse section through *mwp1-R* lateral bud. Husk leaf primordia three and four have pairs of ectopic outgrowths on the abaxial side that express *zyb9* (arrowheads). (D) Close-up of ectopic outgrowths on husk leaf four. *zyb9* is expressed at the tip of each outgrowth. Arrowhead indicates medial region of husk leaf four, arrows indicate margins of husk leaf three. Note also that the prophyll is unfused and the keel on the right is subdivided into two points. Scale bars in (A) and (D) = 200 μ m. Scale bars in (B) and (D) = 50 μ m.

4.3.2 Prophyll phenotypes

The prophyll is the organ most severely affected by *mwp1-R*, although the phenotype varies in both penetrance and expression.

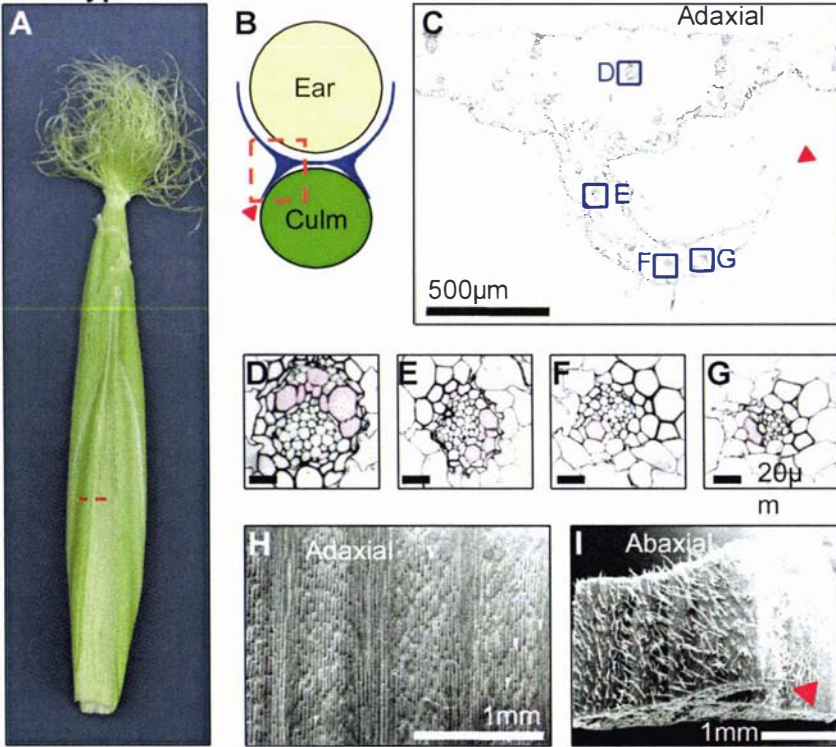
Wild-type prophylls

The prophyll is the first organ produced by a newly initiated lateral meristem (Arber, 1934). At maturity, the prophyll has two outer margins that enclose the ear, and two prominent keels that wrap around the culm (Figure 4.5, Figure 4.6 A-C) (Scanlon and Freeling, 1998). The two keel regions are connected by membranous tissue. Wild-type prophylls bifurcate at the very tip.

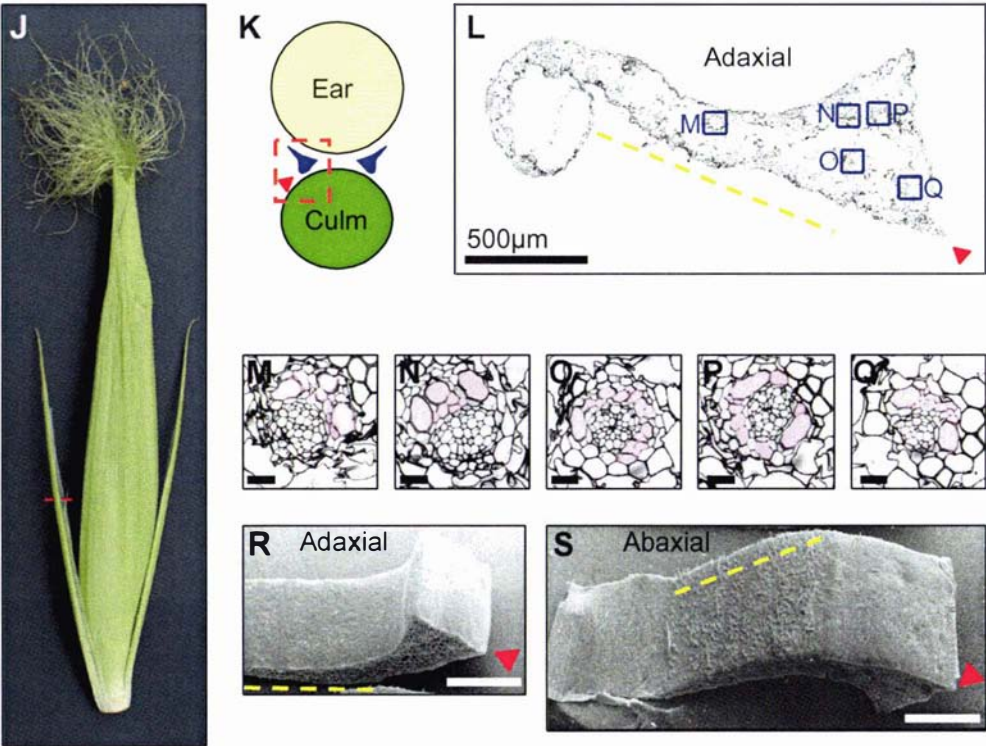


The adaxial epidermis of the wild-type prophyll is relatively smooth, with only shorter prickle-like hairs (Figure 4.6 H). The abaxial epidermis, including the keel region, is covered in longer hairs (Figure 4.6 I). Most veins are oriented with xylem at the adaxial pole and phloem at the abaxial pole (Figure 4.6 D, F, G). However, it was observed that individual veins in the keel often had a different orientation to veins in flanking regions (Figure 4.6 E, Figure 4.7). This

Wild-type



milkweed pod1-R



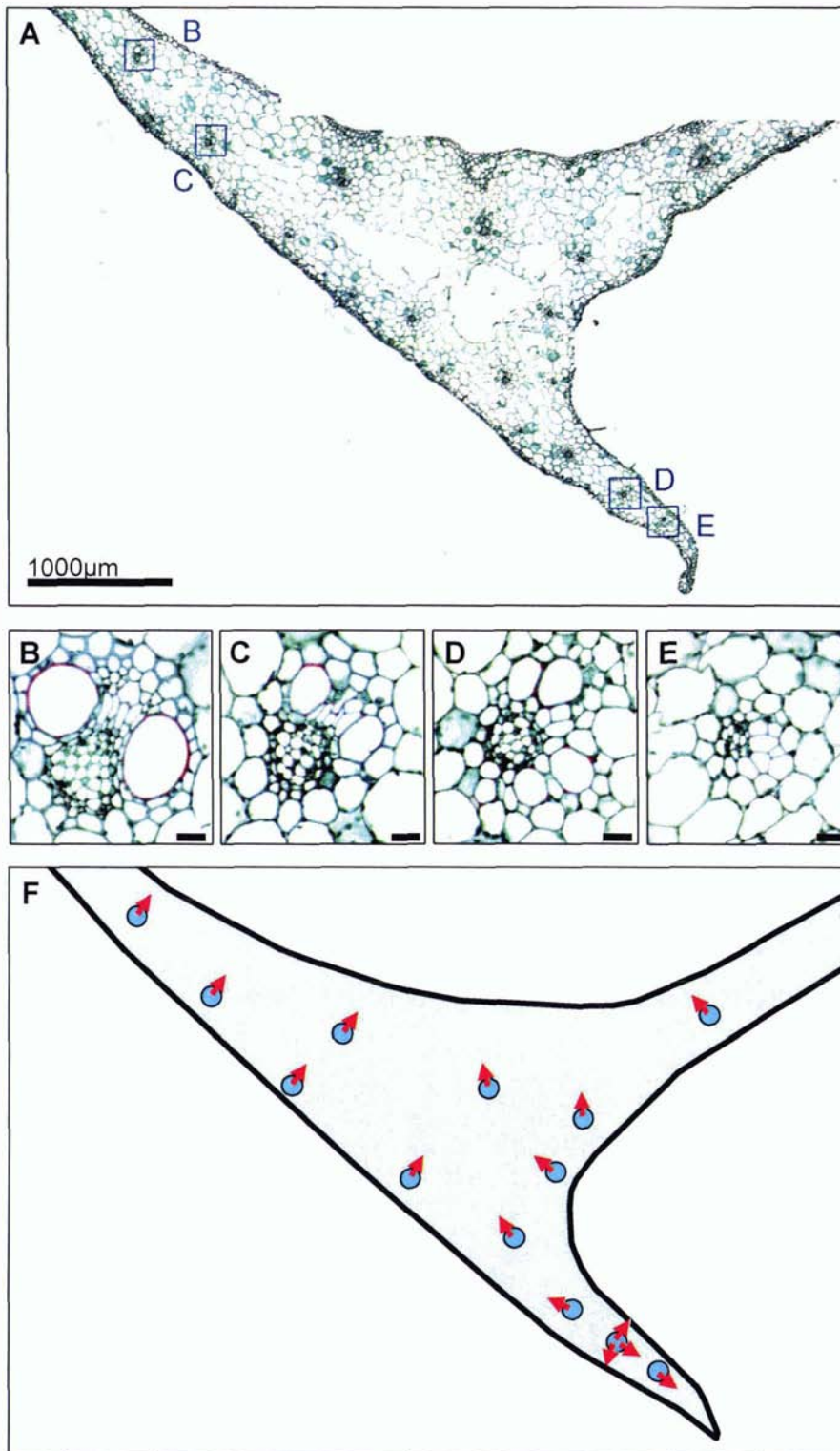


Figure 4.7. Vascular polarity in wild-type prophyll keel. (A) Transverse section through wild-type prophyll keel. (B-E) Close-ups of veins indicated by blue boxes in (A). (B, C) Veins in regions adjacent to the keel are oriented with xylem to the adaxial side and phloem to the abaxial side. (D) Partially radialised vascular bundle in keel. (E) Vein in keel with opposite orientation to veins adjacent to the keel. Sections are stained with safranin and fast green. Xylem elements stain red, whereas phloem cells stain green. (F) Schematic of vein orientation in keel region. Phloem is indicated by blue circles, xylem by red arrows. Scale bars in (B-E) = 20µm.

was observed in 4/5 examples in A188 prophylls and 4/4 times in W23 prophylls.

***mwp1-R* unfused prophyll phenotype**

The prophyll is the organ most strongly affected by *mwp1-R*. In the most severe cases the prophyll is reduced to two unfused prongs (Figure 4.6 J-L). The central membrane and much of the outer margins are deleted. In addition, keel outgrowth is significantly reduced.

The adaxial epidermis of *mwp1-R* prophyll prongs appears normal (Figure 4.6 R). The abaxial side has normal looking epidermal features in the central part (indicated by yellow dotted line). However, the epidermis near the edges of the prong is smooth and more similar to adaxial epidermis (Figure 4.6 S). The orientation of vascular bundles within the prong varies. Bundles near the edge of the prong have a relatively normal orientation (Figure 4.6 M, N, Q), whereas bundles in more central regions may be completely or partially radialised (Figure 4.6 O, P). Within *mwp1-R* prophyll prongs, the distortions in vascular polarity are more extreme and affect a greater number of vascular bundles than the differently oriented vascular bundles seen in the keel region of wild-type prophylls.

Comparison of *mwp1-R* and wild-type prophyll development

To characterise normal prophyll development, and to determine when the *mwp1-R* unfused prophyll defect first becomes apparent, an investigation of prophyll development in *mwp1-R* and wild-type plants was undertaken by SEM (Figure 4.8). Leaf primordia are numbered in the order initiated, with primordia 1 and 2 comprising the prophyll and primordium 3 the first husk leaf. In wild-type, the first two primordia are connected by a strip of tissue at the time they emerge (Figure 4.8 A, B). At a similar stage, the two primordia comprising the *mwp1-R* prophyll also have a connecting membrane (Figure 4.8 E, F). By plastochron 4 (Figure 4.8 C), the fused region of wild-type prophylls has grown upward (along the proximal-distal axis) and the tips have grown laterally. The third primordium, the first husk leaf, can just be seen between the prophyll tips. In contrast, the connecting membrane of the *mwp1-R* prophyll has undergone little growth along the proximal-distal axis, and the tips have not grown laterally, leaving the

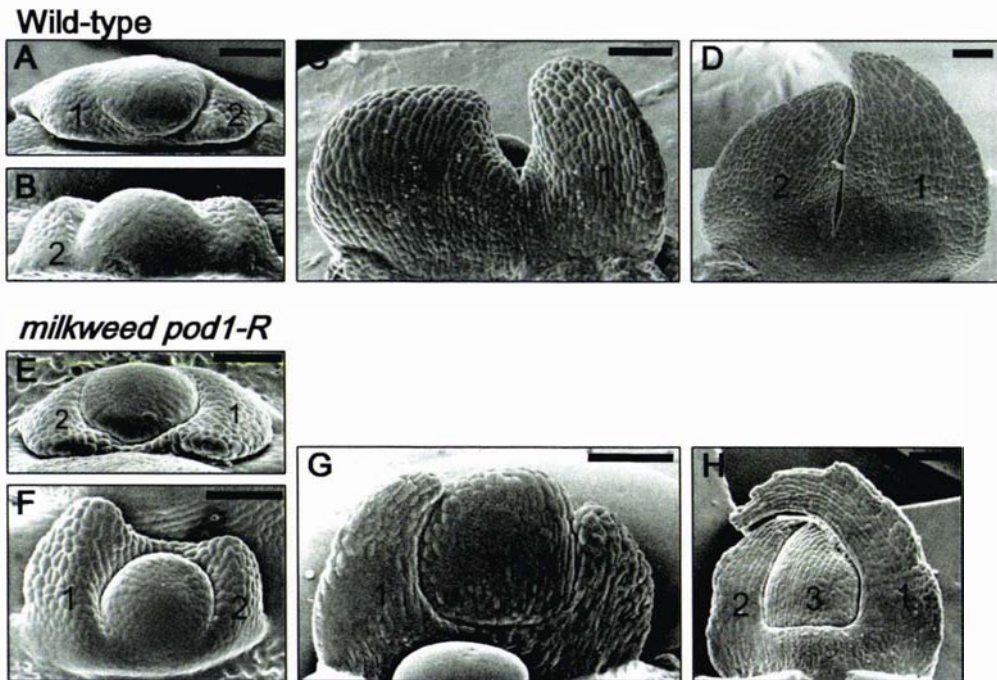


Figure 4.8. The *mwp1-R* prophyll defect is apparent by plastochron 4.

SEMs of wild-type (A-D) and *mwp1-R* (E-H) axillary buds with developing prophylls. At the earliest visible stages of prophyll development, the two primordia that comprise the prophyll are connected by a strip of tissue in both wild-type (A, B) and *mwp1-R* (E, F). By plastochron 4, the *mwp1-R* defect is apparent. In wild-type (C), leaves 1 and 2 have grown laterally and the central membrane has grown upwards, concealing the third primordium. In *mwp1-R* (G), leaves 1 and 2 have undergone little lateral growth and the central membrane has not elongated, leaving leaf 3 exposed. Later in development, these differences are even more pronounced (D, H). Early stage prophylls are shown from above (A, E) and from the side furthest from the culm (B, F). Later stages show the side adjacent to the culm (C, D, G, H). Leaves are numbered in the order of initiation. All scale bars = 100 μ m

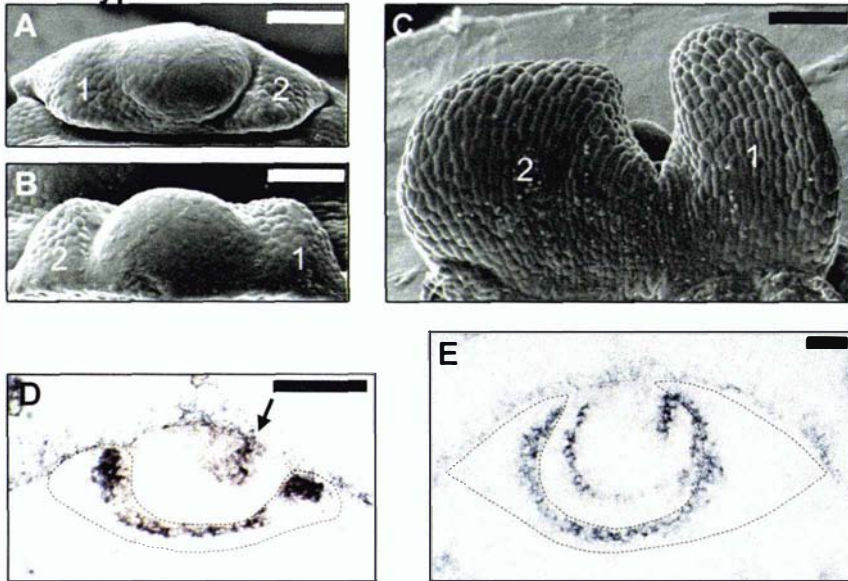
third primordium exposed (Figure 4.8 G). At later stages this difference is even more apparent. In wild-type, the third primordium is enclosed by the prophyll (Figure 4.8 D), whereas in *mwp1-R* there is wide gap between the prongs that leaves the third primordium completely exposed (Figure 4.8 H).

***rd1* expression in early stage prophyll development**

rd1 expression was analysed in early stage prophylls of wild-type and *mwp1-R* plants (Figure 4.9). Transverse sections of lateral buds are shown, with SEMs illustrating equivalent stages. In wild-type prophylls, *rd1* is expressed adaxially (Figure 4.9 D, E). Figure 4.9 D shows a young bud that is just initiating the third primordium (first husk leaf). Only one margin of the husk leaf can be seen in this section (arrow), as husk leaf primordia are initiated at an angle rather than perpendicular to the main shoot axis. In very early stage prophylls, a block of expression is often seen at the outer edge, such that a boundary of *rd1* expression extends along the keel axis (Figure 4.9 D, Figure 4.10). This block of expression is not seen at later stages, when expression becomes confined to the adaxial side of the prophyll (Figure 4.9 E). Expression persists at the outer margins and on the adaxial side of the central membrane, but often fades in the intervening region.

rd1 expression was analysed in *mwp1-R* prophylls, in a genetic background that consistently exhibits the unfused prophyll phenotype. Unlike wild-type prophylls, *rd1* expression is seen on the abaxial side of the *mwp1-R* prophyll very early in development (arrowhead in Figure 4.9 I). One margin of the third primordium (first husk leaf) can be seen (arrow). Figure 4.9 J shows a bud at a later stage, equivalent to the wild-type bud shown in Figure 4.9 E. The prophyll is clearly unfused and the two prongs show patchy *rd1* expression throughout. The husk leaves display a normal-looking adaxial expression pattern.

Wild-type



milkweed pod1-R

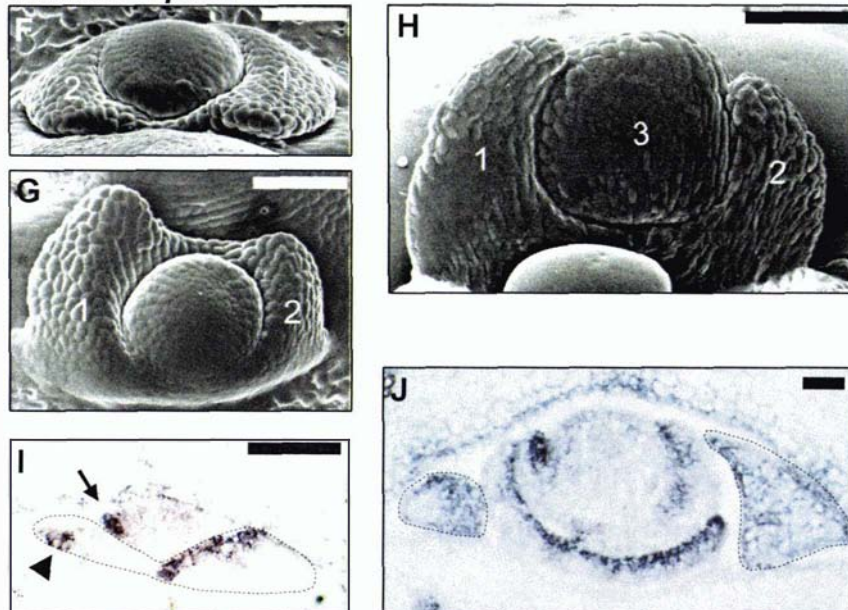


Figure 4.9. The *mwp1-R* unfused prophyll phenotype is associated with *rld1* misexpression early in development.

SEMs of lateral buds showing early stages of prophyll development in wild-type (A-C) and *in situ* hybridisation of *rld1* in transverse sections of equivalent stage buds (D, E). *rld1* is normally expressed on the adaxial side of developing prophylls and husk leaves (D, E). Blocks of *rld1* expression can be seen at the prophyll outer margins early in development (D). These fade at later stages (E).

SEMs (F-H) and *in situ* hybridisation of *rld1* (I, J) in *mwp1-R* lateral buds. In *mwp1-R*, *rld1* expression is seen on the abaxial side of the prophyll early in development (arrowhead in I). Later, diffuse *rld1* expression is seen throughout the two prongs of the unfused prophyll primordium (J). Prophyll primordia are outlined with dotted lines in (D), (E), (I) and (J). Arrows in (D) and (I) indicate P3 leaf primordia. Scale bars = 100 μ m.

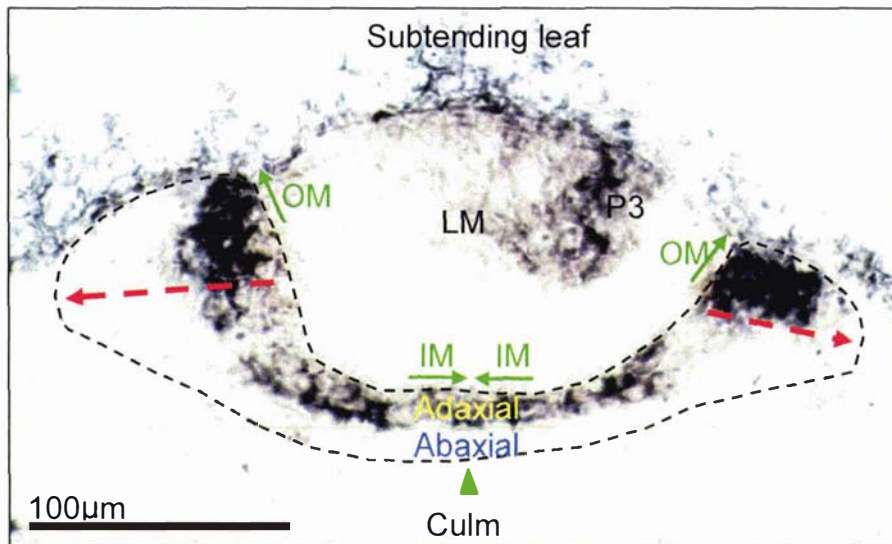


Figure 4.10. *rld1* expression in wild-type prophyll primordium. *rld1* is expressed on the adaxial side of the prophyll primordium (outlined), and in blocks at the outer margins. Boundaries of expression extend along the keel axes (red dotted lines). Two sets of margins are indicated by green arrows. *rld1* expression persists at the margins and fades from the intervening regions. Green arrowhead represents the point at which the two primordia fuse according to the fused phytomer model. OM=outer margins, IM=inner margins. LM = lateral meristem. P3 = plastochron 3 leaf primordium, the first husk leaf to be initiated after the prophyll.

Morphometric analysis of *mwp1-R* and wild-type prophylls

To investigate prophyll growth further, the length of the fused region was compared in *mwp1-R* and normal prophylls at different stages of development. The length of the fused region was plotted against overall prophyll length (Figure 4.11). At the earliest stages (up to about 1 mm overall length) the length of the fused region appears similar in *mwp1-R* and normal prophylls. For prophylls over 1 mm in length, there is a clear difference between the length of the fused region in *mwp1-R* and wild-type. This difference becomes increasingly apparent as growth proceeds. In wild-type the fused region appears to grow rapidly, whereas in *mwp1-R* this region grows very slowly. By the time the prophylls were 10 mm in height, all wild-type prophylls had a fused region of 4 mm or longer, whereas none of the *mwp1-R* fused regions had reached 2 mm.

***mwp1-R* unfused prophylls with tabs**

A variation of the unfused prophyll phenotype is the development of prophylls that are unfused, but have a "tab" of tissue extending from the membranous strip that links the two prongs (Figure 4.12). On either side of the tab are U-shaped sinuses that never elongate. The tabs vary in size and distribution of

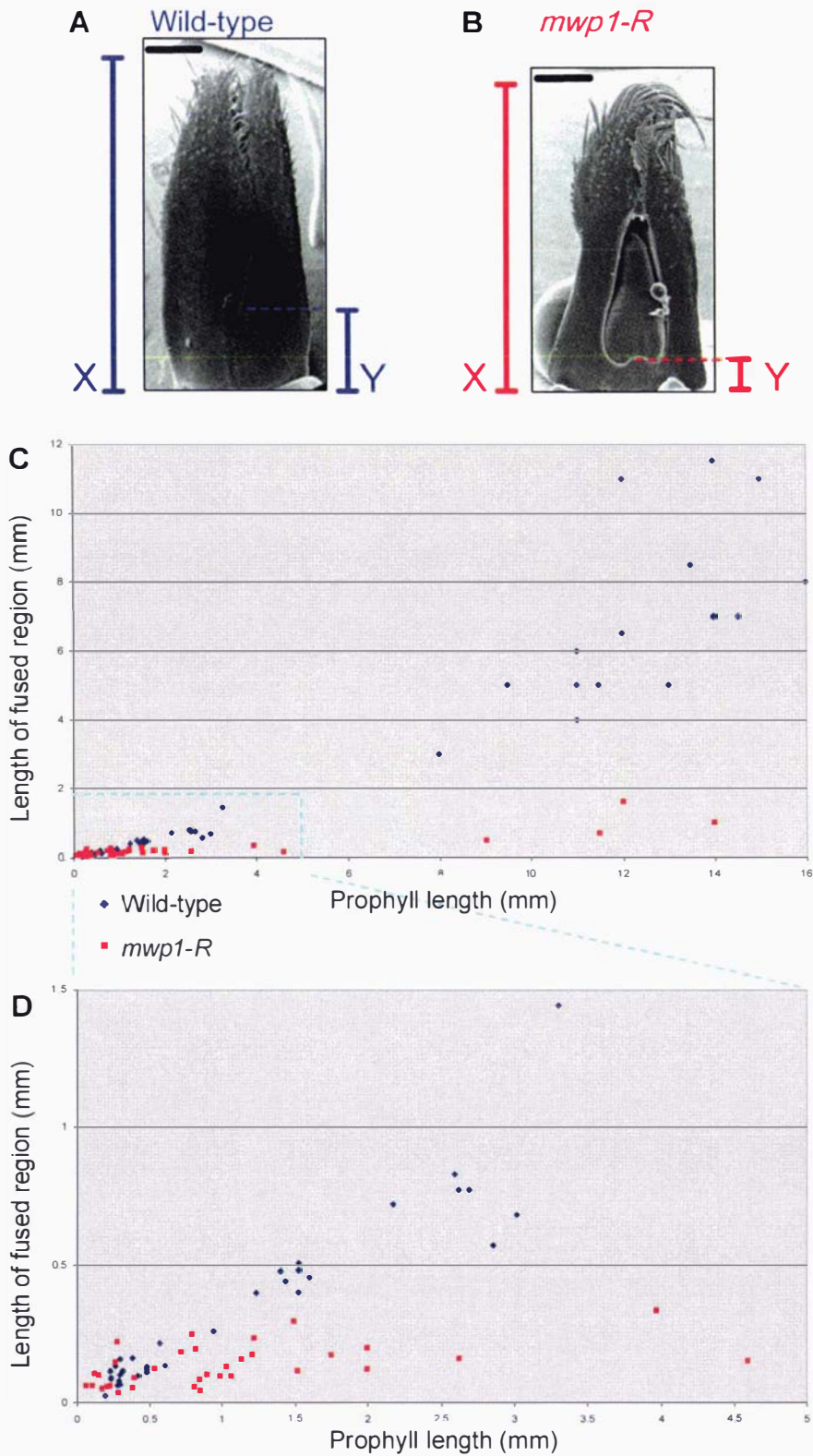


Figure 4.11. Morphometric analysis of *mwp1-R* and wild-type prophyll development.

Prophyll length and the length of the fused region were measured in developing wild-type and *mwp1-R* prophylls (illustrated in A and B). The length of the fused region was plotted against overall prophyll length (C). (D) is an enlargement of the boxed portion in (C). Scale bars in (A) and (B) = 500 μ m.

adaxial and abaxial cell types. Figure 4.12 (D-F) shows a narrow tab that has relatively normal adaxial (E) and abaxial (F) cell types. Figure 4.12 (G-I) shows a wider tab. The adaxial surface has normal looking epidermal characteristics while the abaxial surface has a series of outgrowths. The polarity of veins within prophyll tabs varied from relatively normal to partially radialised, with xylem surrounding phloem.

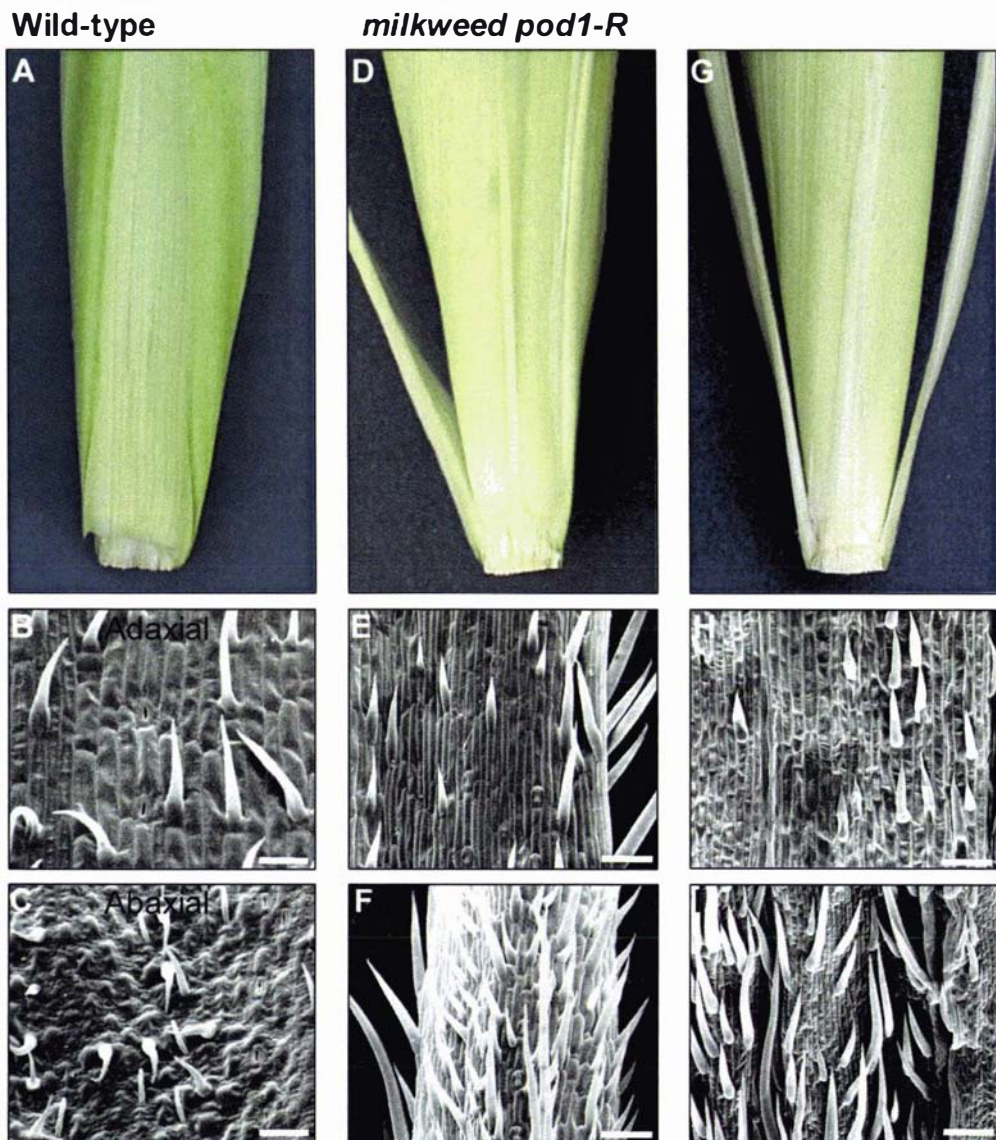


Figure 4.12. The *mwp1-R* prophyll “tab” phenotype. Photographs and SEMs of wild-type prophyll (A-C) and *mwp1-R* prophylls with tabs (D-I). (A) The wild-type prophyll is fused. (B) The adaxial surface of the central membrane is relatively smooth with prickle-type hairs. (C) Cells on the abaxial surface are more rounded. (D) *mwp1-R* prophyll with narrow tab. The adaxial (E) and abaxial (F) epidermis of the tab appear relatively normal. (G) *mwp1-R* prophyll with wider tab. (H) The adaxial epidermis of the tab appears normal. (I) The abaxial side of the tab has ectopic outgrowths. Scale bars = 100µm.

***rld1* expression in *mwp1-R* prophylls with developing tabs**

Expression of *rld1* was examined in a *mwp1-R* prophyll with a developing tab, and in a wild-type prophyll at an equivalent stage (Figure 4.13). The wild-type prophyll is fused, and *rld1* expression is adaxial (Figure 4.13 A, B). The SEM shows a prophyll at a slightly later stage than the section. The dotted line indicates the position equivalent to the plane of the section.

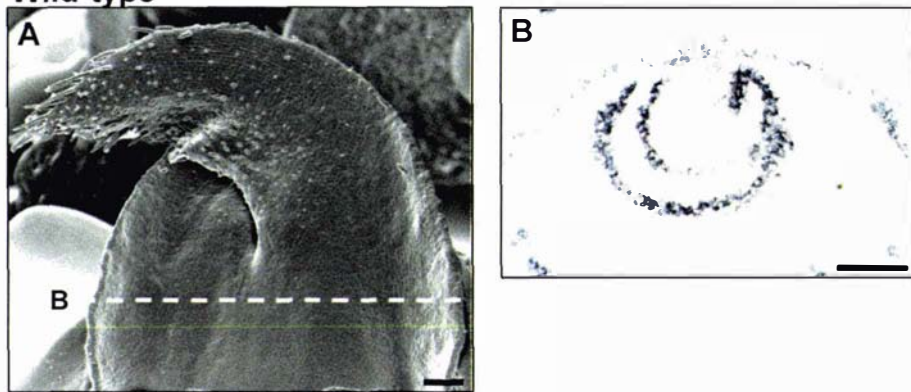
The SEM in Figure 4.13 C shows a *mwp1-R* prophyll with a developing tab. Figure 4.13 D-F are serial sections of a *mwp1-R* prophyll at a slightly earlier stage. Sections are shown corresponding to the fused region at the base of the prophyll (E, F) and a more distal section where the tab and two prophyll prongs are separate (D). In D, an island of tissue corresponding to the tab can be seen (asterisk). Dotted lined in Figure 4.13 C indicate positions equivalent to where sections were taken. In the proximal sections (Figure 4.13 E, F), adaxial *rld1* expression is seen in two patches just below the U-shaped sinuses (arrowheads). The region immediately below the tab retains a more polar pattern of expression, although expression is somewhat patchy (arrows).

***mwp1-R* subdivided keel phenotype**

In the W23 background, *mwp1-R* prophylls were generally fused. However, in many cases each of the keels was replaced by a complex series of outgrowths (Figure 4.14 A-C). Vascular bundles in the keel region were partially or completely radialised, with xylem surrounding a central strand of phloem tissue (Figure 4.14 E-G). Vascular bundles in regions adjacent to the keel had a more normal orientation (Figure 4.14 D).

rld1 and *zyb9* expression patterns were examined in developing prophylls of W23 plants and *mwp1-R* introgressed into W23. In wild-type W23 plants, *rld1* is expressed on the adaxial side of the prophyll and expression persists at the margins and in developing vascular bundles. *rld1* is not expressed in the keels of later stage W23 prophylls (Figure 4.14 H). In the *mwp1-R* prophyll shown in Figure 4.14 I, the keels appear blunter than normal and the keel on the left is divided into two points. *rld1* expression is similar to wild-type at the margins and in developing vascular bundles (Figure 4.14 I). However, *rld1* expression is seen in the keel, particularly in patches where outgrowths are developing

Wild-type



milkweed pod1-R

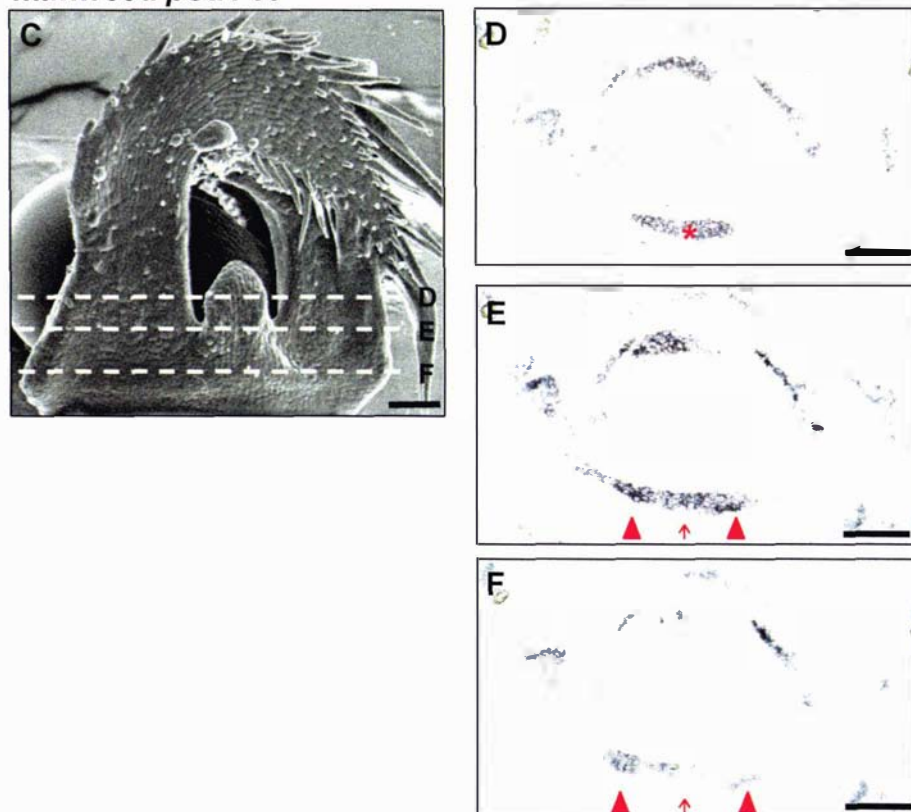
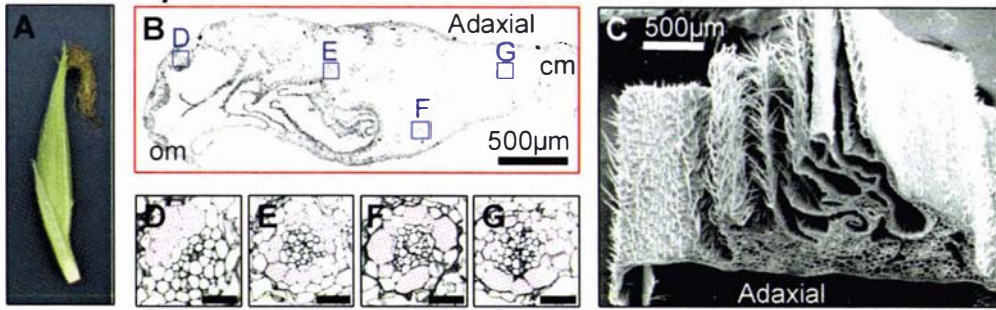
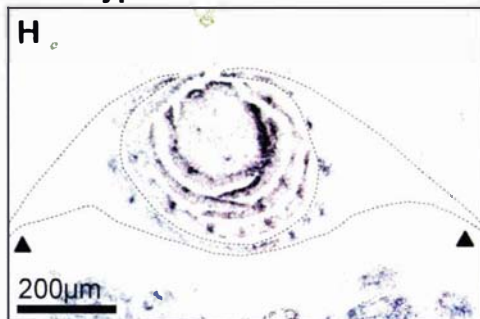


Figure 4.13. *rld1* expression in *mwp1-R* prophyll exhibiting the “tab” phenotype. (A) SEM of wild-type prophyll. (B) *In situ* hybridisation of *rld1* in wild-type prophyll at slightly earlier stage than (A). Dotted line in (A) indicates approximate position of section shown in (B). *rld1* expression is confined to the adaxial side of the prophyll. (C) SEM of *mwp1-R* prophyll with developing tab. (D-F) *In situ* hybridisation of *rld1* in *mwp1-R* prophyll at slightly earlier stage than (C). Dotted lines in (C) indicate approximate position of sections in (D-F). (D) Section taken proximal to fused region. The tab appears as an island of tissue separate from the two prophyll prongs (asterisk). (E,F) Sections through the fused region. *rld1* is expressed on both the adaxial and abaxial sides in the regions immediately below the sinuses (arrowheads). *rld1* expression is largely confined to the adaxial domain in the region immediately below the tab (arrows). Scale bars in (A) and (C) = 200µm, Scale bars in (B) and (D-F) = 100µm.

milkweed pod1-R



Wild-type



milkweed pod1-R

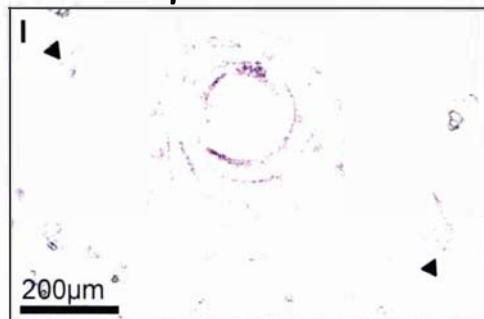


Figure 4.14. *mwp1-R* subdivided keel phenotype. (A) *mwp1-R* ear with prophyll exhibiting the subdivided keel phenotype. The prophyll is narrow and twists away from the ear. Transverse section (B) and SEM (C) of *mwp1-R* keel. The keel is reduced to a complex series of outgrowths. The prophyll outer margin (om) and central membrane (cm) continue out of the plane of the photograph (B). (D-G) Enlargements of veins shown in (B). Veins in the keel region (E-G) are radialised, with xylem (false coloured pink) surrounding phloem. (H) *In situ* hybridisation of *rld1* in transverse section of wild-type lateral bud. Prophyll is outlined with dashed line. *rld1* is not expressed in the prophyll keels (arrowheads). (I) *In situ* hybridisation of *rld1* in *mwp1-R* lateral bud. Patches of *rld1* expression are seen in the prophyll keels (arrowheads). The keels are blunter, and the keel on the left is subdivided into two points. Scale bars in (D-G) = 50µm.

(arrowheads Figure 4.14 I). *zyb9* and *rld1* have similar expression patterns in wild-type prophyll primordia and *zyb9* is misexpressed in *mwp1-R* prophyll primordia in a pattern similar to *rld1* misexpression (data not shown).

4.3.3 *mwp1-R* sheath margin phenotype

The sheaths of *mwp1-R* vegetative leaves develop pairs of outgrowths similar to those seen on *mwp1-R* husk leaves, but these are generally less prominent. Pronounced single outgrowths often occur at the sheath margins (Figure 4.15 D, E). The true margins of affected sheaths are blunt compared to wild-type sheath margins which are normally tapered (arrows Figure 4.15 A, E). Outgrowths occur on the abaxial side, adjacent to the true margin (Figure 4.15 E). These outgrowths are tapered and look more like normal margins. The epidermis on the outer side of sheath outgrowths is smooth and similar to normal adaxial epidermis (Figure 4.16 A, E), whereas the epidermis on the side nearer the midrib is hairy like abaxial epidermis (Figure 4.16 B, F). The vascular bundles near the true margin of the *mwp1-R* leaf have xylem on both sides, with phloem at the centre (Figure 4.15 F, G). Cells on the marginal side of *mwp1-R* sheath outgrowths were shorter than wild-type adaxial sheath margin cells (Figure 4.16 D, E).

rld1 expression was examined in wild-type leaf primordia and *mwp1-R* leaf primordia with developing sheath margin outgrowths. *rld1* is normally expressed on the adaxial side of young leaf primordia. Expression persists at the margins and in developing vascular bundles of older leaf primordia (Figure 4.15 C, I, J; (Juarez *et al.*, 2004b)). In the *mwp1-R* leaf shown, *rld1* expression is seen throughout the sheath margin (Figure 4.15 I, J). An outgrowth is developing along the boundary of *rld1*-expressing and non-expressing tissue. The other sheath margin shows a normal *rld1* expression pattern and is developing normally.

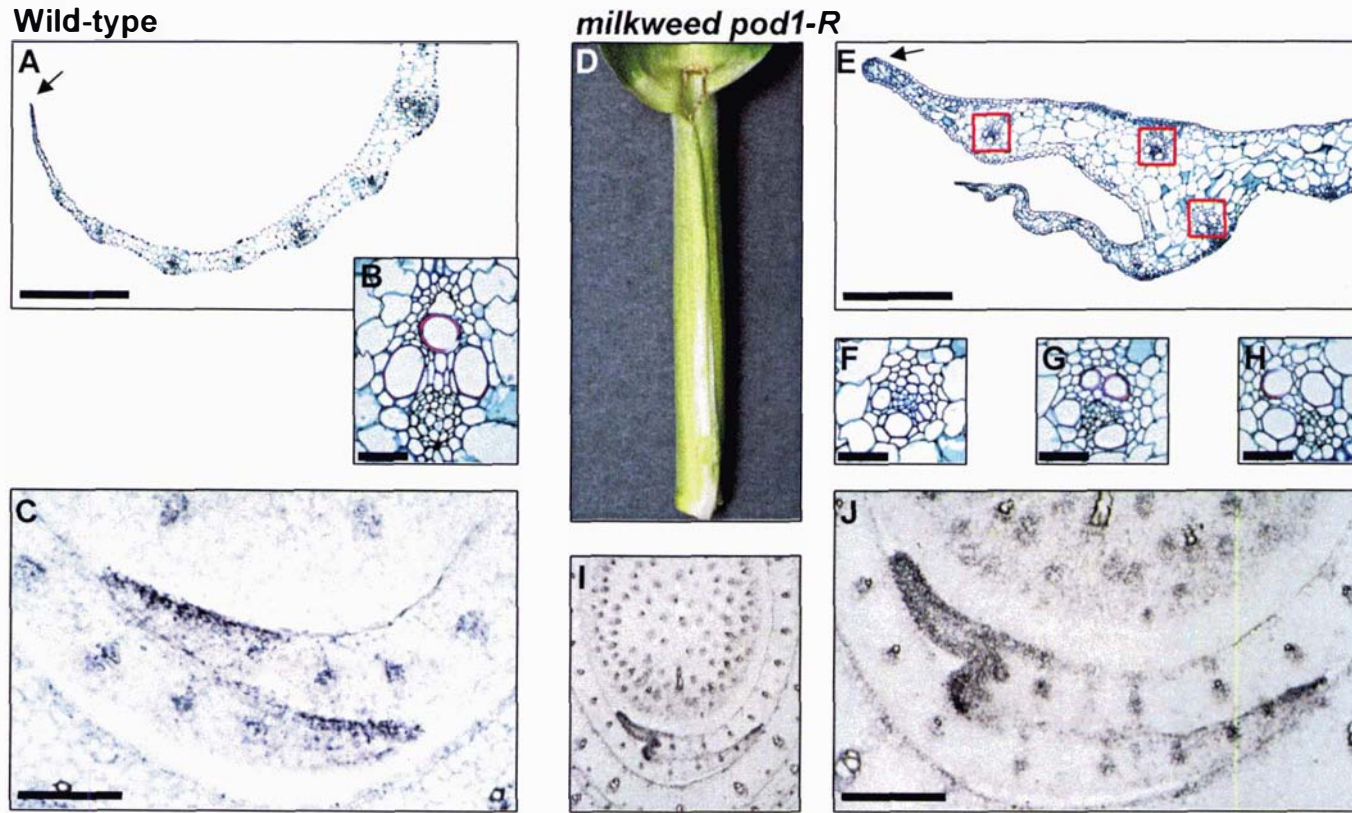


Figure 4.15. Outgrowths at *mwp1-R* sheath margins are associated with ectopic *rld1* expression.

In wild-type leaves, the sheath margin is tapered (arrow in A) and vascular bundles are oriented with xylem on the adaxial side and phloem on the abaxial side (B). (C) *In situ* hybridisation in wild-type leaf primordia shows *rld1* is expressed on the adaxial side of developing leaves and persists at the margins. *mwp1-R* leaves often develop ectopic outgrowths at the sheath margins (D, E). The true sheath margin is blunt (arrow), whereas the ectopic outgrowth is tapered and more similar to a normal sheath margin. Vascular bundles are often radial or mis-oriented (F, G, H). (I) and (J) show a *mwp1-R* sheath margin with an emerging outgrowth. *rld1* is expressed throughout the true margin and the outgrowth coincides with the boundary of *rld1* expression. The other margin (below) expresses *rld1* on the adaxial side and is developing normally. Sections shown in (A), (B) and (E-H) are stained with safranin and fast green. Xylem elements stain red, whereas phloem cells stain green. Scale bars in (A, C, E, J) = 200µm. Scale bars in (B and F-H)=50µm.

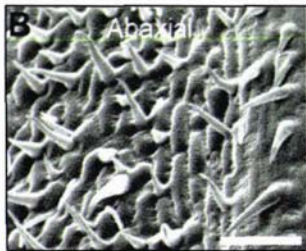
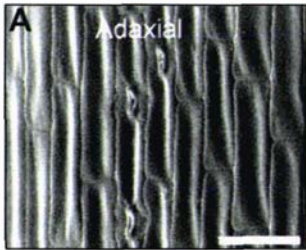
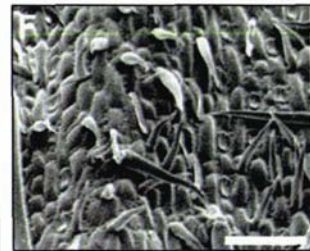
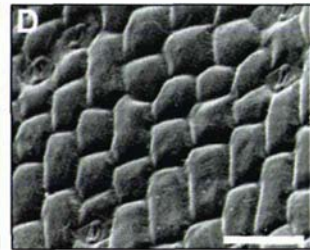
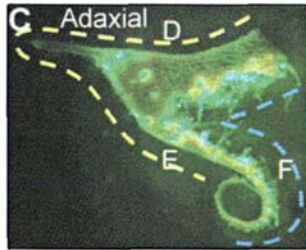
Wild-type***milkweed pod1-R***

Figure 4.16. Adaxial epidermal characteristics continue onto the abaxial side of *mwp1-R* sheath margins with ectopic outgrowths. (A) The adaxial epidermis of wild-type sheath margin is smooth with long, brick-like cells. (B) The abaxial epidermis is hairy and the cells are more rounded. (C) Handsection of *mwp1-R* sheath margin with ectopic outgrowth. (D) The adaxial epidermis of the *mwp1-R* sheath margin is smooth like wild-type adaxial epidermis, but the cells appear shorter. (E) The side of the outgrowth nearest the margin is smooth with brick-like cells, similar to normal adaxial epidermis, although the cells appear shorter. (F) The epidermis on the other side of the ectopic outgrowth has the features of normal abaxial epidermis. Yellow dotted line in (C) indicates the extent of adaxial epidermal characteristics, which appear to wrap around the true margin. Blue dotted line indicates abaxial epidermal characteristics. Scale bars = 100 μ m.

4.3.4 *mwp1-R* floral organ phenotypes

Floral organs such as glumes, paleae and carpels are homologous to leaves. Mutations that disrupt leaf development may affect other lateral organs in a similar manner (Bossinger *et al.*, 1992; Scanlon and Freeling, 1998). Therefore, *mwp1-R* floral organs were examined to determine if they exhibit a phenotype.

Glumes and paleae

The *mwp1-R* glumes and paleae that were examined by SEM did not have any obvious outgrowths or ectopic tissues. When entire male spikelets were examined by SEM, the florets were visible in *mwp1-R* spikelets but not in wild-type spikelets. This suggested that *mwp1-R* glumes may be narrower than wild-type glumes.

Silks

Wild-type (A188) silks are long and straight, with regular files of cells and hairs on the outer edges (Figure 4.17 A, B). Wild-type silks are oval in transverse section, with veins at either end and an indented region (arrow) between the veins (Figure 4.17 C).

In the A188 background, *mwp1-R* silks frequently had a kinked or twisted appearance – this was particularly pronounced near the base of the silk (Figure 4.17 D, E). Extensive folds of tissue occur in the indented region (arrow Figure 4.17 E). In addition, *mwp1-R* silks often had less pronounced outgrowths along their outer edges. In transverse section, the shape of *mwp1-R* silks is less regular and the veins appear closer together than in wild-type silks (Figure 4.17 F). Epidermal cells appear larger and are oriented differently, with some elongated perpendicular to the epidermis.

mwp1-R silks in the W23 background also showed some twisting, but this was less pronounced than in the A188 background.

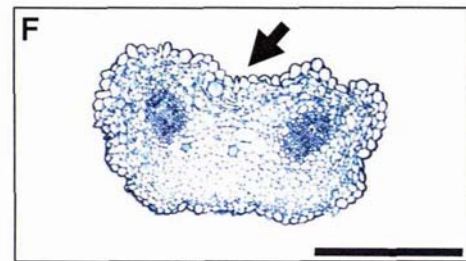
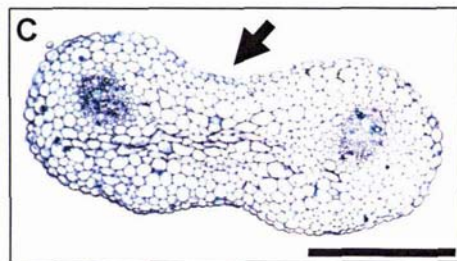
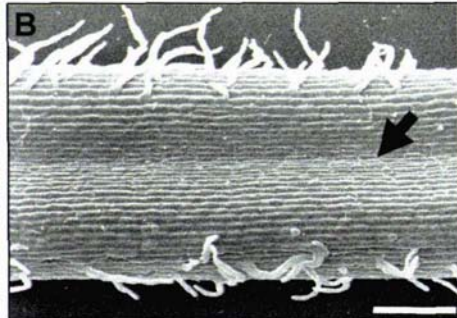
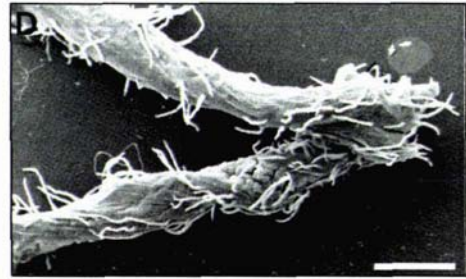
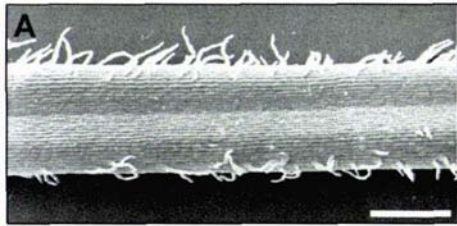
Wild-type***milkweed pod1-R***

Figure 4.17. *mwp1-R* silks are twisted and have ectopic outgrowths. (A, B) Wild-type silks are straight, with regular files of cells and hairs along the outer edges. (C) Wild-type silks are oval in transverse section, with veins at either edge. Arrows in (B) and (C) indicate indented region. (D, E) The *mwp1-R* silk is twisted, with ectopic outgrowths in the indented region (arrow). Less pronounced outgrowths occur along the outer edge. (F) The *mwp1-R* silk is narrower and less regular in shape. Epidermal cells are larger than in wild-type and some are elongated perpendicular to the surface of the silk. Scale bars = 200 μ m.

4.3.5 Measurements of mature wild-type and *mwp1-R* lateral organs

To investigate the effects of *mwp1-R* on lateral organ growth, mature leaves and floral organs were measured. The mean dimensions of *mwp1-R* and wild-type lateral organs were compared. The plant material used for these measurements was wild-type W23 and A188 and *mwp1-R* introgressed into the W23 and A188 backgrounds.

Prophylls

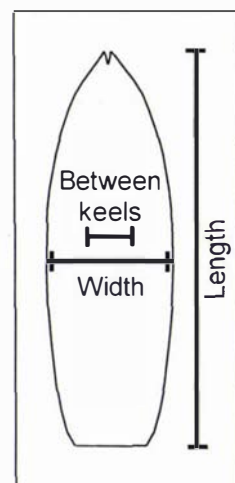
In the W23 background, *mwp1-R* prophylls were significantly narrower than wild-type prophylls (Table 4.1 A). The distance between the keels was also significantly narrower in *mwp1-R*. On average, wild-type prophylls were 43.6 mm wide and *mwp1-R* prophylls were 20.8 mm wide. The average distance between the keels was 16.4 mm in W23 and 7.5 mm in *mwp1-R*. Thus, *mwp1-R* prophylls were 48% as wide as wild-type prophylls, and the distance between the keels was 46% as wide. There was no significant difference in prophyll length between *mwp1-R* and wild-type prophylls in the W23 background.

In the A188 background, *mwp1-R* prophylls were narrower than wild-type prophylls, although the difference was not as great as in the W23 background (Table 4.1 B). *mwp1-R* prophylls were also significantly shorter than wild-type prophylls in this background. On average, wild-type prophylls were 38.2 mm wide and *mwp1-R* prophylls were 24.2 mm wide. The average distance between the keels was 12.4 mm in A188 and 7.6 mm in *mwp1-R*. The average prophyll length was 181.5 mm in wild-type and 120.7 mm in *mwp1-R*. Thus, *mwp1-R* prophylls were 67% as wide as wild-type prophylls, the distance between the keels was 63% as wide, and *mwp1-R* prophylls were 67% as long as wild-type prophylls.

Table 4.1. Measurements of mature *mwp1-R* and wild-type prophylls. (A) W23 background. (B) A188 background. Prophyll length was measured from base to tip. Prophyll width and the distance between the keels were measured at a point midway between the base and tip of the prophyll. Mean values were calculated separately for *mwp1-R* and wild-type prophylls. Means were compared by Student's t-test to determine if they are significantly different at the 0.05 confidence level. * indicates values that are significantly different. SE = standard error. Numbers in brackets are the *mwp1-R* value represented as a percentage of the wild-type value.

A

Prophyll W23 background		Wild-type (n=13)	<i>mwp1-R</i> (n=15)	P-value
Length (mm)	Mean	154.6	148.5	0.480
	SE	5.5	6.3	
Width (mm)	Mean	43.6	20.8 (48%)	<0.001*
	SE	2.4	2.1	
Between keels (mm)	Mean	16.4	7.5 (46%)	<0.001*
	SE	0.8	0.8	



B

Prophyll A188 background		Wild-type (n=13)	<i>mwp1-R</i> (n=13)	P-value
Length (mm)	Mean	181.5	120.7(67%)	<0.001*
	SE	4.6	3.8	
Width (mm)	Mean	38.2	24.2 (63%)	<0.001*
	SE	1.1	1.6	
Between keels (mm)	Mean	12.4	7.6 (61%)	<0.001*
	SE	0.2	0.4	

Husk leaves

In the W23 background, *mwp1-R* husk leaves were significantly narrower than wild-type husk leaves (Table 4.2 A). Husk leaf length was not significantly different. Husk leaves 1, 4 and 8 (with 1 being the outermost husk leaf) were measured. The average width of the first husk leaf was 89.9 mm in wild-type plants and 53.1 mm in *mwp1-R*. The average width of husk leaf 4 was 108.3 mm in wild-type plants and 83.6 mm in *mwp1-R*. The average width of husk leaf 8 was 83.2 mm in wild-type plants and 55.2 mm in *mwp1-R*.

In the A188 background, husk leaves 1, 4 and 8 were all significantly narrower and shorter than equivalent wild-type husk leaves (Table 4.2 B). The average width of husk leaf 1 was 85.2 mm in wild-type plants and 51.3 mm in *mwp1-R*. The average length was 189.5 mm in wild-type plants and 171.4 mm in *mwp1-R*. The average width of husk leaf 4 was 98.3 mm in wild-type plants and 79.9 mm in *mwp1-R*. The average length was 194.2 mm in wild-type plants and 168.9 mm in *mwp1-R*. The average width of husk leaf 8 was 63.5 mm in wild-

type plants and 53.2 mm in *mwp1-R*. The average length was 181.8 mm in wild-type plants and 155.8 mm in *mwp1-R*.

Table 4.2. Measurements of mature wild-type and *mwp1-R* husk leaves. (A) W23 background. (B) A188 background. Husk leaves one, four and eight were measured, with one being the outermost husk leaf. Husk leaf length was measured from the base to the blade-sheath boundary. Width was measured at a point midway between the base and tip of the leaf. Mean values were calculated separately for wild-type and *mwp1-R* husk leaves. Means were compared by Student's t-test to determine if they are significantly different at the 0.05 confidence level. * indicates values that are significantly different. SE = standard error. Numbers in brackets are the *mwp1-R* value represented as a percentage of the wild-type value.

A

Husk leaf 1 W23 background		Wild-type (n=11)	<i>mwp1-R</i> (n=15)	P-value
Length (mm)	Mean	185.5	187.2	0.853
	SE	6.6	6.4	
Width (mm)	Mean	89.9	53.1 (59%)	<0.001*
	SE	4.7	1.9	

Husk leaf 4 W23 background		Wild-type (n=11)	<i>mwp1-R</i> (n=15)	P-value
Length (mm)	Mean	173.5	173.7	0.992
	SE	9.3	8.4	
Width (mm)	Mean	108.3	83.6 (77%)	0.008*
	SE	6.8	5.3	

Husk leaf 8 W23 background		Wild-type (n=11)	<i>mwp1-R</i> (n=13)	P-value
Length (mm)	Mean	145.3	153.5	0.540
	SE	9.1	9.3	
Width (mm)	Mean	83.2	55.2 (66%)	<0.001*
	SE	6.2	3.6	

B

Husk leaf 1 A188 background		Wild-type (n=13)	<i>mwp1-R</i> (n=13)	P-value
Length (mm)	Mean	189.5	171.4(90%)	0.013*
	SE	5.6	3.6	
Width (mm)	Mean	85.2	51.3 (60%)	<0.001*
	SE	2.1	2.4	

Husk leaf 4 A188 background		Wild-type (n=13)	<i>mwp1-R</i> (n=13)	P-value
Length (mm)	Mean	194.2	168.9(87%)	0.027*
	SE	8.0	7.1	
Width (mm)	Mean	98.3	79.9 (81%)	0.016*
	SE	5.8	4.0	

Husk leaf 8 A188 background		Wild-type (n=13)	<i>mwp1-R</i> (n=12)	P-value
Length (mm)	Mean	181.8	155.8(86%)	0.0097*
	SE	8.0	4.1	
Width (mm)	Mean	63.5	53.2 (84%)	0.037*
	SE	3.8	2.7	

In both backgrounds, prophyll width was more severely affected than later husk leaves. *mwp1-R* had a more severe effect on prophyll and husk leaf width in the W23 background than in A188, but did not significantly affect husk leaf length in the W23 background. In the A188 background, *mwp1-R* affected both the width and length of prophylls and husk leaves.

Vegetative leaves

Vegetative leaf size was not affected by *mwp1-R* in either the W23 or A188 backgrounds. No significant differences were seen in blade length, sheath length, blade width or sheath width in *mwp1-R* leaves compared to wild-type leaves (Table 4.3 A, B).

Table 4.3. Measurements of mature wild-type and *mwp1-R* vegetative leaves. (A) W23 background. (B) A188 background. Leaves eight, nine and ten were measured (counting down from the tassel). Blade length was measured from the blade-sheath boundary to the tip of the leaf. Sheath length was measured from the base of the leaf to the blade-sheath boundary. Half leaf widths were measured from midrib to margin in the blade and sheath. Blade width was measured at the base of the blade. Sheath width was measured at a point midway between the base of the leaf and the blade-sheath boundary. Mean values were calculated separately for wild-type and *mwp1-R* husk leaves. Means were compared by Student's t-test to determine if they are significantly different at the 0.05 confidence level. SE = standard error.

A

Vegetative leaf 8 A188 background		Wild-type (n=10)	<i>mwp1-R</i> (n=10)	P-value
Blade length (mm)	Mean	691.4	662.5	0.092
	SE	11.6	11.4	
Sheath length (mm)	Mean	130.3	120.4	0.075
	SE	3.1	4.2	
Blade width (mm)	Mean	35.4	36.2	0.792
	SE	2.7	1.3	
Sheath width (mm)	Mean	40.8	37.1	0.121
	SE	1.9	1.3	

Vegetative leaf 9 A188 background		Wild-type (n=10)	<i>mwp1-R</i> (n=10)	P-value
Blade length (mm)	Mean	672.1	684.4	0.639
	SE	22.8	12.0	
Sheath length (mm)	Mean	148.0	132.4	0.067
	SE	3.2	5.7	
Blade width (mm)	Mean	32.5	35.7	0.325
	SE	2.9	1.1	
Sheath width (mm)	Mean	36.8	35.6	0.648
	SE	1.7	1.9	

Continued on next page.

Vegetative leaf 10 A188 background		Wild-type (n=8)	<i>mwp1-R</i> (n=8)	P-value
Blade length (mm)	Mean	635.3	652.3	0.599
	SE	25.6	18.5	
Sheath length (mm)	Mean	172.3	154.5	0.060
	SE	5.0	6.5	
Blade width (mm)	Mean	32.1	33.9	0.607
	SE	3.1	1.2	
Sheath width (mm)	Mean	32.9	32	0.728
	SE	1.4	2.0	

B

Vegetative leaf 8 W23 background		Wild-type (n=10)	<i>mwp1-R</i> (n=11)	P-value
Blade length (mm)	Mean	569.7	605.2	0.123
	SE	18.4	11.5	
Sheath length (mm)	Mean	138.2	137.2	0.87
	SE	5.8	4.7	
Blade width (mm)	Mean	30.2	29.4	0.657
	SE	1.2	1.2	
Sheath width (mm)	Mean	33.3	35.5	0.095
	SE	0.7	1.0	

Vegetative leaf 9 W23 background		Wild-type (n=10)	<i>mwp1-R</i> (n=10)	P-value
Blade length (mm)	Mean	613.8	602.7	0.675
	SE	18.3	19.3	
Sheath length (mm)	Mean	143.9	147.4	0.563
	SE	4.4	4.1	
Blade width (mm)	Mean	24.6	28.1	0.193
	SE	2.6	0.9	
Sheath width (mm)	Mean	32.8	33.3	0.74
	SE	1.1	0.9	

Vegetative leaf 10 W23 background		Wild-type (n=10)	<i>mwp1-R</i> (n=8)	P-value
Blade length (mm)	Mean	626.1	616.5	0.760
	SE	20.6	23.0	
Sheath length (mm)	Mean	149.1	154.0	0.463
	SE	4.5	4.6	
Blade width (mm)	Mean	27.2	27.1	0.966
	SE	1.4	0.9	
Sheath width (mm)	Mean	32.7	33.6	0.635
	SE	1.3	1.4	

Glumes

In the W23 background, *mwp1-R* glumes were significantly narrower than wild-type glumes (Table 4.4 A). The average glume width was 4.1 mm in wild-type plants and 3.5 mm in *mwp1-R* plants. Thus, *mwp1-R* glumes were 85% as wide as wild-type glumes. The length of *mwp1-R* glumes was not significantly different from wild-type glumes in the W23 background.

In the A188 background, *mwp1-R* glumes were significantly narrower and shorter than wild-type glumes (Table 4.4 B). The average glume width was 3.9 mm in wild-type and 3.3 mm in *mwp1-R*. Thus, *mwp1-R* glumes were 83% as wide as wild-type glumes. The average glume length was 9.6 mm in wild-type and 8.9 mm in *mwp1-R*. Thus, *mwp1-R* glumes were 92% as wide as wild-type glumes in the A188 background.

Table 4.4. Measurements of mature wild-type and *mwp1-R* glumes. (A) W23 background. (B) A188 background. Length was measured from the base to the tip of the glume. Width was measured from margin to margin at the widest point. Mean values were calculated separately for wild-type and *mwp1-R* glumes. Means were compared by Student's t-test to determine if they are significantly different at the 0.05 confidence level. * indicates values that are significantly different. SE = standard error. Numbers in brackets are the *mwp1-R* value represented as a percentage of the wild-type value.

A

Glumes W23 background		Wild-type (n=20)	<i>mwp1-R</i> (n=20)	P-value
Length (mm)	Mean	8.1	8.1	0.810
	SE	0.1	0.2	
Width (mm)	Mean	4.1	3.5 (85%)	<0.001*
	SE	0.1	0.1	

B

Glumes A188 background		Wild-type (n=15)	<i>mwp1-R</i> (n=15)	P-value
Length (mm)	Mean	9.6	8.9 (92%)	0.039*
	SE	0.2	0.3	
Width (mm)	Mean	3.9	3.3 (83%)	0.001*
	SE	0.1	0.2	

Paleae

In the W23 background, *mwp1-R* paleae were significantly narrower than wild-type paleae (Table 4.5 A). The average palea width was 3.8 mm in wild-type and 3.5 mm in *mwp1-R*. Thus, *mwp1-R* paleae were 92% as wide as wild-type

paleae. The length of *mwp1-R* paleae and distance between the keels were not significantly different from wild-type in the W23 background.

In the A188 background, the length and width of *mwp1-R* paleae was not significantly different from wild-type paleae (Table 4.5 B). The distance between the keels of *mwp1-R* paleae was significantly narrower than in wild-type paleae.

Table 4.5. Measurements of mature wild-type and *mwp1-R* paleae. (A) W23 background. (B) A188 background. Length was measured from the base to the tip of the palea. Palea width and the distance between the keels were measured at the widest point. Mean values were calculated separately for wild-type and *mwp1-R* paleae. Means were compared by Student's t-test to determine if they are significantly different at the 0.05 confidence level. * indicates values that are significantly different. SE = standard error. Numbers in brackets are the *mwp1-R* value represented as a percentage of the wild-type value.

A

Palea W23 background		Wild-type (n=25)	<i>mwp1-R</i> (n=25)	P-value
Length (mm)	Mean	7.9	7.7	0.325
	SE	0.1	0.1	
Width (mm)	Mean	3.8	3.5 (92%)	0.010*
	SE	<0.1	0.1	
Between keels (mm)	Mean	1.3	1.2	0.613
	SE	<0.1	0.1	

B

Palea A188 background		Wild-type (n=20)	<i>mwp1-R</i> (n=20)	P-value
Length (mm)	Mean	8.2	8.2	0.880
	SE	0.1	0.1	
Width (mm)	Mean	3.8	3.5	0.073
	SE	0.1	0.1	
Between keels (mm)	Mean	1.7	1.4	<0.001*
	SE	<0.1	0.1	

Silks

In the W23 background, the distance between the veins of *mwp1-R* silks was significantly narrower than in wild-type silks (Table 4.6 A). This distance was 315 μm in wild-type and 282 μm in *mwp1-R*. Thus, the intervein distance was 89% as wide in *mwp1-R* compared to wild-type. The distance from the vein to the outer edge of the silk was greater in *mwp1-R* than in wild-type silks, measuring 65 μm in wild-type and 84 μm in *mwp1-R*.

In the A188 background, the distance between the veins of *mwp1-R* silks was significantly narrower than in wild-type silks (Table 4.6 B). This distance was 352 μm in wild-type and 255 μm in *mwp1-R*. Thus, the intervein distance was 73% as wide in *mwp1-R* compared to wild-type. The distance from the vein to the outer edge of the silk was greater in *mwp1-R* than in wild-type silks, measuring 77 μm in wild-type and 105 μm in *mwp1-R*.

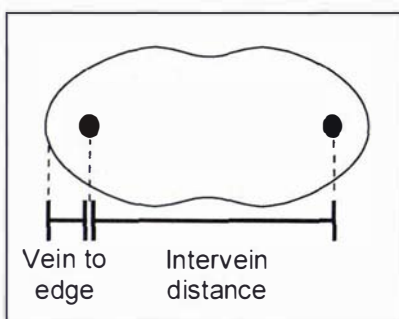
Table 4.6. Measurements of wild-type and *mwp1-R* silks. (A) W23 background. (B) A188 background. Measurements were made from transverse sections of wild-type and *mwp1-R* silks. Measurements were made of the distance between the veins, and from the vein to the outer edge of the silk. Mean values were calculated separately for wild-type and *mwp1-R* silks. Means were compared by Student's t-test to determine if they are significantly different at the 0.05 confidence level. * indicates values that are significantly different. SE = standard error. Numbers in brackets are the *mwp1-R* value represented as a percentage of the wild-type value

A

Silk width W23 background		Wild-type (n=8)	<i>mwp1-R</i> (n=8)	P-value
Intervein distance (μm)	Mean	315	282 (89%)	0.018*
	SE	8.1	9.5	
Vein to outer edge (μm)	Mean	65	84 (129%)	<0.001*
	SE	1.4	3.2	

B

Silk width A188 background		Wild-type (n=8)	<i>mwp1-R</i> (n=10)	P-value
Intervein distance (μm)	Mean	352	255 (73%)	<0.001*
	SE	11.7	12.0	
Vein to outer edge (μm)	Mean	77	105 (137%)	0.001*
	SE	4.2	5.4	



4.3.6 The *mwp1-R;Wab1-R* leaf blade phenotype

To determine if *mwp1-R* affects the polarity of ectopic sheath tissue, *mwp1-R* was crossed to *Wab1-R*, *Kn1-R* and *Rs1-R*. In *mwp1-R* vegetative leaves, disruption of adaxial-abaxial polarity is generally confined to the sheath. However, in *mwp1-R;Wab1-R* double mutants, adaxial-abaxial polarity is disrupted in blade tissue adjacent to ectopic sheath-like tissue (Figure 4.18). Bulliform cells and macrohairs are normally found only on the adaxial surface of the blade (Figure 4.18 B, C). In *mwp1-R;Wab1-R* mutants, bulliform cells and macrohairs are seen on both the adaxial and abaxial surfaces of the blade in regions near ectopic sheath-like tissue (D, E). Small outgrowths of blade tissue occur immediately adjacent to ectopic sheath-like tissue (D, E). Vascular polarity in these regions is disrupted in a similar manner to veins associated with outgrowths on *mwp1-R* husk leaves. Veins within outgrowths are oriented with xylem toward the inner surface of ectopic outgrowths (D) and in some cases are completely radialised (F). It was not clear whether adaxial-abaxial polarity was disrupted within the ectopic sheath-like tissue itself, as clearings tend to be narrow with few veins. Epidermal characteristics of cleared regions appeared to have normal adaxial-abaxial polarity, with smoother epidermis on the adaxial side and epidermal hairs on the abaxial side.

Similar disruptions to blade adaxial-abaxial polarity were associated with ectopic sheath-like tissue in *mwp1-R;Kn1-R* and *mwp1-R;Rs1-R* double mutants (data not shown).

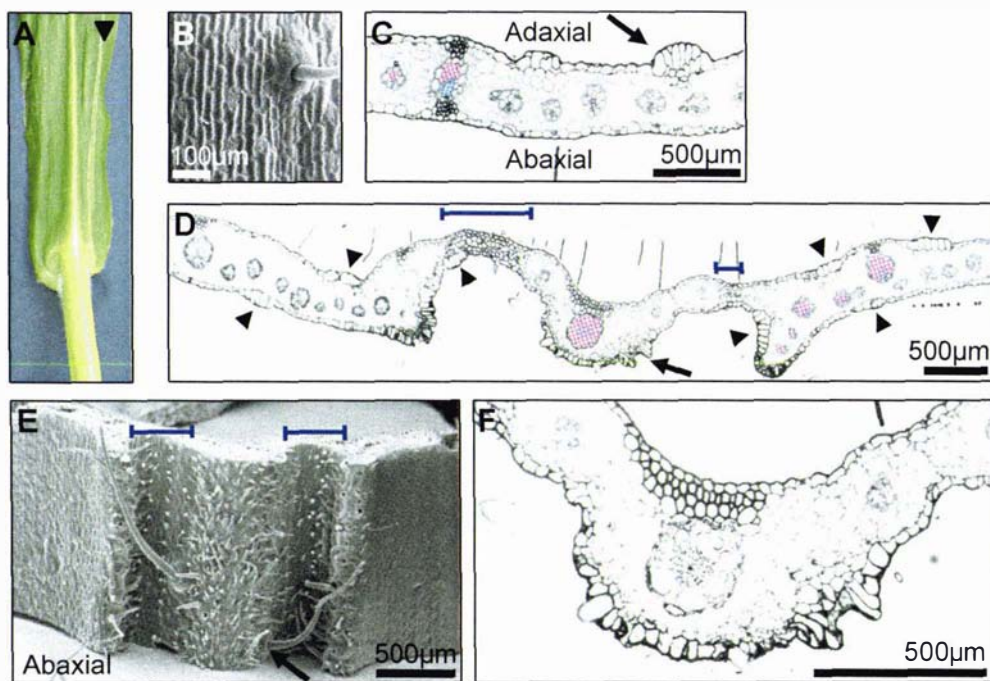


Figure 4.18. Adaxial-abaxial polarity is disrupted in regions adjacent to ectopic sheath-like tissue in *mwp1-R;Wab1-R* leaf blades.

(A) *mwp1-R;Wab1-R* leaf blade with ectopic sheath-like tissue (arrowhead). (B) SEM of wild-type blade adaxial surface. (C) Transverse section of wild-type leaf blade. Normal blade tissue has macrohairs and bulliform cells on the adaxial epidermis (B, arrow in C). Vascular bundles are oriented with xylem on the adaxial side (false coloured pink) and phloem on the abaxial side (false coloured blue). (D) Transverse section of *mwp1-R;Wab1-R* leaf blade. (E) SEM of *mwp1-R;Wab1-R* leaf blade abaxial surface. Narrow strips of ectopic sheath-like tissue are indicated by blue bars in (D) and (E). *mwp1-R;Wab1-R* leaf blades develop outgrowths adjacent to ectopic sheath-like tissue (D,E). Adjacent blade tissue has macrohairs (arrows) and bulliform cells (arrowheads) on the abaxial surface. Vascular polarity is distorted in ectopic outgrowths, and in some cases veins are completely radialised (D,E).

4.4 Discussion

Characterisation of the *mwp1-R* phenotype revealed that *mwp1-R* affects a range of lateral organs, including vegetative leaves, husk leaves, prophylls and floral organs. *mwp1-R* lateral organs were characterised by ectopic outgrowths on the abaxial surface associated with patches of ectopic adaxial tissue. Leaf margins were particularly affected. The misexpression of adaxial polarity genes in *mwp1-R* lateral organ primordia is consistent with this phenotype. The most severe phenotypes were seen in the prophylls and silks. It is hypothesised that these organs form via phytomer fusion (Cronquist, 1988; Bossinger et al., 1992; Scanlon and Freeling, 1998). Therefore, the severity of the prophyll and silk phenotypes may be attributable to their each having two sets of margins.

Most of the *mwp1-R* lateral organs investigated were narrower than wild-type. In some backgrounds *mwp1-R* lateral organs were also shorter. These observations are consistent with a model in which the adaxial-abaxial boundary promotes growth along both the lateral and proximal-distal axes. A detailed discussion of these results is presented below.

4.4.1 *mwp1-R* disrupts adaxial-abaxial polarity

***mwp1-R* husk leaves develop pairs of ectopic outgrowths**

mwp1-R husk leaves are characterised by paired flaps of ectopic tissue on the abaxial surface (Figure 4.1, Figure 4.2). These are similar to abaxial margin tissue on their outer surfaces and more similar to adaxial epidermis on their inner surfaces. The orientation of veins also suggests that the tissue between outgrowths has adaxial identity. Veins in *mwp1-R* outgrowths are oriented with their xylem poles toward the inner surfaces of outgrowths. In some cases veins are partially or completely radialised, with xylem surrounding a central core of phloem, similar to those seen in *Arabidopsis phb-1d* mutants (McConnell et al., 2001). *In situ* hybridisation showed that *rld1*, which is normally expressed on the adaxial side of husk leaf primordia, is misexpressed on the abaxial side of *mwp1-R* husk leaves, between pairs of outgrowths (Figure 4.3, Figure 4.4). This

result further supports the hypothesis that *mwp1-R* husk leaves are partially adaxialised.

The *mwp1-R* phenotype is consistent with the model proposed by Waites and Hudson, in which the juxtaposition of adaxial and abaxial cell types is required for lamina outgrowth (Waites and Hudson, 1995). This model predicts that new boundaries form where a patch of ectopic adaxial tissue is interspersed with normal abaxial tissue, thus initiating a pair of ectopic outgrowths. The margin-like characteristics of *mwp1-R* husk leaf flaps also support the idea that a boundary between adaxial and abaxial cell types is required for the development of margin characteristics (Sawa *et al.*, 1999). This aspect of the phenotype is common to other polarity mutants, such as *Arabidopsis kan1;kan2* mutants, which have leaves that are nearly radial, with marginal cell types found around the entire circumference (Eshed *et al.*, 2004).

Expression of the maize *YAB* gene, *zyb9*, was less polarised than *rdl1* expression in older husk leaves (Figure 4.4). In wild-type husk leaves, expression persists at the margins and in developing vascular bundles but fades in medial regions. *zyb9* expression was observed in ectopic outgrowths in medial regions of *mwp1-R* husk leaves. Expression was strongest in the tip of each outgrowth. This pattern is similar to the misexpression of *zyb9* and *zyb14* in ectopic outgrowths on *lb11* and *Rld1-O* leaf primordia (Juarez *et al.*, 2004a).

Juarez *et al.* (2004a) observed that *zyb* expression in older leaf primordia is associated with less determined cell types, such as the margins and central layer of ground tissue. The hypothesis that maize *YAB* genes promote leaf outgrowth is supported by the observation that ectopic outgrowths on the adaxial side of *lb11* leaf primordia and the abaxial side of *Rld1-O* leaf primordia both express *zyb9* and *zyb14* (Juarez *et al.*, 2004a). Thus, misexpression of *zyb9* in *mwp1-R* husk leaves may be associated with less determined cells and the outgrowth of ectopic laminae, rather than altered polarity *per se*.

Single outgrowths develop at the margins of *mwp1-R* sheaths

The sheaths of *mwp1-R* vegetative leaves have phenotypes similar to husk leaves, but are less severely affected. The most consistently observed

phenotype was a single outgrowth immediately adjacent to the sheath margin (Figure 4.15). These outgrowths were confined to the sheath and never extended into the leaf blade. Similar marginal outgrowths occur on husk leaves. The actual margins of affected leaves are blunt, whereas the outgrowths are tapered and look more similar to normal sheath margins. Adaxial-type epidermis extends onto the abaxial side of the leaf to the tip of the outgrowth, so that the adaxial epidermis appears to wrap around the margin (Figure 4.16). Veins in this region are radial and adaxialised. *rd1* expression is not confined to the adaxial side of affected leaf primordia, as in wild-type leaves, but is expressed uniformly throughout the leaf margin. Outgrowths develop at the boundary between ectopic *rd1* expression and non-expressing cells. These observations are consistent with the idea that the adaxial-abaxial boundary is required for the development of marginal characteristics, as well as for lateral growth (Sawa *et al.*, 1999), as normal margin characteristics develop where there is a distinct adaxial-abaxial boundary. Outgrowths at the margins occur singly, rather than in pairs. The most likely explanation is that only one boundary is created when adaxialised sectors occur at the margins. When adaxial tissue is flanked by abaxial tissue on both sides, two boundaries are created and a pair of outgrowths is initiated.

Outgrowths were frequently observed at the margins of *mwp1-R* vegetative leaf sheaths that had otherwise normal polarity. This may indicate that adaxial and abaxial domains are specified normally during early development, but are not maintained in *mwp1-R* sheaths. In maize, differentiation proceeds basipetally and from the midrib to margins (Sharman, 1942). Thus, the sheath margins are the last part of the leaf to differentiate. Based on the *mwp1-R* phenotype, we predict that *Mwp1* may act late in vegetative leaf development to maintain the abaxial domain.

The *gram* (*yab*) mutant in *Antirrhinum* has a leaf margin phenotype that is similar to *mwp1-R* (Golz *et al.*, 2004). *gram* leaf margins are blunt and adaxial cell types "wrap around" to the abaxial side. The *HD-ZIPIII* gene, *AmPHB* is misexpressed in *gram* leaves in a similar pattern to *rd1* misexpression in *mwp1-R* mutants. However, outgrowths have not been observed at *gram* leaf margins. This may be explained if one of the normal functions of *GRAM* is to

promote lamina outgrowth, as has been proposed for *GRAM* and other *YAB* family members (Siegfried *et al.*, 1999; Eshed *et al.*, 2004; Golz *et al.*, 2004). In *mwp1-R*, *YAB* function is not compromised so could still act to promote ectopic lamina outgrowth.

***mwp1-R* affects prophyll development in a variety of ways**

Normal morphology and development of the prophyll

Normal prophylls have two outer margins that enclose the ear and two prominent keels that wrap back around the culm (Figure 4.5). The keels are connected by a membranous tissue that lies between the ear and the culm of the mature plant. Epidermal features are similar to regular husk leaves. The adaxial surface is relatively smooth, whereas, the abaxial surface is hairier and the cells are more rounded. In the terminology of Bossinger *et al.* (1992), the prophyll is a type two phytomer - it is a fused organ produced by a newly initiated meristem.

The prophyll is initiated on the side of the lateral meristem adjacent to the main shoot axis and furthest from the subtending leaf (Figure 4.5). The two primordia appear to be initiated simultaneously. At the earliest observable stage the two primordia are connected by a strip of tissue that will form the central membrane (Figure 4.8). These observations support the idea that fusion occurs congenitally (Scanlon and Freeling, 1998). The prophyll grows upward and laterally so that the lateral meristem and subsequent primordia are concealed.

In situ hybridisation shows that *rld1* is expressed on the adaxial side of the prophyll (Figure 4.9). Very early in development, a block of *rld1* expression is seen on the side of the prophyll adjacent to the subtending leaf. Cells immediately adjacent to these strongly expressing cells appear to lack *rld1* expression, or to express *rld1* at much lower levels. The boundary between *rld1*-expressing and non-expressing cells extends along the presumptive keel axis (Figure 4.10). This block of expression was not observed in later stage prophylls. We hypothesise that this transient expression pattern may set up a boundary that initiates keel outgrowth. This model is discussed in Section 4.4.8. *rld1* expression persists in the prophyll outer margins and in the central membrane, but often fades from the intervening tissue. It has been observed

previously that *rld1* expression persists in vegetative leaf margins (Juarez *et al.*, 2004b). The persistence of *rld1* expression in the prophyll central membrane is consistent with the idea that the central membrane represents the fused margins of two leaf primordia (Bossinger *et al.*, 1992; Scanlon and Freeling, 1998).

It was observed that the polarity of individual vascular bundles in wild-type prophyll keels often differed from those in the rest of the prophyll (Figure 4.7). In the outer margins, and in the central membrane, veins were orientated with xylem on the adaxial side and phloem on the abaxial side. Veins in the keel were often rotated relative to veins in flanking regions, and some had two xylem poles. This observation suggests that specification of polarity in the keel region may differ from that of the rest of the prophyll.

Unfused prophylls are associated with rld1 misexpression early in development

The most severe manifestation of the *mwp1-R* phenotype was the reduction of the prophyll to two unfused prongs corresponding to the two midrib regions (Figure 4.6). The central membrane and most of the outer margin regions were deleted. The prongs were usually connected at the very base by a residual strip of membranous tissue. According to the fused phytomer model, the deleted parts correspond to the margin domains of two phytomers. Keel outgrowth was also significantly reduced.

Adaxial-abaxial polarity was distorted in the midrib regions (prongs) of unfused prophylls. Veins were often partially or fully radialised. Analysis of epidermal features indicated that adaxial-type epidermal features continued onto the abaxial side of each prong, so that only the central portion of the abaxial side had normal abaxial epidermal features. This phenotype is reminiscent of the "wrapping around" of epidermal features seen at the sheath margins.

An analysis of prophyll development by SEM indicated that *mwp1-R* prophylls are initiated normally (Figure 4.8). Early in development the two primordia are connected by a central membrane, similar to wild-type prophylls. By plastochron four there are clear differences between *mwp1-R* and wild-type prophylls. In the wild-type prophyll the central membrane has elongated and the two tips have

grown laterally. In contrast, the membrane of the *mwp1-R* prophyll has undergone very little growth and the two tips have elongated, but have not grown laterally. The difference becomes more pronounced later in development. These observations imply that *Mwp1* is not required for prophyll initiation, but may act to specify or maintain polarity after emergence. These data are consistent with the idea that the two midrib regions are patterned before the margins.

Measurements of developing prophylls also support the idea that unfused prophylls result from a growth defect that occurs after emergence (Figure 4.11). Early in development, the central membrane regions of *mwp1-R* and wild-type prophylls are the same height. As the overall height of wild-type prophylls increases the membrane also grows rapidly. In contrast, the central membrane of *mwp1-R* prophylls grows very slowly relative to overall prophyll height. Given that maturation of maize leaves proceeds basipetally, it seems likely that growth of the basal portion of the primordium contributes most of the height of the prophyll, with the unfused tips differentiating early in development and contributing relatively little to overall height of the mature prophyll. This is supported by the observation that the prophyll tips develop hairs early in development, when the prophyll is less than 3 mm high (see SEMs, Figure 4.11). Wild-type prophylls bifurcate at the very tip (Scanlon and Freeling, 1998). The bifurcated tip is likely to correspond to the unfused portion of the wild-type prophyll primordium.

rld1 is misexpressed early in the development of *mwp1-R* prophylls that exhibit the unfused phenotype (Figure 4.9). In the central membrane of wild-type prophyll primordia, *rld1* expression is confined to the adaxial side. In the corresponding part of early *mwp1-R* primordia, *rld1* is expressed both adaxially and abaxially. This suggests that the adaxial-abaxial boundary is required for lateral and proximal-distal growth of the membrane. Loss of adaxial-abaxial polarity in *mwp1-R* may result in the loss of growth along the proximal-distal axis. *rld1* is also ectopically expressed in a patchy manner in *mwp1-R* prophyll prongs. This is consistent with the phenotypic analysis which shows distorted polarity. It is likely that loss of distinct adaxial and abaxial domains is

responsible for the lack of proximal-distal growth of the central membrane and lateral growth of the margins.

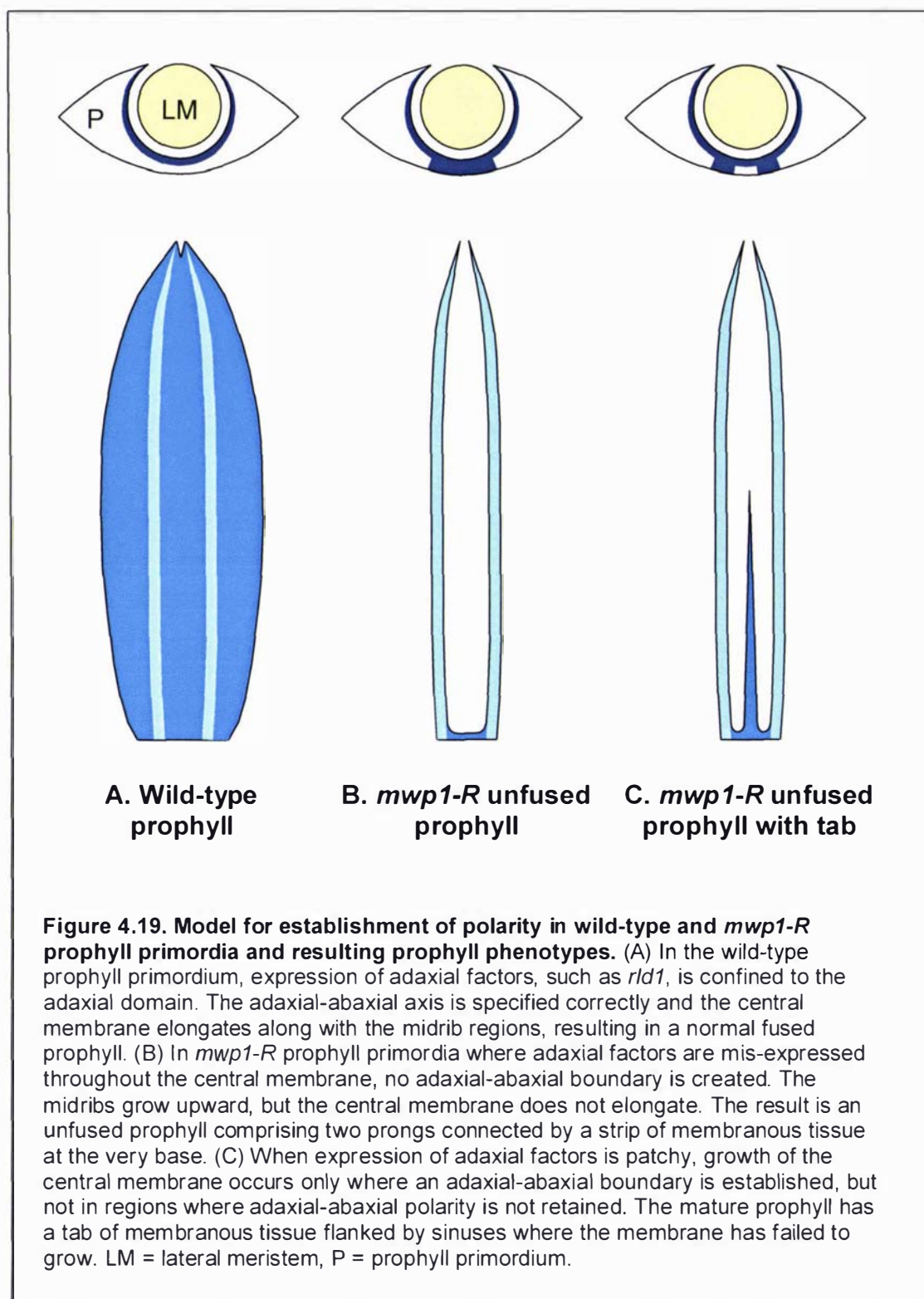
The mwp1-R prophyll tab phenotype is due to irregular disruption of polarity

A variation of the unfused prophyll phenotype is the development of prophylls that are unfused, but have a tab of tissue extending distally from the central membrane between the two prongs (Figure 4.12). The tabs vary in size and morphology. Some appear to have normal epidermal features, whereas others have outgrowths associated with regions of adaxial identity interspersed with normal abaxial tissue. It seems likely that the phenotypic variation corresponds to irregular disruption of polarity during development. The *rld1* expression pattern in prophylls with developing tabs supports this theory. In Figure 4.13, *rld1* is misexpressed in the abaxial domain, just below the U-shaped sinuses on either side of the tab. Patchier *rld1* expression can be seen in the tab itself and in the region immediately below, but with some retention of a polar expression pattern. This pattern suggests that the development of tabs occurs in regions where some adaxial-abaxial polarity is retained, while growth is retarded in areas where polarity is lost completely. The fact that very long tabs were observed demonstrates that when adaxial and abaxial domains are established, the central membrane region of the prophyll can undergo extensive growth along the proximal-distal axis.

Prophyll fusion defects are due to failure of the central membrane to elongate

Although the most severely affected *mwp1-R* prophylls are unfused at maturity, my results indicate that the primary defect is a growth defect rather than a fusion defect *per se*. Firstly, *mwp1-R* prophylls are initiated normally and the two primordia are connected by a central membrane at the earliest stages. By plastochron 4 the two prongs are physically separated, with connecting membrane only at the very base. Measurement data indicate that the prongs elongate but the central membrane fails to grow (Figure 4.11). Secondly, the tab phenotype demonstrates that the central membrane is capable of significant growth along the proximal-distal axis when adaxial-abaxial polarity is retained. The tab is physically separate from the two prongs. Therefore, it cannot be derived from lateral growth and fusion of the prongs. Figure 4.19 summarises

the *rld1* expression pattern in the central membrane of *mwp1-R* and wild-type prophyll primordia and the corresponding mature prophyll phenotypes.



The mwp1-R subdivided keel phenotype is associated with rld1 misexpression later in development

mwp1-R prophylls that develop as fused organs often exhibit severe defects in the keel region (Figure 4.14). This phenotype was most common in the W23 inbred background. In these prophylls, each keel was transformed into a complex series of outgrowths, often with multiple orders of bifurcation. Veins within the keel region were radialised, whereas those in flanking regions had normal polarity. Less pronounced outgrowths were also seen on other parts of the prophyll, similar to those seen on husk leaves. This phenotype suggests that the keel region may be particularly sensitive to disruptions to normal polarity.

rld1 transcript was detected in the prophyll keels in *mwp1-R* families that express the subdivided keel phenotype, whereas, *rld1* expression was never seen in wild-type keels at equivalent stages (Figure 4.14). *rld1* misexpression occurred much later than in families with unfused prophylls, and tended to be in isolated patches. *rld1* expression was frequently associated with regions where the keel was beginning to divide, suggesting that outgrowths and bifurcations occur at points where polarity is disrupted. The finding that *rld1* misexpression occurs relatively late in development, and that prophylls with subdivided keels are fused suggests that polarity is established correctly, allowing early development to proceed normally. However, polarity is not maintained at later stages and causes aberrant development as the keel is being elaborated. It is plausible that other factor(s) in this background repress *rld1* early in development, but do not act at later stages.

Expression of the maize *YAB* gene, *zyb9*, was investigated in prophyll primordia exhibiting the subdivided keel phenotype. The results indicate that *zyb9* is misexpressed in *mwp1-R* prophyll keels in a pattern that mirrors *rld1* misexpression. *zyb9* expression was detected in regions where the keel was bifurcated. The *YAB* genes have been implicated in lamina outgrowth in both dicots and monocots (Siegfried *et al.*, 1999; Eshed *et al.*, 2004; Golz *et al.*, 2004; Juarez *et al.*, 2004a). It is likely that misexpression of *zyb9*, and probably other *YAB* genes, mediates the outgrowth of ectopic laminae in the keel region of *mwp1-R* prophylls.

***mwp1-R* silks are most severely affected in marginal domains**

Like the prophyll, the silks are thought to derive from the congenital fusion of two primordia. However, the mode of fusion is different. It is proposed that the two primordia are folded at the midrib and fuse along two sets of margins (Figure 1.6 D). Thus, the two veins correspond to the midribs, and the indented regions correspond to the fused margins (Cronquist, 1988; Scanlon and Freeling, 1998). This model is supported by the finding that in *ns* mutants, which delete leaf margins, the veins are closer together whereas the distance between the veins and the outer edge of the silk is unchanged (Scanlon and Freeling, 1998).

It was observed that *mwp1-R* silks had the most extensive proliferation of ectopic tissue in the indented regions, the regions corresponding to the fused margins (Figure 4.17). This phenotype is consistent with the folded phytomer model, as the margins are the most severely affected part of other *mwp1-R* organs. Less pronounced outgrowths were seen along the outer edges of silks in the regions corresponding to the midrib domains. The base of the silk, which corresponds to the lower leaf zone, was more severely affected than distal parts (Scanlon and Freeling, 1998).

mwp1-R silks often had a kinked or twisted appearance, particularly at the base. Differential growth of opposite sides of the silk is likely to be responsible for this twisting. Epidermal cells were frequently elongated perpendicular to the surface of the silk, suggesting that the plane of cell expansion is disrupted by *mwp1-R*.

4.4.2 *mwp1-R* affects lateral and proximal-distal growth

***mwp1-R* lateral organs are narrow**

Measurements of *mwp1-R* and wild-type lateral organs showed that *mwp1-R* prophylls, husk leaves, paleae and glumes are significantly narrower than wild-type organs in the W23 background. However, organ length was not affected in this background. In the A188 background, *mwp1-R* prophylls, husk leaves and glumes were significantly narrower and shorter than wild-type organs. The width and length of *mwp1-R* paleae were not significantly different from wild-type

paleae in this background. Vegetative leaf size was not affected by *mwp1-R* in either the W23 or A188 backgrounds. This may reflect the fact that *mwp1-R* has only a mild phenotype in the sheaths of vegetative leaves and has no obvious blade phenotype.

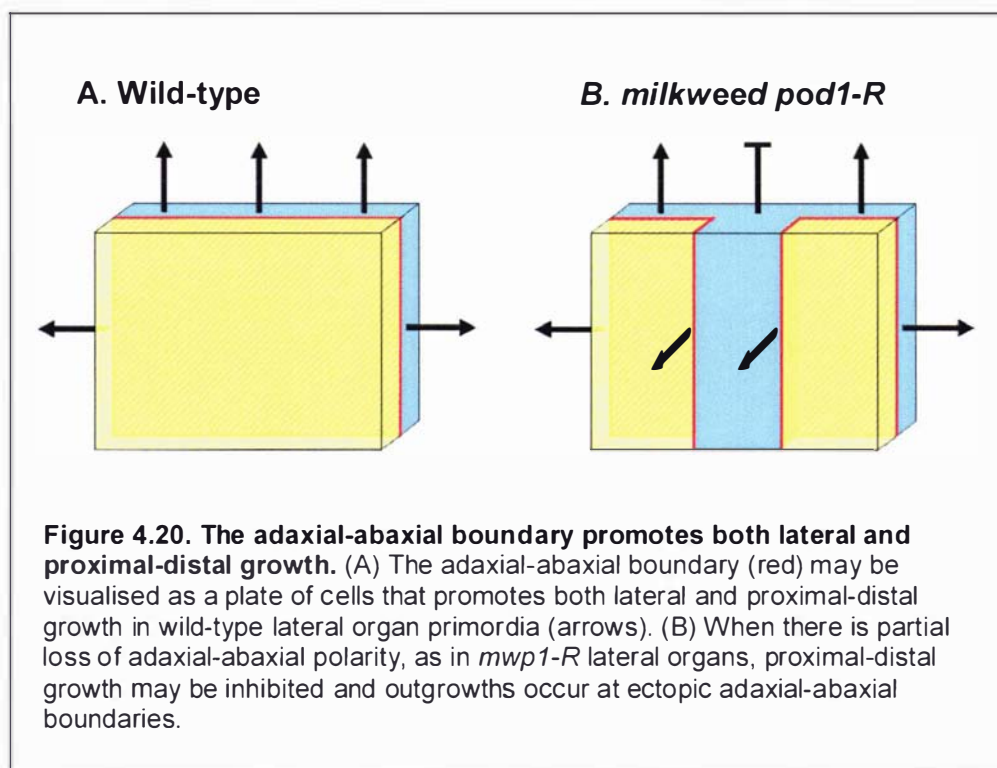
Maize *ns* mutants have narrow leaves that lack normal margin characteristics due to the deletion of a marginal domain (Scanlon *et al.*, 1996; Scanlon and Freeling, 1997; Scanlon, 2000). *mwp1-R* lateral organs appear to be initiated normally and generally have normal margin characteristics, with the exception of sheaths exhibiting marginal outgrowths. These observations suggest that the narrowness of *mwp1-R* lateral organs is more likely due to reduced lateral growth than to the deletion of a specific domain.

Narrow lateral organ phenotypes are common in other mutants that affect adaxial-abaxial polarity, indicating that correct specification of the adaxial-abaxial axis is required for lateral growth (Waites and Hudson, 1995; Eshed *et al.*, 2001; Kerstetter *et al.*, 2001; Golz *et al.*, 2004). *YAB* genes have been implicated in lateral growth and one theory is that the juxtaposition of *YAB* expressing and non-expressing cells is required to promote growth (Eshed *et al.*, 2004). My results show that *rld1* and *zyb9* are misexpressed in *mwp1-R* lateral organs. Thus, the lack of differential *YAB* expression may contribute to reduced lateral growth of *mwp1-R* leaves. In normal leaves, there is coordinated cell expansion and division along the lateral axis. In *mwp1-R* mutants there are multiple ectopic boundaries. Therefore, in these regions cell expansion and division is reorientated along the new axes, at right angles to the plane of the leaf.

The data indicate that *mwp1-R* affects proximal-distal growth as well as lateral growth. *mwp1-R* lateral organs in the A188 background were significantly shorter, as well as narrower, than wild-type lateral organs. Growth in both dimensions was similarly affected in this background. In unfused prophylls, growth of the central membrane along the proximal-distal axis is severely affected. Reductions in lateral organ length have been observed in other mutants that affect organ polarity (Waites and Hudson, 1995; Eshed *et al.*, 1999; Eshed *et al.*, 2004). It was observed that epidermal cells associated with

ectopic outgrowths at *mwp1-R* sheath margins were shorter than wild-type adaxial sheath margin cells (Figure 4.16). This observation is consistent with the theory that *mwp1-R* disrupts cell elongation along the proximal-distal axis.

It is not surprising that disruptions to the adaxial-abaxial boundary affect proximal-distal growth as well as lateral growth. Although this boundary is frequently depicted as a line, it may be more accurately visualised as a plane of cells between adaxially-specified and abaxially-specified cells (Figure 4.20). Waites and Hudson (1995) describe the boundary as a plate of cells that changes its division pattern to lateral proliferation, thereby forming the lamina. Cells at the boundary could direct cell expansion and division along both the lateral and proximal-distal axes. An analogous mechanism exists in *Drosophila*, where loss of the dorsally expressed gene *apterous* leads to loss of growth in both the proximal-distal and lateral directions (Butterworth and King, 1965).



Fused organs are strongly affected by *mwp1-R*

mwp1-R prophylls exhibit more severe growth defects than husk leaves. In the most extreme cases, the membrane between the two midribs fails to elongate and the prophyll develops as an unfused, two-pronged structure. In the case of

fused prophylls, *mwp1-R* generally had a greater effect on the width of prophylls than on husk leaves in the same background. One possible reason is that leaf margins are particularly affected by *mwp1-R*. As a fused organ, the prophyll has four margin domains, whereas husk leaves have only two. In both the A188 and W23 backgrounds, the distance between the keels was reduced to a similar degree as overall width. This implies a reduction in growth of both the inner and outer margins. An alternative explanation is that organs that are produced earlier are more sensitive to *mwp1-R* than later organs. This would be consistent with the general trend for later husk leaves to be less affected than earlier ones. These two explanations are not mutually exclusive.

Like the prophyll, the palea is a bikeeled organ. It was predicted that, if the palea is a fused organ with four margin domains, then palea width would be more severely affected by *mwp1-R* than glume width. However, *mwp1-R* paleae did not have an obvious phenotype. The size of *mwp1-R* paleae was not significantly different from wild-type paleae in the A188 background. *mwp1-R* paleae were narrower than wild-type paleae in the W23 background. However, they were less affected than glumes in the same background. Scanlon and Freeling (1998) found that the distance between the paleae keels was not significantly reduced in *ns* mutants, although the outer margins were reduced. Thus, their study provided no evidence to support the model that the paleae are fused organs. My results are consistent with this finding.

The silks (stigmas) of *mwp1-R* plants also exhibit altered growth. Measurement data indicate that the veins are closer together in *mwp1-R* silks than in wild-type silks. When interpreted in terms of the folded phytomer model, this phenotype corresponds to a reduction in lateral growth. According to this model, the veins correspond to the two midribs and the indented regions represent the margins of two fused primordia (Cronquist, 1988; Scanlon and Freeling, 1998). Scanlon and Freeling (1998) found that the distance between the veins is reduced in *ns* mutants, whereas, the distance from the veins to the outer edge was unaltered. They also found that *ns* silks lack the surface indentation seen in wild-type silks. The phenotype was interpreted as deletion of the margins. The surface indents were still present in *mwp1-R* silks, although some silks had pronounced

outgrowths in this area. These results point to a reduction in lateral growth in *mwp1-R* silks, rather than deletion of an entire domain.

The distance from the veins to the outer edge of the silk was found to be greater in *mwp1-R* than in wild-type. This could be due to outgrowths in this region, and to the expansion of cells perpendicular to the surface of the silk. This may be due to the loss of adaxial-abaxial polarity and the formation of ectopic boundaries, as is observed in other *mwp1-R* lateral organs.

A number of dicot mutants that affect leaf polarity and growth also have lateral organ fusion defects. In *Antirrhinum*, *gram* mutants often have unfused corolla tubes (Golz *et al.*, 2004). The *gram* phenotype is somewhat similar to *mwp1-R*. *gram* leaves exhibit adaxial-abaxial polarity defects, particularly at the margins, and lateral organs are narrower in *gram* mutants than in wild-type. Thus, the fusion defect may be attributable to reduced lateral growth or to the loss of margin characteristics.

Defects in carpel fusion are seen in *Arabidopsis* mutants of *crabs claw* (*crc*), a YAB gene, and *spatula* (*spt*), a basic-helix-loop-helix transcription factor (Alvarez and Smyth, 1999; Bowman and Smyth, 1999; Heisler *et al.*, 2001). *crc* carpels are unfused in the upper third, and this is attributed to the upper part of *crc* carpels being narrower than the lower regions (Alvarez and Smyth, 1999). *SPT* is expressed in the margins of developing carpels and in the septum, a structure derived from the postgenital fusion of outgrowths from the carpel margins (Heisler *et al.*, 2001). These tissues are reduced or lost in *spt-2* mutants, suggesting that *SPT* promotes growth of carpel margin tissue. It is suggested that *SPT* may promote congenital fusion of the carpels directly or, alternatively, the failure to fuse may be a consequence of disrupted lateral growth (Alvarez and Smyth, 1999).

4.4.3 *Mwp1* interacts with networks that establish leaf polarity

Given that *mwp1-R* is a recessive mutation, the adaxialisation of *mwp1-R* lateral organs suggests that *Mwp1* normally acts to promote abaxial identity or to repress adaxial identity. The disruption of vascular polarity in *mwp1-R* lateral

organs suggests a role for *Mwp1* in vascular patterning. *rld1* is misexpressed in affected organs, indicating that *Mwp1* may act to repress *rld1* during normal development. In *Arabidopsis*, an antagonistic relationship between *HD-ZIPIII* and *KAN* family members functions in the establishment of polarity in lateral organs and vascular tissue (Eshed *et al.*, 2001; Kerstetter *et al.*, 2001; Emery *et al.*, 2003; Eshed *et al.*, 2004).

Henderson *et al.* (2006) found that the maize *KAN* gene, *Zm*KAN2*, is expressed in a complementary pattern to *rld1*. Their finding is consistent with, although does not prove, an antagonistic interaction between maize *KANs* and *HD-ZIPIII* genes. Analysis of *KAN* expression in a *Rld1* mutant background would help clarify whether such an antagonistic relationship exists.

miRNA165/166 has been shown to regulate *rld1* expression in maize (Juarez *et al.*, 2004b). Indeed, miRNA-directed cleavage of *HD-ZIPIII* mRNAs is conserved throughout the land plants (Floyd and Bowman, 2004). In addition, there is evidence that *rld1* expression is controlled in part at the transcriptional level (Juarez *et al.*, 2004b). *KAN* genes, such as *Mwp1*, may act at this level.

There are several scenarios as to how *HD-ZIPIII* and *KAN* genes might interact to specify adaxial and abaxial domains. Firstly, there could be an antagonistic relationship, with *HD-ZIPIII* genes specifying adaxial fate, and *KANs* specifying abaxial fate. In *mwp1-R* mutants, a loss of *KAN* function allows *HD-ZIPIII* misexpression on the abaxial side of leaf primordia. Reduced levels of *KAN* coupled with ectopic *HD-ZIPIII* expression would then result in cells in these regions adopting adaxial identity. Alternatively, adaxial and abaxial domains may be determined by regions of *HD-ZIPIII* expression and non-expression respectively. In this scenario, the main role of *KAN* genes would be to repress *HD-ZIPIII* expression rather than to specify abaxial fate directly. A similar mechanism has been proposed to pattern *Arabidopsis* vasculature (Emery *et al.*, 2003). Finally, it may be the relative levels of *HD-ZIPIII* and other factors that determine cell identity. This model is supported by the finding that misexpression of *rld1* is sufficient to switch adaxial and abaxial cell identities (Nelson *et al.*, 2002).

Maize *YAB* (*zyb*) genes are expressed in lateral organs in a similar pattern to *rld1* (Juarez *et al.*, 2004a), although my data indicate that *zyb9* expression in older husk leaves is less polarised than *rld1*. *zyb* expression is increased in *Rld1* mutants, suggesting that *zyb* genes are downstream of *rld1* (Juarez *et al.*, 2004a). However, *Rld1* misexpression is not sufficient to induce *zyb* expression on the abaxial side of young *Rld1* primordia, suggesting that other factors, in addition to *HD-ZIPIII* genes, control *zyb* expression (Juarez *et al.*, 2004a).

My results show that *zyb9* is misexpressed in *mwp1-R* lateral organs, in a pattern that mirrors *rld1* misexpression. This pattern could indicate that *YAB* genes are downstream of *HD-ZIPIII* genes in maize, as suggested by Juarez *et al.* (2004b). Alternatively, *Mwp1* may repress *zyb* expression directly. Thus, *Mwp1* and other *KAN* genes may constitute the additional factors controlling *zyb* expression. It is possible that *zyb* genes are positively regulated by *HD-ZIPIII* genes and negatively regulated by *KAN* genes. The current results do not allow me to distinguish between these possibilities.

rld1 is misexpressed in both *mwp1-R* and *Rld1* mutants, and both mutants show adaxialisation of abaxial tissues (Nelson *et al.*, 2002; Juarez *et al.*, 2004b). However, there are differences between the mutant phenotypes. *rld1* causes adaxialisation of sectors of the blade, whereas, the *mwp1-R* phenotype is generally confined to sheath tissue. In *mwp1-R*, vegetative leaves are less severely affected than husk leaves, whereas, no husk leaf phenotype has been described for *Rld1* mutants. *Rld1* leaves sometimes exhibit a switching of adaxial and abaxial epidermal identities (Nelson *et al.*, 2002). This was not observed in *mwp1-R* mutants.

There are a number of factors that may account for these phenotypic differences. Firstly, the redundant activity of additional *KAN* family members may mean that *rld1* is only misexpressed in specific tissues in *mwp1-R* mutants. Secondly, the temporal and spatial patterns and the level of *rld1* misexpression are likely to differ in the two mutants. In *mwp1-R* leaf primordia, *rld1* is misexpressed in patches, whereas, in *Rld1-O* mutants, *rld1* is misexpressed in a more uniform manner (Juarez *et al.*, 2004b). In *Rld1* mutants, *rld1* misexpression is due to loss of regulation by miRNAs, whereas, in *mwp1-R*

mutants *rd1* misexpression is due to the loss of one *KAN* function. Thirdly, in *Rld1* mutants only a single *HD-ZIPIII* gene is misexpressed, whilst it is possible that multiple *HD-ZIPIII* genes are misexpressed in *mwp1-R* mutants.

mwp1-R mutants exhibit a more severe disruption of vascular polarity than has been reported for *Rld1* mutants. Veins at the junctions of *mwp1-R* husk leaf outgrowths and sheath margins may be partially or completely radialised, whereas *Rld1* major veins are unaffected and minor veins may be lost or mis-oriented (Nelson *et al.*, 2002; Juarez *et al.*, 2004a). In wild-type leaf primordia, *rd1* is expressed in immature vascular strands and becomes localised to pro-xylem cells (Juarez *et al.*, 2004b). Expression in vascular bundles is not altered by loss of *lbl1* function (Juarez *et al.*, 2004a). Given that *Lbl1* operates in the miRNA pathway (per. comm. Marja Timmermans), this finding suggests that *rd1* is regulated independently of miR165/166 in vascular bundles. Thus, *rd1* expression may be relatively normal in *Rld1* vascular bundles, but misexpressed in *mwp1-R* vascular bundles. It is likely also that *HD-ZIPIII* genes other than *rd1* are misexpressed in *mwp1-R* leaves, and these may contribute to vascular patterning. For example, a maize *PHB* homologue is expressed specifically in pro-xylem cells during normal development (Juarez *et al.*, 2004b).

4.4.4 Expression of the *mwp1-R* phenotype varies in different inbred backgrounds

Maize is genetically very diverse. Mutant phenotypes may vary in different backgrounds due to the variability of modifying genetic factors and differences in developmental rate (Bertrand-Garcia and Freeling, 1991; Tenaillon *et al.*, 2001; Fu and Donner, 2002; Song and Messing, 2003; Brunner *et al.*, 2005). The expression levels of homologous genes have been found to differ in different inbred backgrounds (Song and Messing, 2003; Guo *et al.*, 2004). Thus, the pattern and level of expression of genes in interacting networks is likely to influence mutant phenotypes in different backgrounds. There are also morphological differences between inbred lines. For example, the size of the SAM varies in different inbred lines and is correlated with penetrance of the *kn1-E1* phenotype (Vollbrecht *et al.*, 2000).

The *mwp1-R* phenotype varies depending on the background in which it was expressed. The phenotype is very mild in the B73 background, so was not examined in detail in this background (per. comm., Hector Candela and Sarah Hake). B73 is a late flowering line (Bertrand-Garcia and Freeling, 1991). It is possible that additional factors expressed later in development could compensate for loss of *Mwp1* function in this background.

The prophyll phenotype shows considerable variation depending on background. These differences are correlated with temporal differences in *rld1* misexpression. In its most severe form, the prophyll is unfused. This phenotype was most consistently observed in a non-introgressed background, and occasionally in the W23 background. The unfused prophyll phenotype is associated with *rld1* misexpression early in development. In the W23 background, the most commonly observed prophyll defect was the subdivision of the keel into a series of outgrowths. This subdivided keel phenotype is associated with patchy misexpression of *rld1* later in development.

The *mwp1-R* subdivided keel phenotype was seldom seen in the A188 background. A188 is a fast-maturing line. One possibility is that prophyll primordia in the A188 background reach a later stage of differentiation before polarity is disrupted by loss of *Mwp1* function. Such disruptions may occur too late to affect morphogenesis, but could still affect subsequent growth. Alternatively, there may be subtle differences in the way *HD-ZIPIII* genes are regulated in different inbred backgrounds.

The effects of *mwp1-R* on lateral organ growth also differed in A188 and W23. In general, in the W23 background *mwp1-R* lateral organs were reduced in width, but organ length was not significantly different. In the A188 background, both the width and length of *mwp1-R* lateral organs were reduced. The reduction in width was generally greater in the W23 background. The adaxial-abaxial boundary can be conceived as a plate of cells that directs growth along the lateral and proximal-distal axes (Figure 4.20). It is likely that multiple factors are involved in setting up this boundary and in directing growth along the axes. There may be subtle differences in these networks that account for the different growth defects in the W23 and A188 backgrounds. The expression of potential

interacting genes would need to be studied in more detail before any conclusions could be drawn about the effects of background-dependent factors on the *mwp1-R* phenotype.

4.4.5 *mwp1-R* specifically affects sheath tissue

mwp1-R affects a range of lateral organs. However, the phenotype is generally confined to sheath tissue and husk leaf phenotypes are more severe than vegetative leaf phenotypes. Given that there are at least 11 *KAN* genes in maize, it is likely that there is a high level of redundancy and subfunctionalisation in this gene family (per. comm., Hector Candela and Sarah Hake). Thus, *Mwp1* may act primarily in sheath tissue, with other *KAN* family members fulfilling a similar role in blade tissue. Likewise, *Mwp1* may be more important in husk leaf development, with additional *KANs* acting in a partially redundant manner during vegetative leaf development.

In *Arabidopsis* there are four *KAN* genes, and they act in a partially redundant manner. Single mutants have very mild phenotypes compared to double and triple *kan* mutants (Kerstetter *et al.*, 2001; Eshed *et al.*, 2004). *KAN4* expression is limited to ovules and is required for development of the inner integument, whilst *KAN1* and *KAN2* act redundantly to provide a homologous function in the outer integument (McAbee *et al.*, 2006). *KAN* genes in maize may have similarly specialised functions, indeed there is likely to be a higher level of subfunctionalisation due to the larger maize *KAN* family.

4.4.6 *mwp1-R* interacts with proximal-distal patterning mutants

mwp1-R phenotypes are generally confined to the sheath or basal parts of lateral organs. However, blade tissue adjacent to ectopic sheath-like tissue in *mwp1-R;Wab1-R* double mutants also exhibits disrupted adaxial-abaxial polarity (Figure 4.18). This was not observed in *Wab1-R* single mutants. Blade tissue adjacent to ectopic sheath tissue exhibited disrupted adaxial-abaxial polarity, with bulliform cells and macrohairs on the abaxial surface and misoriented or radialised vascular bundles. Similar phenotypes are seen in *mwp1-R;Rs1-R* and *mwp1-R;Kn1-R* double mutants, indicating that this interaction isn't specific to *Wab1-R*. One explanation is that *Mwp1* is specifically required for patterning of

sheath tissue or basal tissue types. There may be blade-specific *KAN* genes that act in normal blade tissue, but are not expressed in ectopic sheath tissue. It is possible that, once incorrect adaxial-abaxial patterning is established in ectopic sheath tissue, this positional information is transmitted to adjacent blade tissue.

4.4.7 Comparison of grass and dicot modes of growth

Differences in the phenotypes of dicot and grass leaf polarity mutants may reflect differences in the way that leaves are initiated and elaborated. In dicots, a number of mutants that affect adaxial-abaxial polarity have leaves that are radial or almost radial. The leaf primordia of dicots such as tobacco emerge as peg-like structures. The lamina is initiated subsequently from cells on the flanks of the primordium (Poethig and Sussex, 1985a). In maize, the leaf lateral axis is established within the SAM and the primordium has a flattened lamina at the time of emergence. Only mutations that affect founder cell recruitment, such as *lbf1*, result in radial leaves (Timmermans *et al.*, 1998).

Elaboration and differentiation of maize leaves proceeds basipetally and from the midrib to margins. Thus, the sheath margins are the last part of the leaf to differentiate (Sharman, 1942; Sylvester *et al.*, 1996; Scanlon, 2003). *mwp1-R* lateral organs are generally most affected in the sheath margin domains. One possible explanation is that *Mwp1* is required to maintain abaxial identity at later stages of development. Maize leaves grow for a more prolonged period than many dicot leaves. In maize, growth persists at the margins and contributes substantially to the width of the leaf base. This is evidenced by wide marginal clonal sectors (Poethig, 1984; Poethig and Szymkowiak, 1995). In dicots, the margin plays only a minor role in growth of the lamina. Cells at the margins begin differentiation early in leaf development and marginal clonal sectors are relatively narrow (Poethig and Sussex, 1985a; Poethig and Sussex, 1985b). These differences in growth patterns may explain why *mwp1-R* phenotypes are most pronounced in margin domains, whereas, in dicots, the leaf margins do not show particularly strong *kan* phenotypes.

Mutations that specifically affect either the upper or lower leaf zone may also manifest differently, as the maize leaf is comprised almost entirely of lower leaf zone, whereas the dicot leaf is mainly upper leaf zone (Figure 1.7) (Troll, 1955; Kaplan, 1973; Nardmann *et al.*, 2004). *mwp1-R* defects are generally specific to sheath tissue. The sheath corresponds to the basal portion of the lower leaf zone. Therefore, equivalent defects in dicot leaves may be difficult to detect, as the lower leaf zone forms only a minor part of the mature leaf.

Outgrowths on *mwp1-R* leaves tend to occur as long flaps that run parallel to lateral veins, whereas, outgrowths on the leaves of *Arabidopsis kan* mutants are radial (Eshed *et al.*, 2004). A linear arrangement of tissues is characteristic of grass leaves (Sylvester *et al.*, 1996). Lateral veins form parallel to the midrib and clonal sectors are generally confined along vascular boundaries (Cerioli *et al.*, 1994). In dicots, veins are initiated at an oblique angle to the midrib and clonal sectors tend to be isodiametric (Poethig and Sussex, 1985a; Poethig and Sussex, 1985b). In dicots, cells expand isotropically, whereas, in grass leaves, cell expansion is polarised longitudinally (Poethig, 1984). Differences between *mwp1-R* and *Arabidopsis kan* phenotypes may reflect differences in the structure and development of *Arabidopsis* and maize leaves.

4.4.8 Prophyll morphogenesis

Do existing meristems and leaf primordia influence the development of organs on newly ramified meristems?

The prophyll is the first organ initiated by the newly formed lateral meristem and it is likely that this affects its development and morphology. Unlike subsequent husk leaves, the prophyll is not subject to the influence of existing primordia. The prophyll arises on the adaxial side of the lateral meristem. Thus, it may be subject to the influence of two meristems – the lateral meristem from which it was initiated and the SAM of the main axis. It is unclear how much influence the SAM would exert on the developing prophyll as, by the time the prophyll is initiated by the lateral meristem, the SAM has initiated several additional vegetative leaves.

It is possible that prophyll development is influenced by the proximity of newly initiated vegetative leaves rather than, or in addition to, the SAM. During the early stages of prophyll development, the main shoot axis is compressed and the lateral meristem exists in close proximity to distal primordia of the main axis and to the subtending leaf. Bossinger *et al.* (1992) suggest that the morphology and topology of the first organs initiated by newly ramified meristems (type 2 phytomers) may be influenced by existing leaf primordia. During initiation of the lateral meristem and early prophyll development, the subtending vegetative leaf and leaves at distal nodes express *rd1* and *zyb9*. In addition *Zm*KAN2* is expressed in leaf primordia and in the disk of insertion (Henderson *et al.*, 2006). These, or other factors expressed by leaves adjacent to the lateral meristem may influence prophyll development.

The shape of the lateral meristem may also influence prophyll development. Meristem shape and size are known to influence phyllotaxy, for example in the maize *abphyl1* mutant (Jackson and Hake, 1999; Giulini *et al.*, 2004). The newly initiated lateral meristem is sandwiched between the main axis and the subtending leaf and is elliptical in transverse section. As primordia are initiated, the meristem assumes a more rounded shape. It is possible that the elongated shape of the meristem causes the initiation of two primordia simultaneously. This theory is consistent with the observation that newly formed floret meristems are somewhat elliptical in shape and initiate paleae, which are also fused organs (Bonnett, 1940; Cheng *et al.*, 1983).

Auxin flux in the SAM has been shown to be a crucial factor in leaf initiation and phyllotaxis. According to auxin flux models, existing primordia act as auxin sinks leading to auxin maxima at regions furthest from existing primordia. New primordia arise in these areas of highest auxin concentration (Reinhardt *et al.*, 2000; Reinhardt *et al.*, 2003). Auxin response factors have been implicated in adaxial-abaxial patterning and lamina outgrowth, suggesting that auxin may also function in patterning of lateral organs (Pekker *et al.*, 2005). It is likely that auxin is involved in the unique topology and morphology of lateral organs produced by newly formed meristems. One possibility is that leaf primordia that flank the new lateral meristem could influence auxin flux in the lateral meristem and thus determine the positioning of prophyll primordia. Auxin may also

mediate fusion of the two primordia, as auxin application has been shown to cause fusion of leaf primordia and inhibition of auxin transport results in fusion of sheath margins in maize (Snow and Snow, 1937; Scanlon, 2003). It should be emphasised that these suggestions are speculative. An investigation of auxin flux in lateral meristems and the localisation of associated proteins may elucidate this matter.

The keel is sensitive to disrupted polarity

The maize prophyll has two prominent keels that partially encircle the culm. The keels correspond to the midrib regions of two fused leaves. The keel region is particularly sensitive to disrupted polarity caused by *mwp1-R*. In families where the prophyll is unfused, keel outgrowth is dramatically reduced. In families where *mwp1-R* prophylls remain fused, a phenotype is often observed where each keel is reduced to a convoluted series of outgrowths. The observation that individual veins in wild-type keels are often oriented differently to veins in surrounding tissue, and the dynamic expression pattern of *rd1* in the keel region, suggest that polarity may be established differently in the keel than in adjacent regions.

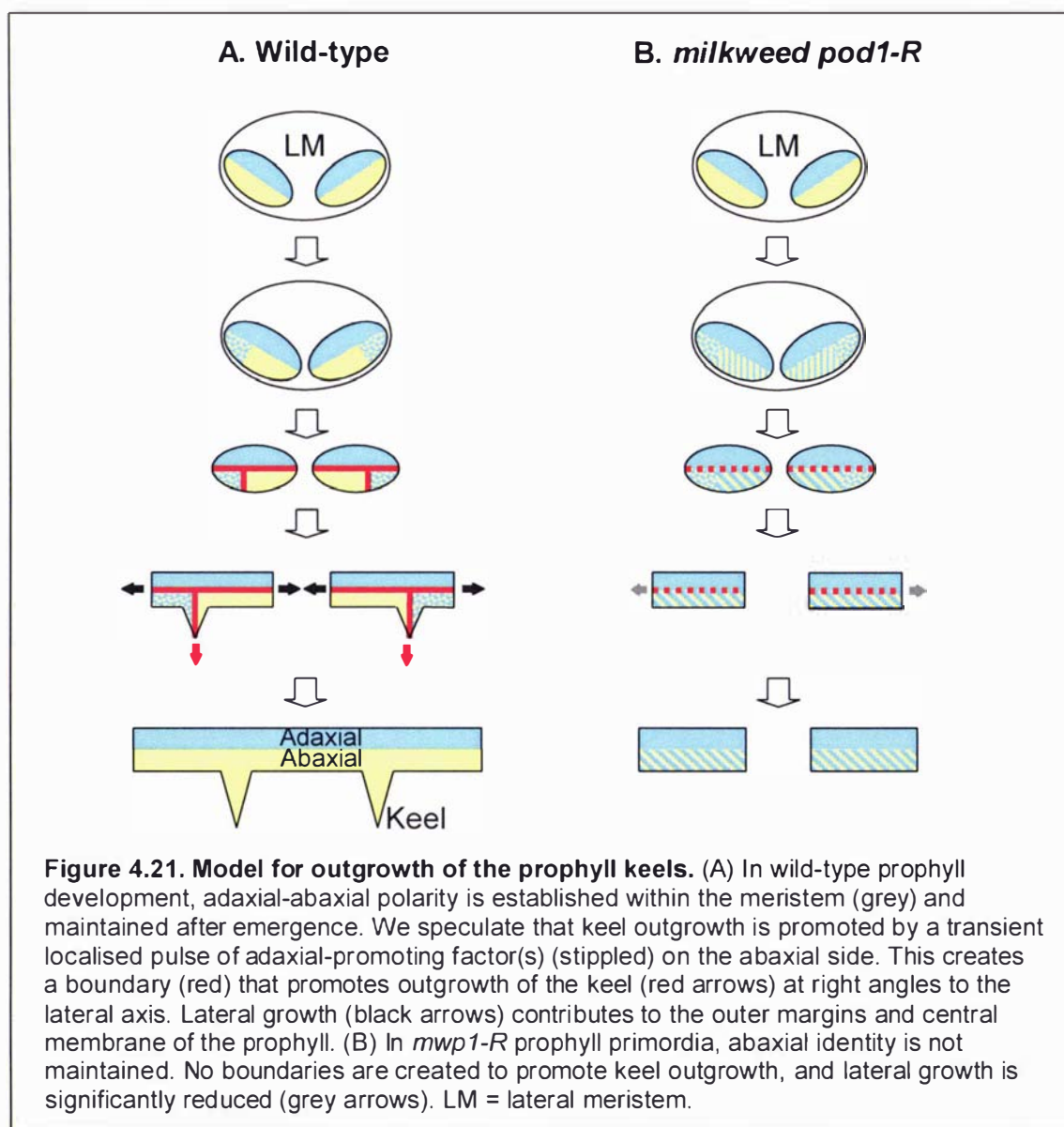
Model for keel outgrowth

We speculate that the adaxial-abaxial patterning system has been co-opted during evolution to promote outgrowth of the keels in normal prophyll development. A model is presented in which a pulse of adaxial identity on the abaxial side of the prophyll generates a new boundary that initiates keel outgrowth (Figure 4.21). In *mwp1-R* prophylls, ectopic expression of adaxial factors means that no distinct boundary is created. Thus, keel outgrowth is significantly reduced.

According to this model, adaxial (blue) and abaxial (yellow) domains are established in the two primordia that comprise the prophyll. This boundary between adaxial and abaxial domains generates the lateral axis. Subsequently, adaxial factor(s) are expressed briefly at the outer edge of each primordium on the abaxial side (stippled). These blocks of adaxial identity set up additional boundaries at right angles to the lateral axis, thereby initiating keel outgrowth. The blocks of *rd1* expression that are seen at the outer edges of early stage

prophylls may correspond to this localised pulse of adaxial identity. The boundary between *rd1*-expressing and non-expressing cells in early stage prophyll primordia aligns with the axis of the emerging keel. The observation that individual veins in wild-type prophyll keels often have a different orientation to surrounding veins is also consistent with this model.

This model could explain the reduction in keel outgrowth seen in unfused *mwp1-R* prophylls. According to the model, adaxial and abaxial domains are initiated normally in *mwp1-R* prophylls. Thus, *mwp1-R* prophylls appear normal shortly after initiation. Without *Mwp1* function, abaxial identity is not maintained. Consequently, there is no strong boundary to promote keel outgrowth. The lateral boundary is also less distinct and, as a result, lateral growth is much reduced.



Analysis of *mwp1-R* prophylls that exhibit the subdivided keel phenotype suggests that the keel region is particularly sensitive to disruptions to abaxial identity. The model for keel outgrowth may explain why the keel is more severely affected than surrounding regions. If the keel axis is established by the transient expression of adaxial identity genes on the abaxial side, then this early exposure to adaxial factors may make cells in the keel region more susceptible to ectopic adaxial factors later in development. The resulting patches of adaxialised cells interspersed with abaxial cells would create multiple ectopic boundaries, generating a complex array of outgrowths.

5. Conclusions and future work

5.1 Conclusions

A fundamental developmental mechanism is the subdivision of fields of cells into smaller compartments and the concomitant initiation of new axes of growth (Diaz-Benjumea and Cohen, 1993; Lawrence and Struhl, 1996). This study focuses on three mutants, *Wab1-R*, *Ig1-R* and *mwp1-R* that disrupt axial patterning of maize leaves. Analyses of mutant phenotypes and gene expression patterns, and a series of mosaic analyses have uncovered interactions between factors involved in defining developmental compartments and growth axes during maize leaf development.

Wab1-R is a dominant mutation that disrupts proximal-distal patterning of maize leaves, resulting in ectopic auricle and sheath tissue in the leaf blade and narrow leaves (Hay and Hake, 2004). Both aspects of the phenotype are exacerbated by *Ig1-R*. A mosaic analysis of *Wab1-R* indicated that *Wab1-R* generally acts cell-autonomously. Examples of *Wab1-R* non-autonomy were only observed in a *Lg1* background, supporting a role for *Lg1* in signal propagation. We suggest that *Lg1* can transmit positional information from *Wab1-R* tissue into *wab1/-* tissue and from *wab1/-* tissue into *Wab1-R* tissue.

Leaf shape and positioning of the blade-sheath boundary are altered in *Ig1-R* mutants, implying a role for *Lg1* in modulating leaf shape. Becraft *et al.* (1990) found that *Lg1* acts cell-autonomously to specify ligule and auricle tissue. My results indicate that *Lg1* also conditions *Wab1-R* ectopic auricle tissue in a cell-autonomous manner. However, the data suggest that *Lg1* promotes lateral growth non-autonomously. Thus, *Lg1* has both cell-autonomous and non-autonomous functions. These functions may be mediated by separate downstream pathways.

Hay and Hake (2004) proposed that the *Wab1-R* narrow leaf phenotype is due to the deletion of a lateral domain. However, a clonal analysis of *Wab1-R* leaves presented in this thesis does not support this hypothesis. *Wab1-R* leaf primordia

appear narrower than wild-type leaf primordia at plastochron three (Hay and Hake, 2004). A comparison of lateral vein initiation in *Wab1-R* and wild-type leaf primordia found a difference in lateral vein number one plastochron later than the observed difference in width. This finding is consistent with a space-filling model rather than a pre-pattern model for vascular initiation.

Analysis of the *mwp1-R* phenotype revealed that adaxial cell-types on the abaxial side of *mwp1-R* lateral organs are associated with ectopic outgrowths. The phenotype is generally confined to sheath tissue. Genes that are normally expressed adaxially are expressed on the abaxial side of *mwp1-R* lateral organs. The *mwp1-R* phenotype is consistent with a model in which the juxtaposition of adaxial and abaxial compartments generates a new axis and promotes lateral growth along this axis (Waites and Hudson, 1995). Given that *mwp1-R* is a recessive mutation, these results suggest that *Mwp1* is required for the establishment or maintenance of abaxial identity in sheath tissue.

The margins of *mwp1-R* lateral organs exhibit the most severe phenotypes. The sheath margin phenotype is consistent with the idea that correct establishment of adaxial-abaxial polarity is required for the development of normal margin characteristics (Sawa *et al.*, 1999). The fact that *mwp1-R* specifically affects sheath tissue and the phenotype is most pronounced at the margins suggests that *Mwp1* acts relatively late in development, as the sheath margins are the last part of the leaf to differentiate. It is likely that other *KAN* family members perform similar functions in other parts of the leaf or at different stages of development.

mwp1-R affects most lateral organs. This supports the concept that common genetic programmes are involved in the patterning of all lateral organs, and implies a shared evolutionary origin (Bossinger *et al.*, 1992). Phenotypic differences are likely to reflect differences in lateral organ morphogenesis. For example, vegetative leaves were most consistently affected at the sheath margins, whereas, the silks had the most severe outgrowths in the central indented regions. The silk phenotype is consistent with the fused phytomer model, in which the indents correspond to the fused margins of two highly modified leaves (Cronquist, 1988; Scanlon and Freeling, 1998).

The prophyll exhibits the most severe *mwp1-R* phenotypes and is also considered to be a fused organ (Bossinger *et al.*, 1992; Scanlon and Freeling, 1998). The prophyll has an unusual morphology, with two prominent keels corresponding to the two midrib domains. The keel region is particularly sensitive to disruptions to adaxial-abaxial polarity by *mwp1-R*. We propose that the adaxial-abaxial patterning system has been co-opted to promote outgrowth of the keels during normal prophyll development (Figure 4.21). Evidence to support this model includes the disruption of keel development by *mwp1-R*, the transient boundary of *rld1* expression along the keel axis and the different orientation of individual veins in the keel region compared to other parts of the prophyll.

Analysis of the *Wab1-R* and *mwp1-R* mutant phenotypes provides evidence that the axes of growth are patterned interdependently. Disruption of either the proximal-distal axis in *Wab1-R* or the adaxial-abaxial axis in *mwp1-R* reduces lateral growth along the medial-lateral axis. In some backgrounds, *mwp1-R* also causes a reduction in growth along the proximal-distal axis. Analysis of the *mwp1-R* "tab" phenotype provides further evidence that adaxial-abaxial patterning is required for proximal-distal growth. The central membrane of the prophyll can undergo extensive growth along the proximal-distal axis in regions where adaxial-abaxial polarity is specified correctly, but not in adjacent regions where polarity is mis-specified. This makes sense if the adaxial-abaxial boundary is conceptualised as a plate of cells that co-ordinates cell division and expansion along both the medial-lateral and proximal-distal axes (Figure 4.20) (Waites and Hudson, 1995).

Correct specification of developmental compartments is crucial for normal leaf development. The axes of growth establish the planes of cell division and expansion, which in turn direct lateral organ morphogenesis. When these axes are disrupted, the final shape of the leaf is altered. Positional information is also required for the appropriate differentiation of specific tissues. As well as the delimitation of compartments and the specification of cell-types, there is a requirement for inter-compartmental signalling to ensure co-ordinated growth of the leaf. Thus, both cell-autonomous and non-autonomous pathways are

necessary for leaf development. The results of this study place *Mwp1*, *wab1* and *Lg1* in a network of genes that regulate leaf polarity and axial patterning.

5.2 Future work

The identity of *wab1* is not yet known. Cloning of *wab1* will facilitate investigations of *wab1* function. It will enable *in situ* hybridisation to determine the *wab1* expression pattern during normal leaf development and in *Wab1* mutants, as well as interactions with other genes. Identifying the molecular lesion(s) in *Wab1* alleles may provide information about the regulation of *wab1*, or about the function of WAB1 protein. Obtaining a *wab1* loss-of-function mutant and analysis of the mutant phenotype will be crucial to determining the normal function of *wab1*.

Mwp1 has recently been cloned and is a member of the *KAN* gene family. Work is currently underway to characterise the *Mwp1* expression pattern. In light of the severe *mwp1-R* phenotypes in prophylls and silks, it will be particularly interesting to characterise the *Mwp1* expression pattern in these organs. In *Arabidopsis*, the *KAN* and *HD-ZIPIII* genes have an antagonistic relationship (Eshed *et al.*, 2001; Kerstetter *et al.*, 2001; Emery *et al.*, 2003). We have shown that *rd1* is ectopically expressed in *mwp1-R* mutant leaves. It is likely that other *HD-ZIPIII* genes are also misexpressed in *mwp1-R*. This could be investigated by analysing the expression patterns of other maize *HD-ZIPIII* genes in wild-type and *mwp1-R* lateral organs. Analysis of the *Mwp1* expression pattern in *Rld1* mutants will help determine if an antagonistic relationship between the *KAN* and *HD-ZIPIII* genes exists in maize

There are at least 11 *KAN* genes in maize. Therefore, there is likely to be a high level of redundancy. Obtaining multiple *kan* loss-of-function mutants may reveal phenotypes that would be obscured by redundancy in single mutants. In particular, blade tissue is generally not affected by *mwp1-R*. It will be interesting to see whether blade phenotypes are observed in other *kan* mutants.

Auxin has been implicated in lateral organ initiation and in leaf polarity (Reinhardt *et al.*, 2000; Reinhardt *et al.*, 2003; Pekker *et al.*, 2005). Auxin flux is

mediated by PIN proteins (Galweiler *et al.*, 1998). Therefore, it may be informative to investigate the pattern of PIN localisation in ectopic outgrowths during *mwp1-R* leaf development and during initiation of the prophyll keel. The prophyll is characteristic of a type two phytomer in that two primordia are initiated simultaneously by a newly ramified meristem (Bossinger *et al.*, 1992). Factors that may influence this unique topology include the elliptical shape of the meristem, and the influence of flanking meristems and leaf primordia. Given that auxin levels determine the positioning of new primordia, it will be interesting to study PIN localisation during prophyll initiation and compare this with initiation of subsequent husk leaves.

We propose that the adaxial-abaxial patterning system has been co-opted to promote outgrowth of the keels during normal prophyll development. This could be investigated further by determining the expression patterns of other polarity genes during normal prophyll development, and by characterising any prophyll phenotypes conditioned by other mutants that disrupt leaf polarity. It may also be informative to analyse the *Mwp1* gene to identify motifs that regulate the *Mwp1* expression pattern in the prophyll.

It is possible that the adaxial-abaxial patterning network has been co-opted to pattern unusual leaf forms in other species. This could be addressed by investigating the function of homologues of known polarity genes in species with diverse lateral organ morphologies.

References

- Alvarez, J., and Smyth, D.R.** (1999). *CRABS CLAW* and *SPATULA*, two *Arabidopsis* genes that control carpel development in parallel with *AGAMOUS*. *Development* **126**, 2377-2386.
- Arber, A.** (1934). *The Gramineae. A study of Cereal, bamboo, and grasses.* (Cambridge: Cambridge University Press).
- Bao, N., Lye, K., and Barton, M.K.** (2004). MicroRNA binding sites in *Arabidopsis* ClassIII *HD-ZIP* mRNAs are required for methylation of the template chromosome. *Developmental Cell* **7**, 653-662.
- Barton, M., and Poethig, R.** (1993). Formation of the shoot apical meristem in *Arabidopsis thaliana* - an analysis of development in the wild-type and in the *shoot meristemless* mutant. *Development* **119**, 823-831.
- Becraft, P., and Freeling, M.** (1991). Sectors of *liguleless-1* tissue interrupt an inductive signal during maize leaf development. *The Plant Cell* **3**, 801-807.
- Becraft, P., and Freeling, M.** (1994). Genetic analysis of *Rough sheath-1* developmental mutants of maize. *Genetics* **136**, 295-311.
- Becraft, P., Bongard-Pierce, D., Sylvester, A.W., Poethig, R.S., and Freeling, M.** (1990). The *liguleless-1* gene acts tissue specifically in maize leaf development. *Developmental Biology* **141**, 220-232.
- Bertrand-Garcia, R., and Freeling, M.** (1991). *Hairy-sheath frayed #1-0*: A systemic, heterochronic mutant of maize that specifies slow developmental stage transitions. *American Journal of Botany* **78**, 747-765.
- Blanc, G., and Wolfe, K.H.** (2004). Widespread paleopolyploidy in model plant species inferred from age distribution of duplicate genes. *The Plant Cell* **16**, 1667-1678.
- Bonnett, O.T.** (1940). Development of the staminate and pistillate inflorescences of sweet corn. *Journal of Agricultural Research* **60**, 25-37.
- Bossinger, G., Lundqvist, U., Rohde, W., and Salamini, F.** (1992). Genetics of plant development in barley. *Barley Genetics VI* **2**, 989-1022.
- Bowman, J.L., and Smyth, D.R.** (1999). *CRABS CLAW*, a gene that regulates carpel and nectary development in *Arabidopsis*, encodes a novel protein with zinc finger and helix-loop-helix domains. *Development* **126**.
- Brink, R.** (1933). Heritable characters in maize XLVI - *Liguleless2*. *Journal of Heredity* **24**, 325-326.
- Brunner, S., Fengler, K., Morgante, M., Tingey, S., and Rafalski, A.** (2005). Evolution of DNA sequence nonhomologies among maize inbreds. *The Plant Cell* **17**, 343-360.
- Burr, B., Chandler, V., Coe, E., Dooner, H., Fauron, C., Langdale, J., Polacco, M., Sachs, M., Scanlon, M., and Stinard, P.** (1995). A standard for maize genetics nomenclature. *Maize Genetics Coop Newsletter* **69**, 182-184.
- Butterworth, F.M., and King, R.C.** (1965). The developmental genetics of *apterous* mutants in *Drosophila melanogaster*. *Genetics* **52**, 1153-1174.
- Carrington, J., and Ambros, V.** (2003). Role of microRNAs in plant and animal development. *Science* **301**, 336-338.
- Cerioni, S., Marocco, A., Maddaloni, M., Motto, M., and Salamini, F.** (1994). Early events in maize leaf epidermis formation as revealed by cell lineage studies. *Development* **120**, 2113-2120.

- Cheng, P.C., Greyson, R.I., and Walden, D.B.** (1983). Organ initiation and the development of unisexual flowers in the tassel and ear of *Zea Mays*. *American Journal of Botany* **70**, 450-462.
- Chuck, G., Lincoln, C., and Hake, S.** (1996). BP induces lobed leaves with ectopic meristems when overexpressed in *Arabidopsis*. *Plant Cell* **8**, 1277-1289.
- Clifford, H.T.** (1988). Spikelet and floral morphology. In *Grass Systematics*, T.R. Soderstrom, K.W. Hilu, S.C. Campbell, and M.E. Barkworth, eds (Washington, D.C., London: Smithsonian Institution Press), pp. 21-30.
- Coe, E.H.** (1994). Genetic experiments and mapping. In *The Maize Handbook*, M. Freeling and V. Walbot, eds (New York: Springer-Verlag Inc.), pp. 189-197.
- Crawford, K., and Zambryski, P.** (2000). Subcellular localization determines the availability of non-targeted proteins to plasmodesmatal transport. *Current Biology* **10**, 1032-1040.
- Cronquist, A.** (1988). *The Evolution and Classification of Flowering Plants*. (New York: The New York Botanical Garden).
- de Bodd, S., Maere, S., and Van de Peer, Y.** (2005). Genome duplication and the origin of angiosperms. *Trends in Ecology and Evolution* **20**, 591-597.
- Diaz-Benjumea, F.J., and Cohen, S.M.** (1993). Interactions between dorsal and ventral cells in the imaginal disc directs wing development in *Drosophila*. *Cell* **75**, 741-752.
- Duarte, J.M., Cui, L.Y., Wall, P.K., Zhang, Q., Leebens-Mack, J., Ma, J., Altman, N., and dePamphilis, C.W.** (2006). Expression pattern shifts following duplication indicative of subfunctionalization and neofunctionalization in regulatory genes of *Arabidopsis*. *Molecular Biology and Evolution* **23**, 469-478.
- Emerson, R.** (1912). The inheritance of the ligule and auricles of corn leaves. *Nebraska Agricultural Experimental Station Annual Report* **25**, 81-88.
- Emery, J., Floyd, S., Alvarez, J., Eshed, Y., Hawker, N., Izhaki, A., Baum, S., and Bowman, J.** (2003). Radial patterning of *Arabidopsis* shoots by Class III HD-ZIP and KANADI genes. *Current Biology* **13**, 1768-1774.
- Esau, K.** (1960). *Plant Anatomy*. (New York: John Wiley and Sons, Inc).
- Esau, K.** (1965). *Vascular Differentiation in Plants*. (New York: Holt, Rinehart and Winston).
- Esau, K.** (1977). *Anatomy of Seed Plants*. (New York: John Wiley and Sons).
- Eshed, Y., Baum, S.F., and Bowman, J.L.** (1999). Distinct mechanisms promote polarity establishment in carpels of *Arabidopsis*. *Cell* **99**, 199-209.
- Eshed, Y., Baum, S., Perea, J., and Bowman, J.** (2001). Establishment of polarity in lateral organs of plants. *Current Biology* **11**, 1251-1260.
- Eshed, Y., Izhaki, A., Baum, S., Floyd, S., and Bowman, J.** (2004). Assymmetric leaf development and blade expansion in *Arabidopsis* are mediated by KANADI and YABBY activities. *Development* **131**, 2997-3006.
- Floyd, S.K., and Bowman, J.L.** (2004). Gene regulation: ancient microRNA target sequences in plants. *Nature* **428**, 485-486.
- Floyd, S.K., and Bowman, J.L.** (2007). The ancestral developmental tool kit of land plants. *International Journal of Plant Sciences*. **168**, 1-35.
- Foster, T., Hay, A., Johnston, R., and Hake, S.** (2004). The establishment of axial patterning in the maize leaf. *Development* **131**, 3921-3929.

- Foster, T., Yamaguchi, J., Wong, B., Veit, B., and Hake, S.** (1999). *Gnarley1* is a dominant mutation in the *knox4* gene affecting cell shape and identity. *Plant Cell* **11**, 1239-1252.
- Foster, T., Lough, T., Emerson, S., Lee, R., Bowman, J., Forster, R., and Lucas, W.** (2002). A surveillance system regulates selective entry of RNA into the shoot apex. *Plant Cell* **14**, 1497-1508.
- Freeling, M.** (1992). A conceptual framework for maize leaf development. *Developmental Biology* **153**, 44-58.
- Freeling, M., and Hake, S.** (1985). Developmental genetics of mutants that specify knotted leaves in maize. *Genetics* **111**, 617-634.
- Freeling, M., and Fowler, J.** (1994). A nine-step way to characterise a morphological mutant. In *The Maize Handbook*, M. Freeling and V. Walbot, eds (New York: Springer-Verlag Inc.), pp. 209-211.
- Fu, H., and Donner, H.K.** (2002). Intraspecific violation of genetic colinearity and its implications in maize. *Proceedings of the National Academy of Science* **99**, 9573-9578.
- Galinat, W.C.** (1959). The phytomer in relation to floral homologies in the American Maydeae. *Botanical Museum Leaflets, Harvard University* **19**, 1-32.
- Galweiler, L., Guan, C., Muller, A., Wisman, E., Mendgen, K., Yephremov, A., and Palme, K.** (1998). Regulation of polar auxin transport by AtPIN1 in *Arabidopsis* vascular tissue. *Science* **282**, 2226-2230.
- Garcia-Bellido, A., Ripoll, P., and Morata, G.** (1973). Developmental compartmentalisation of the wing disc of *Drosophila*. *Nature New Biology* **245**, 251-253.
- Gaut, B.S., and Doebley, J.F.** (1997). DNA sequence evidence for the segmental allotetraploid origin of maize. *Proceedings of the National Academy of Science* **94**, 6809-6814.
- Gilbert, S.F.** (2000). *Developmental Biology*. (Sunderland, Massachusetts: Sinauer Associates).
- Gisel, A., Barella, S., Hempel, F., and Zambryski, P.** (1999). Temporal and spatial regulation of symplastic trafficking during development in *Arabidopsis thaliana* apices. *Development* **126**, 1879-1889.
- Giulini, A., Wang, J., and Jackson, D.** (2004). Control of phyllotaxy by the cytokinin-inducible response regulator homologue *ABPHYL1*. *Nature* **430**, 1031-1034.
- Golz, J.F., Roccaro, M., Kuzoff, R., and Hudson, A.** (2004). *GRAMINIFOLIA* promotes growth and polarity of *Antirrhinum* leaves. *Development* **131**, 3661-3670.
- Guo, M., Rupe, M., Zinselmeier, C., Habben, J., Bowen, B., and Smith, O.S.** (2004). Allelic variation of gene expression in maize hybrids. *Plant Cell* **16**, 1707-1716.
- Hake, S., and Freeling, M.** (1986). Analysis of genetic mosaics shows that the extra epidermal cell divisions in *Knotted* mutant maize plants are induced by adjacent mesophyll cells. *Nature* **320**, 621-623.
- Hake, S., Vollbrecht, E., and Freeling, M.** (1989). Cloning *Knotted*, the dominant morphological mutant of maize using Ds2 as a transposon tag. *EMBO Journal* **8**, 15-22.
- Hake, S., Hester, H., Wassom, J., Widholm, J., and Rocheford, T.** (1999). *Wab* (*Wavy auricle in blades*), a dominant leaf mutation located on chromosome 2L. *Maize Genetics Coop Newsletter* **73**, 3.

- Harper, L., and Freeling, M.** (1996). Interactions of *liguleless1* and *liguleless2* function during ligule induction in maize. *Genetics* **144**, 1871-1882.
- Hay, A., and Hake, S.** (2004). The dominant mutant *Wavy auricle in blade* disrupts patterning in a lateral domain of the maize leaf. *Plant Physiology* **135**, 300-308.
- Heisler, M.G.B., Atkinson, A., Bylstra, Y.H., Walsh, R., and Smyth, D.R.** (2001). *SPATULA*, a gene that controls development of carpel margin tissues in *Arabidopsis*, encodes a bHLH protein. *Development* **128**, 1089-1098.
- Henderson, D.C., Zhang, X., Brooks III, L., and Scanlon, M.J.** (2006). RAGGED SEEDLING2 is required for expression of KANADI2 and REVOLUTA homologues in the maize shoot apex. *Genesis* **44**, 372-382.
- Irish, V., and Sussex, I.** (1992). A fate map of the *Arabidopsis* embryonic shoot apical meristem. *Development* **120**, 405-413.
- Jackson, D.** (1991). *In situ* hybridisation in plants. In *Molecular plant pathology: a practical approach*, D.J. Bowles, S.J. Gurr, and M. McPherson, eds (Oxford: Oxford University Press), pp. 163-174.
- Jackson, D., and Hake, S.** (1999). Control of phyllotaxy in maize by the *ABPHYL1* gene. *Development* **126**, 315-323.
- Jackson, D., Veit, B., and Hake, S.** (1994). Expression of the maize *KNOTTED-1* related homeobox genes in the shoot apical meristem predicts patterns of morphogenesis in the vegetative shoot. *Development* **120**, 405-413.
- Johansen, D.A.** (1940). *Plant Microtechnique*. (New York: McGraw-Hill Book Company, Inc.).
- Juarez, M.T., Twigg, R.W., and Timmermans, M.C.P.** (2004a). Specification of adaxial cell fate during maize leaf development. *Development* **131**, 4533-4544.
- Juarez, M.T., Kui, J.S., Thomas, J., Heller, B.A., and Timmermans, M.C.P.** (2004b). microRNA-mediated repression of *rolled leaf1* specifies maize leaf polarity. *Nature* **428**, 84-88.
- Kaplan, D.** (1973). The monocotyledons: their evolution and comparative biology. VII. The problem of leaf morphology and evolution in the monocotyledons. *The Quarterly Review of Biology* **48**, 437-457.
- Kepinski, S.** (2006). Integrating hormone signaling and patterning mechanisms in plant development. *Current Opinion in Plant Biology* **9**, 28-34.
- Kerstetter, R., Bollman, K., Taylor, R., Bomblies, K., and Poethig, R.** (2001). *KANADI* regulates organ polarity in *Arabidopsis*. *Nature* **411**, 706-709.
- Kidner, C., and Martienssen, R.** (2004). Spatially restricted microRNA directs leaf polarity through *ARGONAUTE1*. *Nature* **428**, 81-84.
- Kim, J., Yuan, Z., and Jackson, D.** (2003). Developmental regulation and significance of KNOX protein trafficking in *Arabidopsis*. *Development* **130**, 4351-4362.
- Kumaran, M.K., Bowman, J.L., and Sundaresan, V.** (2002). *YABBY* polarity genes mediate the repression of *KNOX* homeobox genes in *Arabidopsis*. *The Plant Cell* **14**, 2761-2770.
- Lai, J., Messing, J., and Dooner, K.K.** (2005). Gene movement by *Helitron* transposons contributes to the haplotype variability of maize. *Proceedings of the National Academy of Science* **102**, 9068-9073.
- Langdale, J., Lane, B., Freeling, M., and Nelson, T.** (1989). Cell lineage analysis of maize bundle sheath and mesophyll cells. *Developmental Biology* **133**, 128-139.

- Lawrence, P., and Struhl, G.** (1996). Morphogens, compartments and pattern: lessons from *Drosophila*. *Cell* **85**, 951-961.
- Lee, M.** (1994). Inbred lines of maize and their molecular markers. In *The Maize Handbook*, M. Freeling and V. Walbot, eds (New York: Springer-Verlag Inc.), pp. 423-432.
- Lynch, M., and Conery, J.S.** (2000). The evolutionary fate and consequences of duplicate genes. *Science* **290**, 1151-1155.
- Matsumoto, N., and Okada, K.** (2001). A homeobox gene, *PRESSED FLOWER*, regulates lateral axis-dependent development of *Arabidopsis* flowers. *Genes and Development* **15**, 3355-3364.
- McAbee, J.M., Hill, T.A., Skinner, D.J., Izhaki, A., Hauser, B.A., Meister, R.J., Reddy, G.V., Meyerowitz, E., Bowman, J.L., and Gasser, C.S.** (2006). *ABERRANT TESTA SHAPE* encodes a KANADI family member, linking polarity determination to separation and growth of *Arabidopsis* ovule integuments. *The Plant Journal* **46**, 522-531.
- McConnell, J., and Barton, M.** (1998). Leaf polarity and meristem formation in *Arabidopsis*. *Development* **125**, 2935-2942.
- McConnell, J., Emery, J., Eshed, Y., Bao, N., Bowman, J., and Barton, M.** (2001). Role of *PHABULOSA* and *PHAVOLUTA* in determining radial patterning in shoots. *Nature* **411**, 709-713.
- Moreno, M., Harper, L., Krueger, R., Dellaporta, S., and Freeling, M.** (1997). *liguleless1* encodes a nuclear-localized protein required for induction of ligules and auricles during maize leaf organogenesis. *Genes and Development* **11**, 616-628.
- Morgante, M., Brunner, S., Pea, G., Fengler, K., Zuccolo, A., and Rafalski, A.** (2005). Gene duplication and exon shuffling by helitron-like transposons generate intraspecies diversity in maize. *Nature Genetics* **37**, 997-1002.
- Nardmann, J., Ji, J., Werr, W., and Scanlon, M.** (2004). The maize duplicate genes *narrow sheath1* and *narrow sheath2* encode a conserved homeobox gene function in a lateral domain of shoot apical meristems. *Development* **131**, 2827-2839.
- Nelson, J., Lane, B., and Freeling, M.** (2002). Expression of a mutant gene in the ventral leaf epidermis is sufficient to signal a switch of the leaf's dorsoventral axis. *Development* **129**, 4581-4589.
- Pekker, I., Alvarez, J., and Eshed, Y.** (2005). Auxin response factors mediate *Arabidopsis* organ asymmetry via modulation of KANADI activity. *The Plant Cell* **17**, 2899-2910.
- Phelps-Durr, T.L., Thomas, J., Vahab, P., and Timmermans, M.C.P.** (2005). Maize rough sheath2 and its *Arabidopsis* orthologue ASYMMETRIC LEAVES1 interact with HIRA, a predicted histone chaperone, to maintain *knox* gene silencing and determinacy during organogenesis. *The Plant Cell* **17**, 2886-2898.
- Poethig, R.S.** (1984). Cellular parameters of leaf morphogenesis in maize and tobacco. In *Contemporary Problems of Plant Anatomy*, R. White, Dickinson, W., ed (New York: Academic Press), pp. 235-238.
- Poethig, R.S.** (1988). Heterochronic mutations affecting shoot development in maize. *Genetics* **119**, 959-973.
- Poethig, R.S.** (1994). The Maize Shoot. In *The Maize Handbook*, M. Freeling and V. Walbot, eds (New York: Springer-Verlag), pp. 11-17.
- Poethig, R.S., and Sussex, I.** (1985a). The developmental morphology and growth dynamics of the tobacco leaf. *Planta* **165**, 158-169.

- Poethig, R.S., and Sussex, I.M.** (1985b). The cellular parameters of leaf development in tobacco: a clonal analysis. *Planta* **165**, 170-184.
- Poethig, R.S., and Szymkowiak, E.J.** (1995). Clonal analysis of leaf development in maize. *Maydica* **40**, 67-76.
- Pontig, C., and Aravind, L.** (1999). START: a lipid-binding domain in StAR, HD-ZIP and signalling proteins. *Trends in Biochemical Science* **24**, 130-132.
- Reinhardt, D., Mandel, T., and Kuhlemeier, C.** (2000). Auxin regulates the initiation and radial position of plant lateral organs. *Plant Cell* **12**, 507-518.
- Reinhardt, D., Pesce, E.-R., Stieger, P., Mandel, T., Baltensberger, K., Bennett, M., Traas, J., Friml, J., and Kuhlemeier, C.** (2003). Regulation of phyllotaxis by polar auxin transport. *Nature* **426**, 255-260.
- Rhoades, M., Reinhart, B., Lim, L., Burge, C., Bartel, B., and Bartel, D.** (2002). Prediction of plant microRNA targets. *Cell* **110**, 513-520.
- Russell, S.H., and Evert, R.F.** (1985). Leaf vasculature of *Zea mays* L. *Planta* **164**, 448-458.
- Russo, V.E.A.** (1999). Development: genetics, epigenetics and environmental regulation. (Berlin: Springer).
- Ruzin, S.E.** (1999). Plant Microtechnique and Microscopy. (New York: Oxford University Press).
- Sawa, S., Watanabe, K.G., K., Kanaya, E., Morita, E., and Okada, K.** (1999). *FILAMENTOUS FLOWER*, a meristem and organ identity gene of *Arabidopsis*, encodes a protein with a zinc finger and HMG-related domains. *Genes and Development* **13**, 1079-1088.
- Scanlon, M.** (2000). NARROW SHEATH1 functions from two meristematic foci during founder-cell recruitment in maize leaf development. *Development* **127**, 4573-4585.
- Scanlon, M., and Freeling, M.** (1997). Clonal sectors reveal that a specific meristematic domain is not utilized in the maize mutant *narrow sheath*. *Developmental Biology* **182**, 52-66.
- Scanlon, M., and Freeling, M.** (1998). The *narrow sheath* leaf domain deletion: a genetic tool used to reveal developmental homologies among modified maize organs. *The Plant Journal* **13**, 547-561.
- Scanlon, M., Schneeberger, R., and Freeling, M.** (1996). The maize mutant *narrow sheath* fails to establish leaf margin identity in a meristematic domain. *Development* **122**, 1683-1691.
- Scanlon, M.J.** (2003). The polar auxin transport inhibitor *N*-1-naphthylphthalamic acid disrupts leaf initiation, KNOX protein regulation, and formation of leaf margins in maize. *Plant Physiology* **133**, 597-605.
- Scarpella, E., Marcos, D., Friml, J., and Berleth, T.** (2006). Control of leaf vascular patterning by polar auxin transport. *Genes and Development* **20**, 1015-1027.
- Schneeberger, R., Tsiantis, M., Freeling, M., and Langdale, J.** (1998). The *rough sheath2* gene negatively regulates homeobox gene expression during maize leaf development. *Development* **125**, 2857-2865.
- Sessa, G., Steindler, C., Morelli, G., and Ruberti, I.** (1998). The *Arabidopsis Athb-8, -9* and *-14* genes are members of a small gene family coding for highly related HD-ZIP proteins. *Plant Molecular Biology* **38**, 609-622.
- Sessions, A., Yanofsky, M., and Weigel, D.** (2000). Cell-cell signalling and movement by the floral transcription factors LEAFY and APETALA1. *Science* **289**, 779-782.

- Sharman, B.C.** (1941). Development of the ligule in *Zea Mays* L. *Nature* **147**, 641.
- Sharman, B.C.** (1942). Developmental anatomy of the shoot of *Zea mays* L. *Annals of Botany* **6**, 245-284.
- Siegfried, K., Eshed, Y., Baum, S., Otsuga, D., Drews, G., and Bowman, J.** (1999). Members of the *YABBY* gene family specify abaxial cell fate in *Arabidopsis*. *Development* **126**.
- Sinha, N.R., and Hake, S.** (1990). Mutant characters of *Knotted* maize leaves are determined in the innermost tissue layers. *Developmental Biology* **141**, 203-210.
- Sinha, N.R., Williams, R.E., and Hake, S.** (1993). Overexpression of the maize homeobox gene, *KNOTTED-1*, causes a switch from determinate to indeterminate cell fates. *Genes and Development* **7**, 787-795.
- Smith, L.G., Greene, B., Veit, B., and Hake, S.** (1992). A dominant mutation in the maize homeobox gene, *Knotted-1*, causes its ectopic expression in leaf cells with altered fates. *Development* **116**, 21-30.
- Snow, M., and Snow, R.** (1937). Auxin and leaf formation. *The New Phytologist* **36**, 1-18.
- Snow, M., Snow, R.** (1959). The dorsiventrality of leaf primordia. *New Phytologist* **41**, 13-22.
- Song, R., and Messing, J.** (2003). Gene expression of a gene family in maize based on noncolinear haplotypes. *Proceedings of the National Academy of Science* **100**, 9055-9060.
- Steeves, T.A., and Sussex, I.M.** (1984). *Patterns in Plant Development*. (London: Wiley).
- Steffensen, D.M.** (1968). A reconstruction of cell development in the shoot apex of maize. *American Journal of Botany* **55**, 354-369.
- Sussex, I.** (1955). Morphogenesis in *Solanum tuberosum* L.: experimental investigation of leaf dorsiventrality and orientation in the juvenile shoot. *Phytomorphology* **5**, 286-300.
- Sussex, I.M.** (1954). Experiments on the cause of dorsiventrality in leaves. *Nature* **174**, 351-352.
- Swigonova, Z., Lai, J., Ma, J., Ramakrishna, W., Llaca, V., Bennetzen, J., and Messing, J.** (2004). Close split of sorghum and maize genome progenitors. *Genome Research* **14**, 1916-1923.
- Sylvester, A.W., Cande, W.Z., and Freeling, M.** (1990). Division and differentiation during normal and *liguleless-1* maize leaf development. *Development* **110**, 985-1000.
- Sylvester, A.W., Smith, L.G., and Freeling, M.** (1996). Acquisition of identity in the developing leaf. *Annual review of cell and developmental biology* **12**, 257-304.
- Tang, G., Reinhart, B., Bartel, D., and Zamore, P.** (2003). A biochemical framework for RNA silencing in plants. *Genes and Development* **17**, 49-63.
- Tenaillon, M.I., Sawkins, M.C., Long, A.D., Gaut, R.L., Doebley, J.F., and Gaut, B.S.** (2001). Patterns of DNA sequence polymorphism along chromosome 1 of maize (*Zea mays* ssp. *Mays* L.). *Proceedings of the National Academy of Science* **98**, 9161-9166.
- Timmermans, M., Schultes, N., Jankovsky, J., and Nelson, T.** (1998). *Leafbladeless1* is required for dorsoventrality of lateral organs in maize. *Development* **125**, 2813-2823.

- Timmermans, M.C., Hudson, A., Becraft, P.W., and Nelson, T.** (1999). ROUGH SHEATH2: a Myb protein that represses *knox* homeobox genes in maize lateral organ primordia. *Science* **284**, 151-153.
- Troll, W.** (1955). Concerning the morphological significance of the so-called vorlaeufer Spitze of monocot leaves. A contribution to the typology of monocot leaves. *Beitr. Biol. Pflanz.* **31**, 525-558.
- Tsiantis, M., Schneeberger, R., Golz, J., Freeling, M., and Langdale, J.** (1999). The maize *rough sheath2* gene and leaf development programs in monocot and dicot plants. *Science* **284**, 154-156.
- Veit, B., Vollbrecht, E., Mathern, J., and Hake, S.** (1990). A tandem duplication causes the *Kn1-O* allele of *Knotted*, a dominant morphological mutant of maize. *Genetics* **125**, 623-631.
- Villanueva, J.M., Broadhvest, J., Hauser, B.A., Meister, R.J., Schneitz, K., and Gasser, C.S.** (1999). *INNER NO OUTER* regulates abaxial-adaxial patterning in *Arabidopsis* ovules. *Genes and Development* **13**, 3160-3169.
- Vollbrecht, E., Reiser, L., and Hake, S.** (2000). Shoot meristem size is dependent on inbred background and presence of the maize homeobox gene, *knotted1*. *Development* **127**, 3161-3172.
- Waites, R., and Hudson, A.** (1995). *phantastica*: a gene required for dorsoventrality of leaves in *Antirrhinum majus*. *Development* **121**, 2143-2154.
- Waites, R., Selvadurai, H., Oliver, I., and Hudson, A.** (1998). The *PHANTASTICA* gene encodes a MYB transcription factor involved in growth and dorsoventrality of lateral organs in *Antirrhinum*. *Cell* **93**, 779-789.
- Walker, K.L., and Smith, L.G.** (2002). Investigation of the role of cell-cell interactions in division plane determination during maize leaf development through mosaic analysis of the *tangled* mutation. *Development* **129**, 3219-3226.
- Walsh, J., Waters, C., and Freeling, M.** (1997). The maize gene *liguleless2* encodes a basic leucine zipper protein involved in the establishment of the leaf blade-sheath boundary. *Genes and Development* **11**, 208-218.
- Weatherwax, P.** (1923). *The story of the maize plant.* (Chicago: University of Chicago Press).
- Williams, M.H., Vesk, M., and Mullins, M.G.** (1987). Tissue preparation for scanning electron microscopy of fruit surfaces: comparison of fresh and cryopreserved specimens and replicas of banana peel. *Micron Microsc. Acta* **18**, 27-31.